

In presenting this thesis in partial fulfillment of the requirements for an advanced degree at Idaho State University, I agree that the Library shall make it freely available for inspection. I further state that permission to download and/or print my thesis for scholarly purposes may be granted by the Dean of the Graduate School, Dean of my academic division, or by the University Librarian. It is understood that any copying or publication of this thesis for financial gain shall not be allowed without my written permission.

Signature _____

Hamed Alnagran

Date _____

**BIOKINETICS OF STRONTIUM-90 INJECTED IN NON-HUMAN
PRIMATES USING SAAM SOFTWARE AND IMBA PROFESSIONAL PLUS
SOFTWARE**

By

Hamed M. Alnagran

A thesis

submitted in partial fulfillment

of the requirements for the degree of

Master of Science in Department of Nuclear Engineering and Health Physics

Idaho State University

August 2014

To the Graduate Faculty:

The members of the committee appointed to examine the thesis of Hamed Alnagran find it satisfactory and recommend that it be accepted.

Dr. Richard Brey
Major Advisor

Dr. Jason Harris
Committee Member

Dr. Dewayne Derryberry
Graduate Faculty Representative

ACKNOWLEDGEMENTS

I would like to thank my advisor, Dr. Richard Brey for his guidance and advices on the topics of internal dosimetry and health physics in general. I would like to thank Takehito Hirayama for technical guidance in the use of SAAM II. I would also like to thank Eric Krage and Depesh Poudel for their guidance in the use of IMBA Professional Plus. I would like to thank my committee members Dr. Jason Harris and Dr. Dewayne Derryberry for their comments on my thesis.

TABLE OF CONTENTS

LIST OF FIGURES.....	vii
LIST OF TABLES.....	x
ABBREVIATIONS.....	xii
ABSTRACT.....	xiii
CHAPTER 1 INTRODUCTION.....	1
1.1 The Purpose of the Study.....	1
1.2 Hypothesis Statement.....	2
1.3 Overview.....	4
CHAPTER 2 LITERATURE REVIEW.....	6
2.1 Strontium Properties.....	8
2.2 Internal Contamination Pathway of Strontium.....	10
2.3 Absorption.....	12
2.3.1 Inhalation Exposure.....	12
2.3.2 Oral Exposure.....	12
2.3.3 Dermal Exposure.....	13
2.3.3.1 Ingestion.....	13
2.4 Distribution.....	14
2.4.1 Inhalation Exposure.....	14
2.4.2 Oral Exposure.....	14
2.4.3 Dermal Exposure.....	14
2.5 Total Absorption and Excretion via the Alimentary Tract Model.....	14
2.6 Strontium in Bone.....	16
2.7 Biokinetics of Strontium.....	18

2.7.1 ICRP 67 Systemic Model for Strontium.....	18
CHAPTER 3 MATERIALS AND METHODS	23
3.1 SAAM II	23
3.1.1 SAAM OPERATION.....	24
3.2 Total objective function.....	27
3.3 IMBA Software.....	31
3.4 IMBA Statistics.....	33
3.4.1 Maximum Likelihood Method.....	33
3.4.2 Chi-Square statistics.....	35
3.4.3 Autocorrelation Coefficient.....	36
CHAPTER 4 RESULTS AND DISCUSSION	38
4.1 Non-human Primates Data and SAAM II Predictions Results.....	38
4.2 Modification of Default Parameters based on Intravenously Injected Non- human Primates Data.....	54
4.3 Non-human Primates Data and IMBA Professional Plus Predictions.....	73
4.3.1 Chi-square and Autocorrelation Test Results.....	80
CHAPTER 5 SUMMARY AND CONCLUSIONS.....	91
CHAPTER 6 FUTURE WORK	95
REFERENCES.....	96
APPENDIX A.....	99
APPENDIX B.....	104
APPENDIX C.....	105

LIST OF FIGURES

Figure 1: ICRP 67 systemic biokinetic model for alkaline earth elements (ICRP, 1993).....	21
Figure 2: The Main screen of SAAM II and an example of two- compartment model.....	24
Figure 3: An example of a parameter window in SAAM II.....	25
Figure 4: An example of a data window in SAAM II.....	26
Figure 5: The screen shot of plot in SAAM II.....	27
Figure 6: Compartment model of ICRP 67 systemic model for strontium in SAAM II	30
Figure 7: The Main Screen of IMBA.....	31
Figure 8: Calculated Intake amount with Maximum Likelihood Method “best fit” ...	33
Figure 9: Case R7M, urine and feces are combined.....	39
Figure 10: Case R7M, urine and feces are separate.....	39
Figure 11: Case R8F, urine and feces are combined.....	40
Figure 12: Case R8F, urine and feces are separate.....	40
Figure 13: Case R9M, urine and feces are combined.....	41
Figure 14: Case R9M, urine and feces are separate.....	41
Figure 15: Case R33F, urine and feces are combined.....	42
Figure 16: Case R33F, urine and feces are separate.....	42
Figure 17: Case R34F, urine and feces are combined.....	43
Figure 18: Case R34F, urine and feces are separate.....	43
Figure 19: Case R29F, urine and feces are combined.....	44
Figure 20: Case R29F, urine and feces are separate.....	44
Figure 21: Case R50F, urine and feces are combined.....	45

Figure 22: Case R50F, urine and feces are separate.....	45
Figure 23: Case R51F, urine and feces are combined.....	46
Figure 24: Case R51F, urine and feces are separate.....	46
Figure 25: Case R52F, urine and feces are combined.....	47
Figure 26: Case R52F, urine and feces are separate.....	47
Figure 27: Case R61M, urine and feces are combined.....	48
Figure 28: Case R61M, urine and feces are separate.....	48
Figure 29: Case R191M, urine and feces are combined.....	49
Figure 30: Case R191M, urine and feces are separate.....	49
Figure 31: Scatter plots of the retention fraction of SAAM II prediction and measured values in skeleton.....	53
Figure 32: Strontium-90 retentions in feces predicted by the systemic model using default and geometric mean parameters respectively.....	67
Figure 33: Strontium-90 retentions in urine predicted by the systemic model using default and geometric mean parameters respectively.....	67
Figure 34: Strontium-90 retentions in soft tissue predicted by the systemic model using default and geometric mean parameters respectively.....	68
Figure 35: Strontium-90 retentions in skeleton predicted by the systemic model using default and geometric mean parameters respectively (short term).....	68
Figure 36: Model fitted activity of urine data using default and optimized parameter transfer.....	84
Figure 37: Model fitted activity of feces data using default and optimized parameter transfer.....	84
Figure 38: Model fitted activity of urine data using default and optimized parameter transfer.....	85
Figure 39: Model fitted activity of feces data using default and optimized parameter transfer.....	85

Figure 40: Model fitted activity of urine data using default and optimized parameter transfer.....	86
Figure 41: Model fitted activity of feces data using default and optimized parameter transfer.....	86
Figure 42: Model fitted activity of urine data using default and optimized parameter transfer.....	87
Figure 43: Model fitted activity of feces data using default and optimized parameter transfer.....	87
Figure 44: Model fitted activity of urine data using default and optimized parameter transfer.....	88
Figure 45: Model fitted activity of feces data using default and optimized parameter transfer.....	88

LIST OF TABLES

Table 1: List of Monkeys injected intravenously at Lawrence Berkeley Laboratory (LBL) from 1954 to 1982.....	7
Table 2: Present Natural Occurrence Radioactive Properties of Isotopes of Strontium (ASTDR, 2004).....	9
Table 3: Transfer rates for ICRP 67 biokinetic model for Strontium (ICRP, 1993)....	22
Table 4: An explanation of how the Chi-square test and autocorrelation coefficient are utilized together to assess model “goodness of fit”.....	37
Table 5: Summary of the retention fraction of SAAM II prediction and measured values in skeleton.....	52
Table 6: Summary of the modified transfer rates for each case with the default values described in ICRP 67 (COMBINED).....	56
Table 7: Summary of the modified transfer rates for each case with the default values described in ICRP 67 (COMBINED).....	58
Table 8: Summary of the modified transfer rates for each case with the default values described in ICRP 67 (COMBINED).....	60
Table 9: Summary of the modified transfer rates for some case with the default values described in ICRP 67 (Individually).....	62
Table 10: Summary of the modified transfer rates for some case with the default values described in ICRP 67 (Individually).....	64
Table 11: Summary of Geometric mean and GSD values along with the default values for systemic model for 21 non-human primates <i>using combined</i> urine and feces data.....	65
Table 12: Summary of Geometric mean and GSD values along with the default values for systemic model for 11 non-human primates <i>using separate</i> urine and feces data.....	66

Table 13: Differences in AIC values between default and optimized model.....	71
Table 14: The values of total objective function.....	72
Table 15: Measured and predicted intake values of Strontium activity using combined urine and feces data and the maximum likelihood method in IMBA Professional Plus.....	74
Table 16: Measured and predicted intake values of Strontium activity using combined urine and feces data and the maximum likelihood method in IMBA Professional Plus using optimized Parameter Transfer by SAAM II.....	75
Table 17: Measured and predicted intake values of Strontium activity using urine, feces data separately and the maximum likelihood method in IMBA Professional Plus.....	77
Table 18: Measured and predicted intake values of Strontium activity using urine, feces data separately and the maximum likelihood method in IMBA Professional Plus using optimized Parameter Transfer.....	78
Table 19: Chi-square and Autocorrelation test results for default parameters using combined urine and feces data.....	80
Table 20: Chi-square and Autocorrelation test results for Urine data.....	81
Table 21: Chi-square and Autocorrelation test results for feces data.....	82

LIST OF ACRONYMS AND ABBREVIATIONS

ICRP = International Committee on Radiation Protection

Sr = Strontium

SrCl_2 = Strontium chloride

SrTiO_3 = Strontium titanate

SAAM = Simulation, Analysis and Modeling

IMBA = Integrated Modules for Bioassay Analysis IMBA-PPAE

LBL = Lawrence Berkeley National Laboratory

AIC = Akaike Information Criterion

BIC = Schwarz-Bayesian Information Criterion

GSD = Geometric Standard Deviation

GeoMean = Geometric Mean

Pu = Plutonium

U = Uranium

**BIOKINETICS OF STRONTIUM-90 INJECTED IN NON-HUMAN
PRIMATES USING SAAM SOFTWARE AND IMBA
[PROFESSIONAL PLUS SOFTWARE**

Thesis Abstract - Idaho State University - 2014

This research was intended to examine the efficacy of systemic models for humans using measured non-human primate bioassay data obtained from studies by Durbin et al. Twenty-one non-human primates were injected with strontium and were observed for periods ranging 1 to 7,168 days. The retention activity of strontium in urine, feces and the skeleton was obtained. These data were evaluated using the SAAM II software in accordance with ICRP 67. Furthermore, eleven subjects were analyzed simultaneously and separately, and their Intake was evaluated using the IMBA software with default parameters and optimized parameters respectively. It was realized that the optimized parameter using SAAM II software provided good fits (based on the AIC criterion) between the measured and predicted retention values in urine, feces, and skeleton, while the default parameter underestimated the measured retention values. However, the chi-square test indicate that the default and modified parameters using IMBA provide good fits between measured injected activity and the predicted activity in urine and feces. For the default parameters, the fraction of predicted to measured intake activities varied between 0.523 and 2.29. While for the optimized parameters, the fraction of predicted to measured intake activities varied between 0.64 and 2.40.

(Work performed with partial support from funding from the National Institute of Allergy and Infectious Diseases under contract HHSN272201000046C)

CHAPTER 1: INTRODUCTION

1.1 The Purpose of the Study

The main purpose of this study was to investigate intravenously injected non-human primate bioassay data generated by Durbin et al. to test the effectiveness of the ICRP 67 systematic models for humans. A second purpose as appropriate was to optimize the ICRP 67 transfer rate coefficients for strontium. A tertiary goal of this study was to examine the efficacy of the model by applying the geometric means of a set of optimized parameters obtained using SAAM II software. This was done employing IMBA Professional Plus, and comparing predictions of the ICRP default parameters to the geometric mean of optimized parameters to determine which set of parameters produced better predictive capability.

1.2 Hypothesis Statement

First Null Hypothesis (H1,0): The ICRP 67 optimized model will not accurately predict the retention in excretion and skeleton using SAAM II software.

First Alternative Hypothesis (H1,a): The ICRP 67 optimized model will accurately predict the retention in excretion and skeleton using SAAM II software.

Decision Rule #1: The data is consistent with Alternative Hypothesis if it is determined that the AIC and total objective function values for optimized model are less than the values for default model. If the AIC and total objective function values are greater, the Null Hypothesis is supported.

Second Null Hypothesis (H2,0): The ICRP 67 default model and optimized model using IMBA software will not predict the excretion and deposition of ^{90}Sr from intravenously injected in Rhesus monkeys.

Second Alternative Hypothesis (H2,a): The ICRP 67 default model and optimized model using IMBA software will predict the excretion and deposition of ^{90}Sr from intravenously injected in Rhesus monkeys.

Decision Rule #2: The data is consistent with Alternative Hypothesis if the chi-square (p-value) is less than 0.05. If the p-value is greater than 0.05, the Null Hypothesis is supported.

Third Null Hypothesis (H3,0): The predicted ^{90}Sr intake of urine and feces data using default model and optimized model in IMBA software are significantly different from injected intake.

Third Alternative Hypothesis (H3,a): The predicted ^{90}Sr intake of urine and feces data using default model and optimized model in IMBA software are consistent with the injected intake.

Decision Rule #3: The data is consistent with Null Hypothesis if the difference between the predicted intake and injected intake is not arbitrarily within 20%. If the difference is greater than 20%, the Null Hypothesis is supported

Overview

1.3 Non-human Primates Studies

Durbin et al. engaged in a long-term study conducted between the years 1954 and 1983 on ^{90}Sr biokinetics in primates of the *Macaca mulatta*. The study was conducted in three different sites: Lawrence Berkeley Laboratory (LBL), the University of Rochester (UR), and the Delta Primate Center (Delta). The LBL study was in progress from 1954 to 1983, and studied 37 male and female monkeys that were all injected. The UR study was conducted between the years 1954 and 1964 before moving to the Delta facilities (1964-1968) studied 10 and 24 ^{90}Sr injected and fed monkeys respectively. In summary, a total of 71 both male and female, either ^{90}Sr injected or fed monkeys were studied. 61 out of 71 monkeys were ^{90}Sr injected while the rest (10) were ^{90}Sr fed age (Durbin et al, 1993).

Table 1 below summarizes the experimental treatments undertaken by Durbin et al. on 21 injected Rhesus monkeys and the amounts of activity injected intravenously. This study focused on the distributions of ^{90}Sr concentrations in injected monkeys as examined in blood plasma, excreta, and the whole body. With regards to the table (LBL series), the parameters that were analyzed on the 21 coded monkeys (from Case R7M to R191M) were: injection method, injection date, deaths (number of days a living post-injection), the number of days post-injection when serial blood sampling was conducted days when whole body counts commenced, and percent of ^{90}Sr in plasma otherwise whole blood. The days post-injection spanned from 1 to 7,168. Blood samples were drawn from thirteen monkeys regularly post-injection until death. Also, samples were drawn from five monkeys semiannually; however, this practice commenced at a later stage after injection. Whole-body counts were conducted for four monkeys, immediately

post-injection, and semiannually thereafter. Additionally, semiannual whole-body counts were recorded for six other monkeys; however, were started a few years post-injection whole body count analyses were based on a correlation of the bremsstrahlung radiation detected externally to that thought to be present in the animals. Bremsstrahlung radiation in this case generally arose from high velocity of beta radiation incident on mineral bone. The scope of this evaluation limited itself to the ^{90}Sr plasma, or whole blood concentration data observed in monkeys between 2 and 13.5 years of age (Durbin et al, 1993).

According to Durbin et al., the concentration of ^{90}Sr in plasma of an entire body of a monkey was obtained by the benefit of analysis radio technique. The percentage concentrations of ^{90}Sr ($\% \text{IDmL}^{-1}$) in the plasma/whole blood of a monkey were calculated using the data presented in Table 1. The weight of a monkey together with ^{90}Sr concentrations in a blood sample were the essential parameters considered. The results obtained were expressed as Sr ($\% \text{ID}$) in the entire plasma volume. The densities of plasma and whole blood used to compute these results used the values established for man specifically, a value of 1.027 g/ml was used for plasma while 1.058 g/ml was used for the entire blood. The total ^{90}Sr in blood plasma could only be obtained after establishing the total volume of plasma and/or the whole blood volume per unit weight of a monkey. As reported by Gregerson et al., after they considered a large population of monkeys (both sexes) with weights ranging from 3 to 7 kilograms it appears that plasma volume in monkeys is equivalent to 36.4 mL/Kg, the entire blood volume to 54.1 mL/Kg, and the hematocrit accounted for 0.66 mL/Kg. As for plasma samples, the formula below was used to calculate the Sr ($\% \text{ID}$):

$$\text{Plasma Sr (\%ID)} = 36.4 \times \text{BW} \times \text{\%ID (sample)} \times 1.027 \times w (\text{sample})^{-1} \quad \text{Equation 1}$$

Where: BW = the body weight.

If given sample a whole blood sample, the formula below was used to calculate the Sr (ID%):

$$\text{Plasma Sr (\%ID)} = 36.4 \times \text{BW} \times \text{\%ID (sample)} \times 1.058 \times w (\text{sample})^{-1} \times 0.66. \quad \text{Equation 2}$$

The body weight (BW) was measured in kilograms, and the sample weights were in grams (Durbin et al, 1993).

It is important to note that the entire monkey community in the LBL series underwent TB diagnosis semiannually. It was during this time that they were weighed, tranquilized, and blood samples obtained from their bodies. Additionally, their weights were measured and recorded as they being semiannually whole body counted. If data on body weight (BW) was omitted, then for the purpose of continuity the missing weight was estimated via extrapolation of two consecutive recorded weights (Durbin et al, 1993).

The data recorded on coded monkeys from the UR Delta group (i.e. case 301M to 374M) included: the group number or the case number of a monkey, the date when the monkeys were injected or fed with ⁹⁰Sr, the days to death after injection or feeding, the sites where the species died and the location where analysis radio happened, and the time post-injection or feeding when whole body counting was started. However, as mentioned previously, this review was limited to the ⁹⁰Sr concentrations in plasma and the whole blood of injected monkeys (Durbin et al, 1993).

Case No	Injection method	Injection date	Death (days post-injection)	Start day (blood)	Start day	
					(Whole body)	% ⁹⁰ Sr Body
R7M	iv	3/16/54	181	4	-	24.2
R8F	iv	4/11/54	3506	-	-	3.0
R9M	iv	4/16/54	2520	-	-	21.6
R10F	iv	8/8/55	94	-	-	44.4
R33F	iv	2/21/58	2278	1	-	6.5
R34F	iv	2/21/58	1921	1	-	15.4
R35F	iv	2/21/58	2040	1	-	-
R27F	iv	9/10/58	3159	0 ^e	-	11.3
R28F	iv	9/10/58	2087	0 ^e	-	16.1
R29F	iv	9/10/58	280	0 ^e	-	38.9
R32F	iv	10/27/59	7168	1	327t	5.9
R36F	iv	2/15/60	4	-	-	58.6
R37F	iv	2/15/60	1	-	-	45.3
R50F	iv	11/13/60	1212	-	-	24.6
R51F	iv	11/13/61	441	-	-	28.5
R52F	iv	2/25/61	21	-	-	53.4
R61M	iv	2/25/63	5372	497	2054	2.8
R62M	iv	9/25/63	5853	497	2054	1.2
R83F	iv	9/13/63	3411	287	1850	2.3
R188M	iv	9/9/69	2	-	-a	35.3
R191M	iv	8/8/70	16	0 ^e	-a	51.4

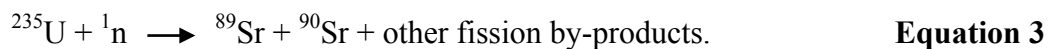
Table 1: List of Monkeys injected intravenously at Lawrence Berkeley Laboratory (LBL) from 1954 to 1982.

CHAPTER 2: LITREATURE REVIEW

2.1 Strontium Properties

Strontium is a vital chemical element found in Group II (II A) of the periodic table. Fundamentally, together with strontium, the entire members of this group including radium, barium, calcium, magnesium and beryllium among others have a common atomic structure that make them members of this group (alkaline earth metals). These members have two electrons on their outer energy level hence the name Group II. On the periodic table, strontium occupies a central position in the group. Strontium is more reactive than all the members above it in the group (e.g. beryllium, magnesium and calcium), and less reactive than all the members that come below it in the group e.g. barium.

The elemental strontium has an atomic number of 38 and an atomic mass of 87.62 amu, and can exist either at 0 or +2 oxidation states. Under ideal environmental conditions the later oxidation state is steady enough vital for practical use since its reaction with both water and oxygen is feasible. Strontium boasts a total of 26 isotopes of which 4 happen naturally. The naturally occurring isotopes including: ^{84}Sr (0.56%), ^{86}Sr (9.86%), ^{87}Sr (7.0%) and ^{88}Sr (82.58%), are the only stable isotopes, the rest are artificial synthesized isotopes and Sr-90 are a consequence usually radioactive. Of great importance in radiology are the isotopes ^{89}Sr and ^{90}Sr . These emanate from a nuclear fission process of radioactive isotopes (^{239}Pu , ^{235}U or, ^{238}U) after bombardment with a high-energy neutron. This process is depicted by the below nuclear equation:



These two radioactive isotopes are both human health concern owing to their potential carcinogenicity. Nevertheless, between the two isotopes ^{90}Sr is the more radiotoxic due to its relatively long half-life (twenty-nine years). ^{90}Sr 's half-life dwarfs ^{89}Sr (51 days) by more than 200 folds. Unlike other radioactive isotopes, strontium decays by isobaric transition emitting a negatron together with the creation of a progeny product Y-90. The table below provides a summary of the radiological properties of the various strontium isotopes (ASTDR, 2004)

Isotope	CAS registry number	Natural abundance (by weight %)	Beta energies, MeV	Half-life	Activity, Ci/gram
^{84}Sr	15758-49-3	0.56	No data	Stable	No data
^{85}Sr	13967-73-2	No data	1.065 ^a	65 days	35,400
^{86}Sr	13982-14-4	9.86	No data	Stable	No data
^{87}Sr	13982-64-4	7.00	No data	Stable	No data
^{88}Sr	14119-10-9	82.58	No data	Stable	No data
^{89}Sr	14158-27-1	No data	1.495	51 days	27,800
^{90}Sr	10098-97-2	No data	0.546	29 years	143
^{91}Sr	14331-91-0	No data	2.707	10 hours	3.4×10^6
^{92}Sr	14928-29-1	No data	1.911	3 hours	1.1×10^7

Table 2: Percent Natural Occurrence and Radioactive Properties of Isotopes of Strontium (ASTDR, 2004).

2.2 Internal Contamination Pathway of Strontium

Currently, anthropogenic activities involving nuclear technology release negligible amounts of ^{90}Sr to the environment and, therefore, do not raise much concern (EPA, 2002). However, the little Sr released can be incorporated into food substances and converted into part of the food chain. Nuclear weapons testing in the mid twentieth century led to the emission of significant amounts of environmental radiostrontium. This was evident from the substantial drop in environmental concentration of ^{90}Sr after the atmospheric test ban treaties. However, the suspension of atmospheric nuclear testing did not eliminate environmental Sr emissions because releases from nuclear plants and from other plants of the nuclear fuel cycle may occur. Apart from weapon facilities, plants that reprocess fuels may contribute to the environmental source term of Sr. As may the utilization of nuclear fission at research reactors and nuclear power plants may lead to Sr-90 releases into the environment.

The Chernobyl accident led to the emission of substantial quantities of radioactive ^{90}Sr to the environment. Both local and global ^{90}Sr concentrations were observed as an aftermath of the Chernobyl accident.

Historically the key route of entry of ^{90}Sr into the human body was arguably through the ingestion of polluted water and food substances. Contaminated air, in addition, may lead to the uptake of radiostrontium in humans. This occurs either when Sr particles that have been adsorbed on dust particles are inhaled or when Strontium oxides are inhaled. However, the hazards associated with ingestion of contaminated food seem to surpass those related to the inhalation of contaminated air (EPA, 2002). Approximately twenty to thirty percent of the ingested ^{90}Sr is absorbed in the gut following the intake of

^{90}Sr -contaminated food while the remaining fraction is excreted (EPA, 2002). Nearly all of the absorbed ^{90}Sr goes to the bones or the skeletal tissues while the rest is disseminated to the peripheral tissues such as blood, soft tissues, extracellular fluids, as well as the surface of the bones. The ^{90}Sr can stay for extended periods of time in these tissues. When eventually excreted it is expelled in urine or feces (EPA, 2002).

As mentioned earlier, ^{90}Sr 's key route of entry into the human body is through its incorporation into the food chain. This occurs when grass grows on ^{90}Sr -contaminated soil. Cows feed on this grass and the strontium becomes absorbed into the cows' gastrointestinal tract and later on passes into milk. The consumption of such milk, therefore, leads to the introduction of radioactive Sr into the human body. Strontium, a radioactive substance decays into ^{90}Y , which is a transitory decay product. Y-90 undergoes a beta decay releasing energy of approximately 0.93 MeV that plays a vital role in the internal dose of ^{90}Sr . ^{90}Sr is a chemical congener of calcium thereby, making it a suitable candidate for absorption mechanisms that are similar to calcium. Consequently, Sr-90 is absorbed, metabolized and integrated into plant and animal tissues. During female lactation, ^{90}Sr that was already incorporated into milk passes a great danger to breastfeeding children. Such children have high chances of developing leukemia and cancer of the bones because of the partial substitution of calcium by strontium in their developing bones (Washington State Department of health, 2002)

Urinalysis is the main method of establishing the levels of strontium in the body. However, the accuracy of the test is higher when taken immediately after the intake than when measured some time after the intake (EPA, 2002). In sum, there are five internal contamination pathways of strontium: inhalation, ingestion, injection, and absorption.

2.3 Absorption

2.3.1 Inhalation Exposure

There is ample evidence from case studies of accidents that Sr-90 may be taken into the body by inhalation. These cases do not provide a clear quantitative account of the absorption of inhaled Sr in humans, but the discovery of radiostrontium in feces and urine undoubtedly reveals that the inhalation of radiostrontium leads to its absorption in the body (ATSDR, 2004).

Animal studies particularly in dogs reveal that the chemical form of the inhaled strontium greatly influences the rate of absorption. Complexes with a high solubility such as SrCl_2 undergo rapid clearance from the lungs. The nasopharyngeal section of the respiratory tract appears to be responsible for the absorption of soluble strontium. An experiment by (Cuddihy and Ozog, 1973) observed that 67% of Sr administered as $^{85}\text{SrCl}_2$ to the nasal tract of hamsters was absorbed within the first four hours. Another 63% was absorbed into the nasopharynx (ATSDR, 2004).

2.3.2 Oral Exposure

The fractional absorption of ingested strontium administered to healthy subjects as SrCl_2 in food was investigated by ATSDR. They compared quantitatively the strontium concentration-time profiles from subjects who had ingested strontium and those who had intravenous injections of strontium. They considered the bioavailability of Sr in the body following different routes of administration. Another approach compared the amount of Sr ingested to that excreted in feces. These studies observed that about 20% of the ingested Sr was absorbed in the alimentary canal (ATSDR, 2004).

A difference in the absorption of Sr with changes in the age of the subjects is a phenomenon that is frequently observed in rat studies. No human data on this changing Sr absorption rates in humans exists. However, owing to this observation in animal models and similarities with humans, it is suggested that there is a likely increase in Sr absorption during the neonatal period in humans. During the rest of the human life cycle, just as in various animal models, it is thought the fraction of ingested Sr is constant, at around 20% (ATSDR, 2004).

2.3.3 Dermal Exposure

The experimental data on the dermal exposure to compounds containing Sr does not give conclusive evidence of systemic toxicity. This implies that there is poor absorption of Sr from the surface of the skin. However, the integrity of the skin tissues determines the extent of absorption. An experiment by Ilyin et al. in 1975 demonstrated that scratched skin allows more absorption than intact skin (ATSDR, 2004).

2.3.3.1 Ingestion

It is possible for strontium to be transmitted across the placenta in a pregnant female animal and in human subjects. However, only one study demonstrates Sr transfer across the placenta following inhalation where an intratracheal dose of ^{89}Sr is given to rats at two weeks of gestation. But there were insignificant differences in Sr absorption rates in the fetuses of control and experimental rodents. . In addition, Sr gets into human mammary glands and can be conveyed to infants during lactation (ATSDR, 2004).

2.4 Distribution:

2.4.1 Inhalation Exposure

There is insufficient information regarding the dispersal of inhaled Sr in humans. Nevertheless, it can be assumed that inhaled strontium and ingested strontium are distributed in a similar manner (ATSDR, 2004).

2.4.2 Oral Exposure

The dispersion of orally ingested Sr mimics calcium absorption with nearly all of the ingested Sr ending up in the bones. This is evident from autopsy reports of human bone samples, which reveal that Sr absorption is a half of the normal Ca absorption (ATSDR, 2004).

2.4.3 Dermal Exposure

Dermal exposure to strontium as $^{85}\text{SrCl}_2$ gets into the patella three hours after exposure. The same Sr takes about six hours to be detected in the forearm suggesting that dermal exposure ultimately leads to absorption in the bones (ATSDR, 2004).

2.5 Total Absorption and Excretion via the Alimentary Tract Model

Several aspects including the level of glucose present in blood and the nutritive value of food modulate the absorption of strontium in human bodies. The presence of minerals such as calcium, phosphorous and magnesium tend to escalate the rate of Sr absorption by the tissues. Diets containing high proportions of milk constituents and vitamin D raise Sr absorption. Fasting plays a vital role in influencing the concentration of glucose in blood and the rate of Sr absorption. Studies by McAughey et al. observed that an all night fast doubles the absorption of Sr. This observation is evident after

comparing the Sr absorption of four subjects who ingested Sr-containing substances after fasting with the absorption of an individual who ingests Sr after taking breakfast. A three-fold reduction of calcium intake causes a two-fold increase in Sr absorption.

A comparison of animal and human data on Sr absorption gives similar outcomes. However, when Sr is administered to rodents as a titanate (SrTiO_3) the rate of absorption is relatively low and gives a rate of 0.01 in contrast with the rate of 0.1 when Sr is issued as SrCl (Métivier, et al, 2004).

Age is thought to play a role in the absorption of Sr. A study by Widdowson et al. in 1960 revealed that the rate of Sr absorption in infants was extremely high at a level of 0.7. It is possible that milk, which is the key diet in infants, contributes to the high levels of Sr absorption since milk rich diets elevate Sr absorption. However, in children between the ages of five and fifteen the rate of Sr absorption is similar to that in adults. Rodent experiments, in addition, reveal an absorption rate of 0.95 in 2-week old rats. Conversely, the absorption values decline to about 0.74 in a sample of five 22-days old rats. Therefore, it can be concluded from these two experiments that Sr absorption declines with an increase in the age of the subject. The probable reason for the high absorption rates in infants is that there is no delay in the transfer of the absorbed Sr to blood. This is because of minimal retention of Sr in the walls of the small intestines (Métivier, et al, 2004).

A systemic biokinetic prototype for alkaline earth metals unequivocally replicates the excretion of Sr through the gastrointestinal tract. The dispensation of radiostrontium through an intravenous injection shows that a quarter of the injected Sr is exuded into the alimentary canal thereby contributing to the endogenous loss of Sr. Excretion through

bile accounts for a tiny fraction of the entire secretion of Sr into the alimentary canal. The ICRP biokinetic model for strontium displays the systemic secretion of Sr as the transfer of blood plasma to the constituents of the large intestines in the upper region of the alimentary canal. This is a simplified version of the whole process, which clearly explains the movement of Sr in biological systems (Métivier, et al, 2004).

2.6 Strontium in Bone

Several studies reveal that the rate of uptake and elimination of different types of radionuclides are greatly influenced by the age of the subject. This is also true for the uptake of strontium in human body as observed from the examination of thousands of human skeletons. It is essential to develop dosimetric models that include the relationship between age and the uptake of the various Sr isotopes in different physical and chemical form (Leggett et al. 1982).

Strontium and calcium experience similar metabolism. The bone, which is the main calcium store, is partitioned into two key sections. These are the structural bone that carries out motorized roles and the metabolic bone that controls calcium quantities in the extracellular fluids. This model relies on the fact that the skeleton comprises three compartments, two of which are coupled with the structural bone (bone volume) and the other compartment that is connected to metabolic processes (surface bone). The bone volume further consists of three vast parts that are soft, compact and hard bone. This model assumes that these three compartments are present during all life stages, but their metabolism differs at various life stages (Leggett et al. 1982).

Increases and reductions of calcium by the bone volume significantly affect the metabolism of Sr. The cortical bones (compartment 1) and the cancellous bones (compartment 2) have little differentiation in terms of structure and function in young people. Therefore, there are no disparities in their uptake and retention of Sr. However, as a person grows old, there are distinct dissimilarities between these two compartments in terms of their Sr uptake and retention. It is thought that the body cannot distinguish between Ca and Sr during metabolism due to their similarities. However, there is a facet of discrimination of Sr before it reaches the skeleton, which is accounted for by the formula $k(t) = 0.7 \exp(-1.2t) + 0.2$ where 't' is age, and 'k' is the bias aspect (Leggett et al. 1982).

Skeleton age greatly affects bone behavior. Young bones have a rich blood and water supply that makes them extremely dynamic. Old bones are much more static in nature because of nearly complete mineralization. Regardless of this change associated with age, the bone proportion available for exchange of calcium remains constant throughout the developmental process. Strontium elimination from bones is the same as calcium removal, which increases with increasing age due to the natural aging process that causes bone loss. The radioactive decay process of about 0.025 annually also contributes to Sr loss. Compact bone and cancellous bones show different Sr removal rates with cancellous bone having a lower rate than compact bone. The product of the discrimination factor and the fraction of calcium that is absorbed by the bones is the proportion of Sr that is ultimately retained by bones (Leggett et al. 1982).

2.7 Biokinetics of Strontium

2.7.1 ICRP 67 Systemic Model for Strontium

The ICRP 67 model is a radionuclide based systemic demonstration of how various alkaline earth metal elements are thought to translocate while inside the human body. The common metallic elements to which the model applies include radium, lead, barium, uranium, and barium. The ICRP model assumes that blood plasma contains a uniform concentration of calcium. However, this is not practically true since in human body tissues, calcium exists both in ionic and solid forms. ICRP does not include the red blood cells (RBC) because the cells do not react with the alkaline earth metals (Leggett et al. 2008)

The demonstration of the rates of intake and retention of strontium and calcium have been demonstrated through radio-calcium experiments. Such experiments demonstrate that on average 0.35 percent of the total radio-calcium intake into an adult body diffuses into the soft tissues. Plasma retains 0.03 percent of the total adult body calcium content. Generally the soft tissues are classified into three sections. These sections include an intermediate turnover section (ST1), a rapid turnover section (ST0) and, a slow turnover section (ST2). The ST0 body calcium content is about 0.09 percent, while that of ST1 is approximately 0.26 percent. The concentration of the calcium ST0 section is determined by the deposition percentage (F) and the associated half-time (T). A sufficient period to investigate ST0 calcium diffusion is thought to be about 124 days post injection after which various ca/sr ratios change (Leggett et al. 2008).

An ST2 section in the ICRP model represents non-absorbable calcium due to tissue dystrophic calcification. Usually, the ST2 is characterized by low absorption of calcium from the plasma within 124 days after the injection. The test of ST2 is carried out through manipulation of F and elimination of T using different elements. An experiment on radio-strontium absorption and retention was carried out on ailing patients just before they died. The experiment revealed that initially the bones and the soft tissues had an almost equal proportion of strontium (Leggett et al. 2008).

Modes of strontium kinetics in the soft body tissue are usually based on comparison of strontium retention in the soft tissue with that of the calcium. The method assumes that the rate of calcium and strontium deposition percentage is equal. Schlenker et al. asserts that approximately 1% of the total strontium consumed is retained in the soft tissues. The ST0 section of the model contains soluble calcium and the interstitial fluid. ST1 contains slowly soluble calcium like dystrophic, mitochondria, and cartilage calcium, ST2 section contains deposits of calcium. The ICRP model does not consider the kidney and the liver as part of soft body tissues (Leggett et al. 2008).

The ICRP 67 model divides the bone structure into trabecular and cortical sections. Each of these parts is further divided into bone volume and surface subsections (Figure1), bone volume is composed of soluble and insoluble pools. The bone surface is responsible for skeleton deposition. After some time, a part of the bone surface diffuses into the soluble bone volume while the rest diffuses to the plasma. It is believed that bone surface can only be recovered from the bone through bone desorption. The rate of elimination of bone surface from the insoluble bone volume is age dependent but not subject to the elements used (Leggett et al. 2008).

An experiment to investigate the absorption and maintenance of the strontium content in the bone was carried out on incurably patient (Leggett et al. 2008). The results of the experiment supported general observations that there exists great variation of strontium in the patients' bodies at different age groups. The experiments further showed that the bone - rebuilding rate is higher for individuals below the age 25 compared to the older individuals. This is because the rate of calcium deposition is higher at younger age than at old age. Consequently, the strontium retention rate is elevated in younger adult compared to elderly people. Research indicates that the rate of deposition of radium, barium, and strontium are similar in the first few hours after injection for skeleton, trabecular, and cortical bones for all elements (Bligh and Taylor 1963; Kshirsagar et al. 1966; Domanski et al. 1969, 1980). It is argued that about 25% of radium, barium, or strontium diffusing out of the plasma in an adult is deposited on the bone surface (Leggett et al. 2008).

The rate of deposition of alkaline earth metals on the either cortical or trabecular surfaces depends on calcium intake in either bone type. The deposition rate in Trabecular bone is 1.25 times higher than that of cortical bone (Leggett et al. 1982). Nevertheless, the average deposition time of alkaline earth metals is not exactly known. Several experiments have demonstrated that the rate of activity turnover is larger in calcium, strontium, and barium in that order. The alkaline earth elements are excreted from the body through faeces and urine. Equally, the rate of element excretion depends on the age of the subject and length of the element intake (Leggett et al. 2008).

Figure 1 illustrates the human biokinetic model for alkaline earth elements, especially for strontium. While Table 3 provides the transfer rates for the ICRP 67 strontium model.

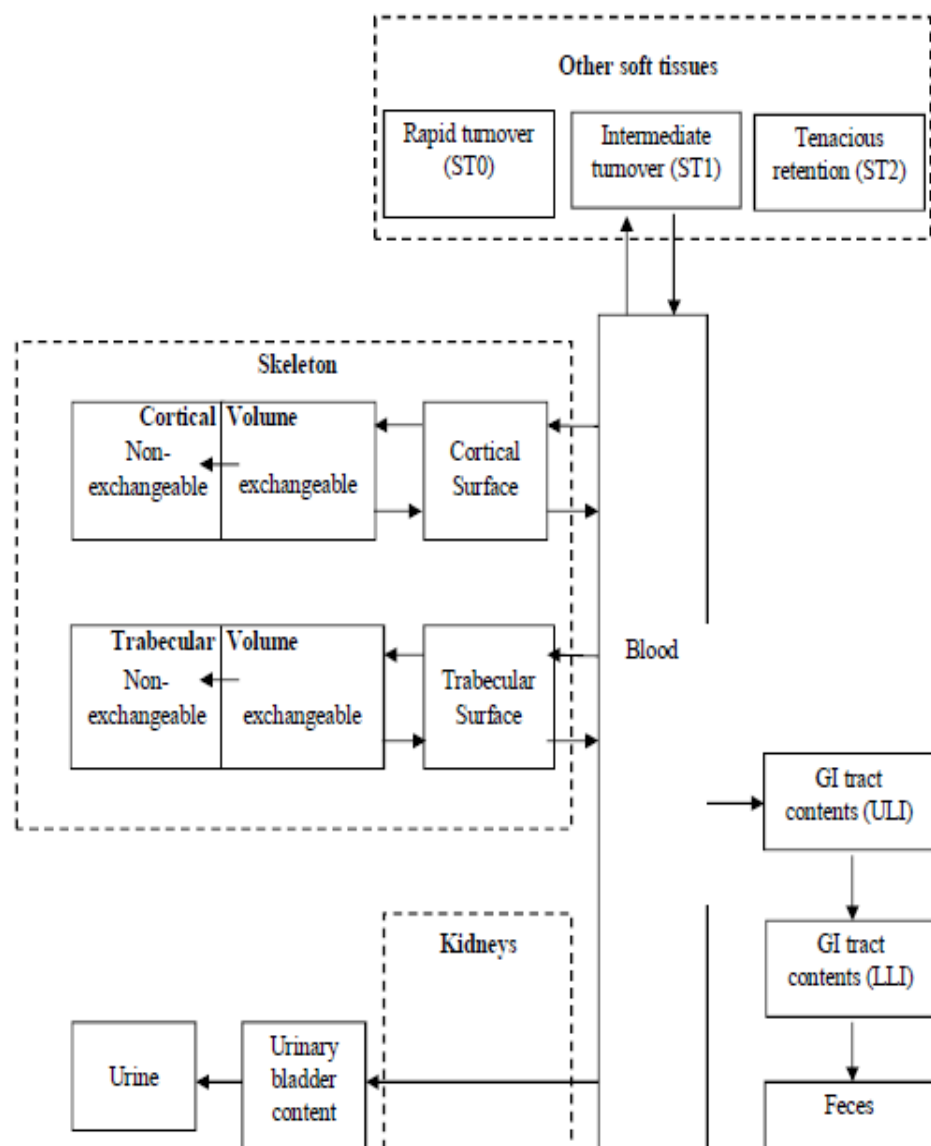


Figure 1: ICRP 67 systemic biokinetic model for alkaline earth elements (ICRP, 1993)

Rote of transfer between Compartments	Transfer rate (d ⁻¹)
Plasma to ST0	7.500
Plasma to Urinary bladder contents	1.730
Plasma to G.I. tract contents	0.525
Plasma to ST1	1.500
Plasma to ST2	0.003
Plasma to Trabecular Surfaces	2.080
Plasma to Cortical Surfaces	1.670
ST0 to Plasma	2.500
ST1 to plasma	0.116
ST2 to plasma	3.8×10^{-4}
Cortical Surface to Cortical exchangeable Vol.	0.116
Bone Surfaces to plasma	0.578
Non-exchangeable Trabecular Vol. to Plasma	4.93×10^{-4}
Non-exchangeable Cortical Vol. to Plasma	8.21×10^{-5}
Trabecular Surface to Trabecular exchangeable Vol.	0.116
Exchangeable Cortical bone vol. to Cortical Surface	4.3×10^{-3}
Exchangeable Trabecular bone vol. to Trabecular Surface	4.3×10^{-3}
Exchangeable Cortical bone vol. to Non-exchangeable cortical vol.	4.3×10^{-3}
Exchangeable Trabecular bone vol. to Non-exchangeable Trabecular vol.	4.3×10^{-3}
Urinary bladder contents to Urine	5.000
G.I. tract contents to Feces	1.000

Table 3: Transfer rates for ICRP 67 biokinetic model for Strontium (ICRP, 1993)

CHAPTER 3: MATERIALS AND METHODS

3.1 SAAM II

The software that was used in this study was SAAM version II* (University of Washington). SAAM II, which means simulation, analysis, and modeling software II, is a pharmacokinetic analysis software package designed for studies of radioactive experiments. The software is very popular among biomedical and bioengineering experts. SAAM II is a dominant instrument in research, education, and project development (Barrett, 1998).

The system provides help for the biomedical problems and services through consultation on the use of the software analysis. With the help of the software, an individual can design compartmental representations, simulate experiments on these representations, and analyze data (SAAM II help)

Urine and fecal bioassay data for Sr-90 were analyzed simultaneously (and separately for eleven cases) using SAAM II software, which employed the default parameters as exemplified in the ICRP 67 to estimate the retention values in urine, feces and skeleton. The multi compartment models were created on the drawing canvas based on the ICRP 67 systemic model. In addition, the excretion and skeleton data were employed in the optimization process with the aid of the Bayesian method available in SAAM software.

* University of Washington

3.1.1 SAAM II OPERATION

The user can design the model using a compartmental application method, which uses either by differential equation or numerical application method in analyses. These approaches allow the user to enter an algebraic equation directly. SAAM II is designed in such a way that it can generate a system of differential equations automatically for each model in use. The user should identify an experiment on a model by selecting from a number of experimental building objects that are illustrated as inputs and outputs. After the user identifies the experiment, SAAM II works out and fits the model to the data (SAAM II help).

The model shown below is used in illustrating the main parts of SAAM II's model construction capability, describing its attributes, developing trials and basic operations such as working out, fitting, and viewing solutions.

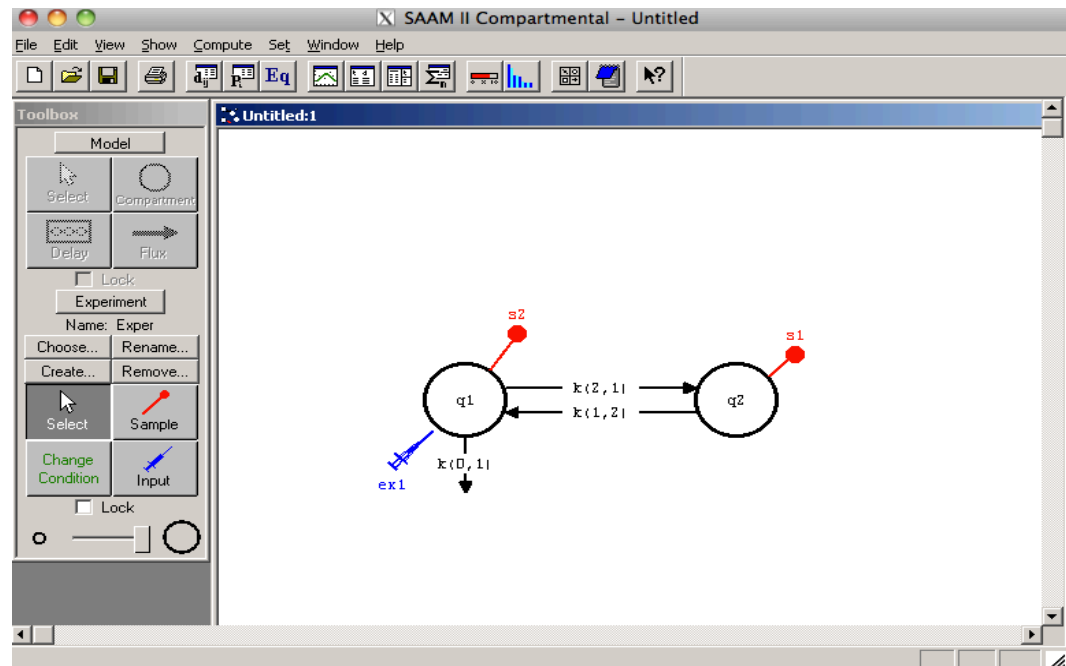


Figure 2: The main screen of SAAM and an example of two- compartment model

Figure 2 shows the main screen of SAAM II along with a two compartmental model containing an essential plasma compartment and a swap compartment. The SAAM II principle for the transfer coefficients is represented as $k(i, j)$ -k (to, from). Based on this illustration, $k(i, j)$ is the transfer rate to compartment i from compartment j . The EX1 is an experiment generated in the model through which the exogenous input in it is stated directly. The input type was bolus and the initial amount was 100 corresponding to 100 % of initial activity. S1 stands for a sample site (SAAM II help).

An important facet of SAAM II is parameter window; an example of parameter window is illustrated in Figure 3 below. The user is free to modify the parameter's type value. For this study the Bayesian option was chosen. When the Bayesian option is selected, mathematical functions such as population mean and SD will be computed (SAAM II help).

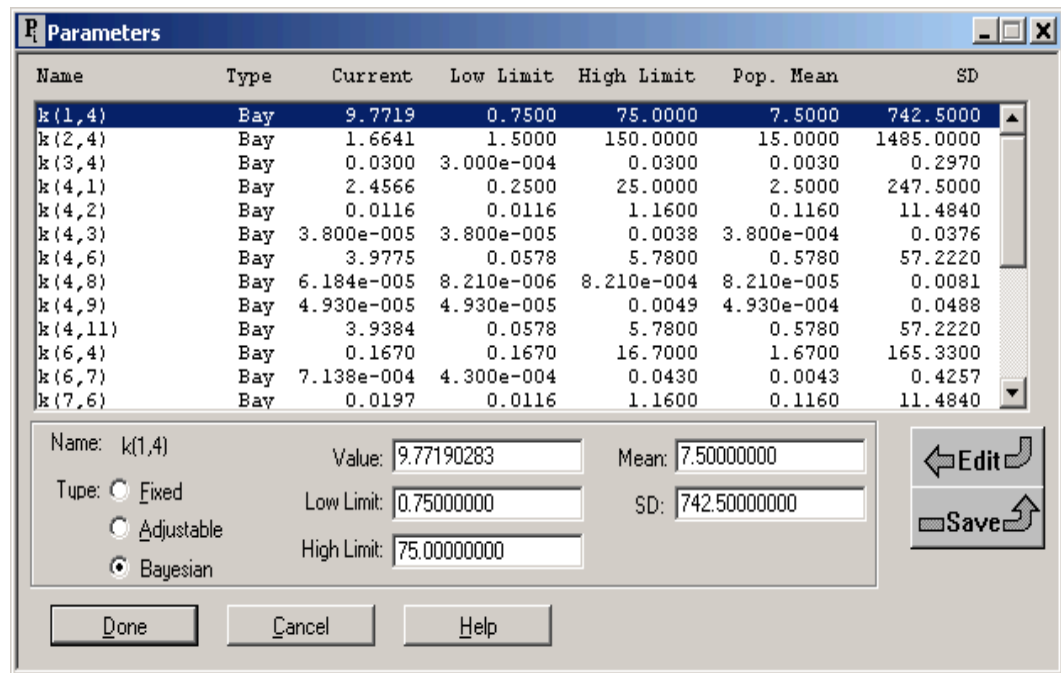
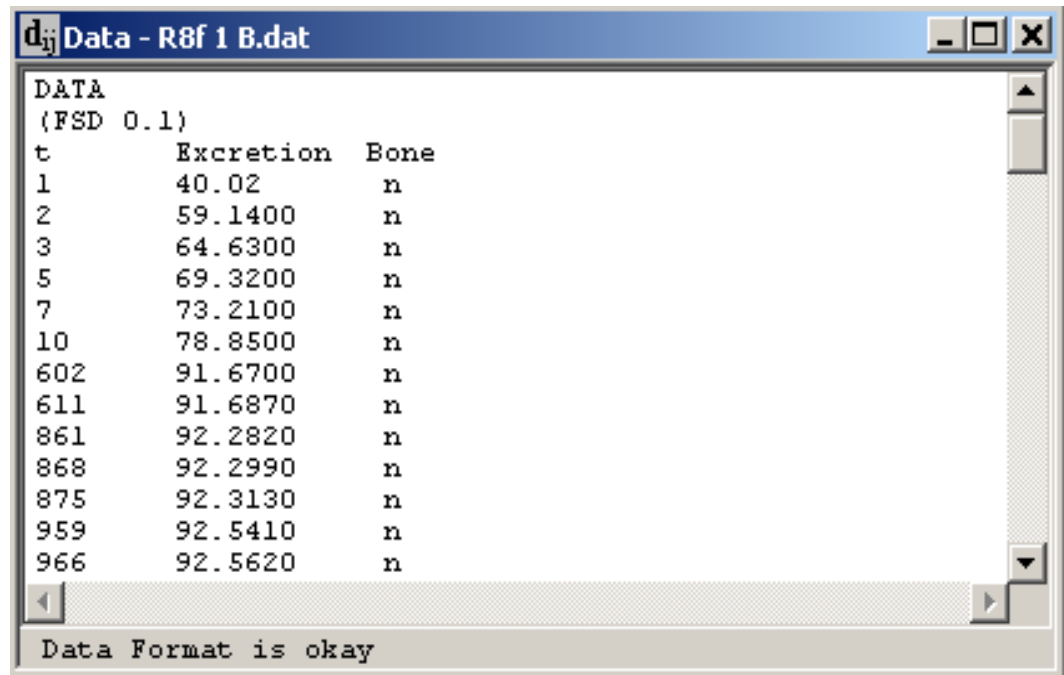


Figure 3: An example of a parameter window in SAAM II

Another important facet of SAAM II is data window. Data window utilizes tables in a specific format, which enables combinations of values for bioassay measurement data such as Excretion and Skeleton. An example of data window is shown in the Figure 4 below (SAAM II help).



The screenshot shows a window titled "Data - R8f 1 B.dat". Inside the window, the text "(FSD 0.1)" is displayed above a table. The table has three columns: "t", "Excretion", and "Bone". The data rows show time points (t) and corresponding values for Excretion and Bone. The Bone column contains the letter "n" for all entries. A status bar at the bottom of the window displays the message "Data Format is okay".

t	Excretion	Bone
1	40.02	n
2	59.1400	n
3	64.6300	n
5	69.3200	n
7	73.2100	n
10	78.8500	n
602	91.6700	n
611	91.6870	n
861	92.2820	n
868	92.2990	n
875	92.3130	n
959	92.5410	n
966	92.5620	n

Figure 4: An example of a data window in SAAM II

With the Plot command, SAAM II provides extended plotting abilities. This helps the user to create a plot for numerous variables; also the user can alter the plot scale settings and limit them. An example of plot is illustrated in Figure 6 below (SAAM II help).

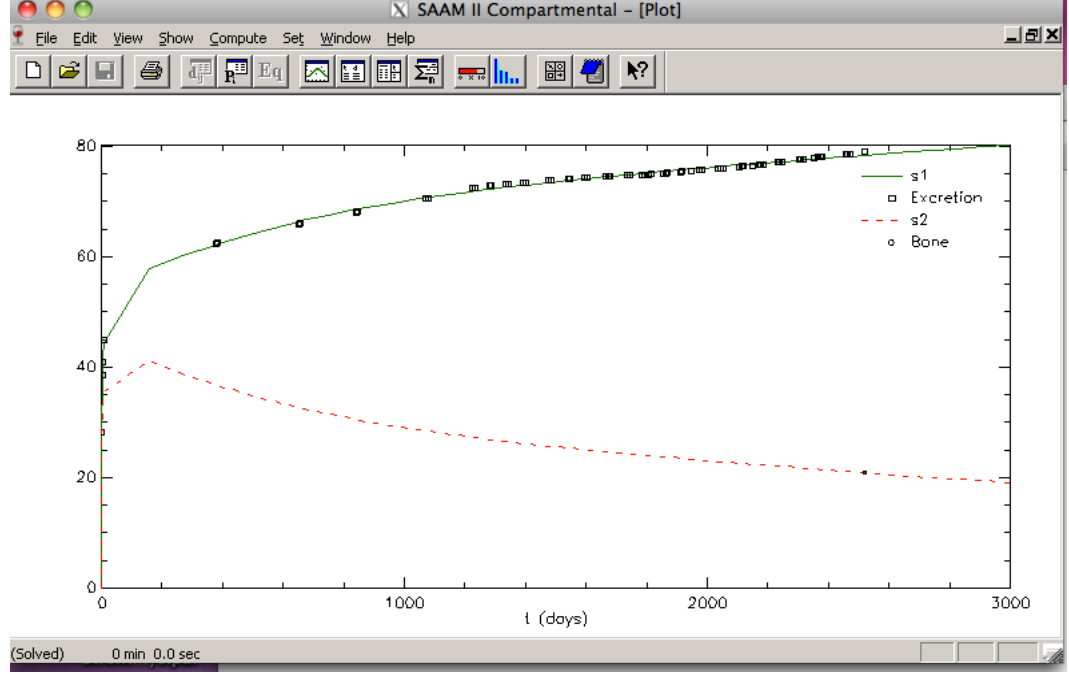


Figure 5: The screen shot of plot in SAAM II

3.2 Total objective function

The total objective function is reduced during the process and the two information criteria. Akaike information criterion, and the Schwarz-Bayesian information criterion can be used in the evaluation process of the model order. In order to attain the best fit, SAAM II should reduce the objective function as indicated in the equation below.

$$R(p) = \frac{1}{M} \left\{ \sum_{j=1}^j \sum_{i=1}^{Ni} \left(\log \left[v_{i,j}(s(p, t_{i,j}), v_{i,j}, \hat{v}_j) \right] + \frac{(y_{i,j} - s(p, t_{i,j}))^2}{v_{i,j}(s(p, t_{i,j}), y_{i,j}, \hat{v}_{i,j})} \right) + \sum_{k=1}^{Nb} \frac{(p_k - m_{p,k})^2}{\sigma_{p,k}^2} + \log(\sigma_{p,k}^2) \right\}$$

Where:

Equation 4

p = the vector of adjustable parameters

R(p) = the objective function, $y_{i,j}$ is the i th datum in the j th data set

$S(p, t_{i,j})$ = the model value (a sample in the compartment module)

v_j = the variance parameter in the j th data set

$V_{i,j}(s(p_{i,j}), y_{i,j}|v_i)$ = the variance model for $y_{i,j}$

J = the number of data sets N_j = the number of the data points in the data set

M = the total number of the data points

$\mu_{p,k}$ = the mean value of p_k over a group of similar subjects (population mean)

$\sigma_{p,k}$ = the standard deviation of p_k in that population

The Akaike information criterion as compared to other related methods offers efficient methods of the relative goodness of fit of a statistical model. This criterion was suggested by Hirotugu Akaike during the early 1970's. The criterion is normally defined using Equation 5.

$$AIC = -2\log(L) + 2K \quad \text{Equation 5}$$

Where: L = the log of the maximized likelihood

K = the number of estimable parameters (Burnham and Anderson, 2002).

Akaike information criterion values are a relative scale and are strongly dependent on sample size. This approach evaluates the relative distance of the likelihood function described by a fitted candidate model from the unknown true likelihood function that generated the data. AIC is generally positive, nevertheless, when an additive constant shifts values, a negative value is obtained. AIC difference values are easy to illustrate and permit a quick evaluation and rating of candidate models. The AIC difference is defined using Equation 6.

$$\Delta_i = AIC - AIC_{\min} \quad \text{Equation 6}$$

Where:

Δ_i = the AIC differences

AIC = the AIC value of the i th model

AIC_{\min} = the smallest AIC value among all candidate models (Burnham, 2002).

It is deemed that those models with $\Delta_i \leq 2$ have significant support, models with values of $4 \leq \Delta_i \leq 7$ have considerably less support and models with $\Delta_i > 10$ do not have the necessary support (Burnham and Anderson 2002).

The ICRP 67 systemic model for Strontium was generated with the aid of SAAM II as shown in Figure 6 below. The transfer rates listed in ICRP 67 have been assigned in each route between compartments.

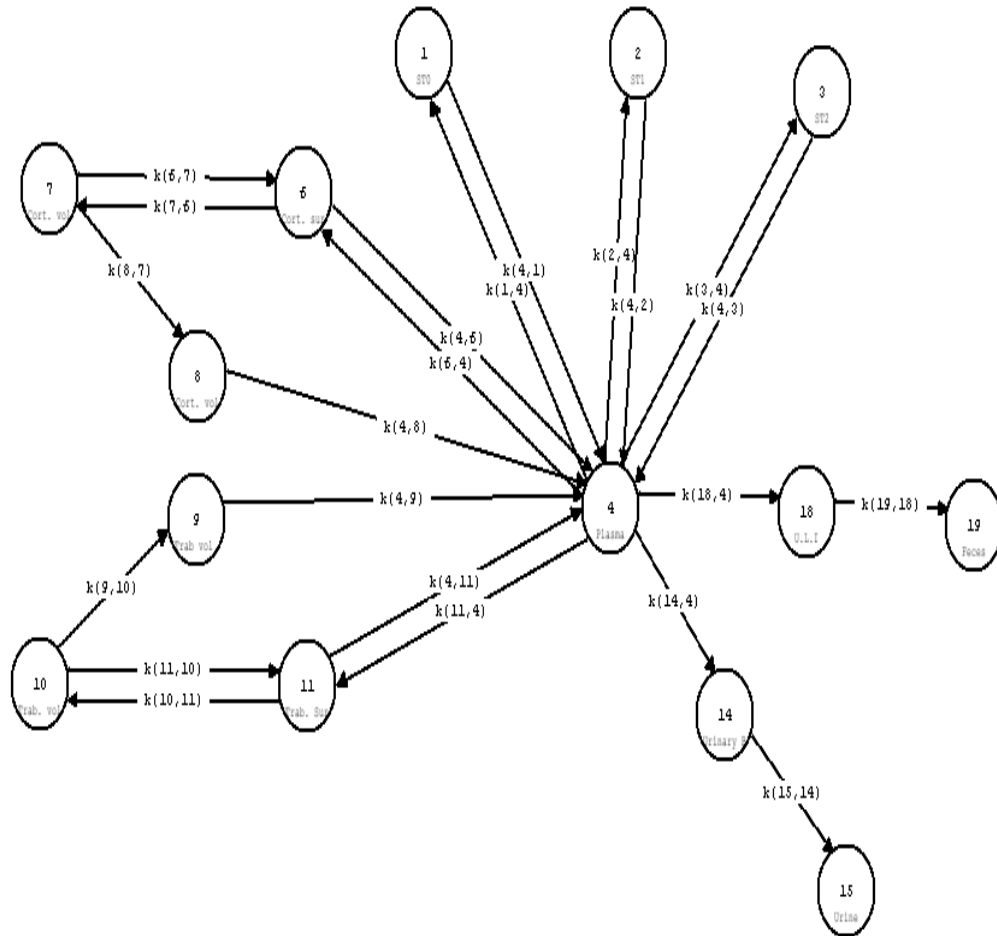


Figure 6: Compartment model of ICRP 67 systemic model for strontium in SAAM II

3.3 IMBA Software

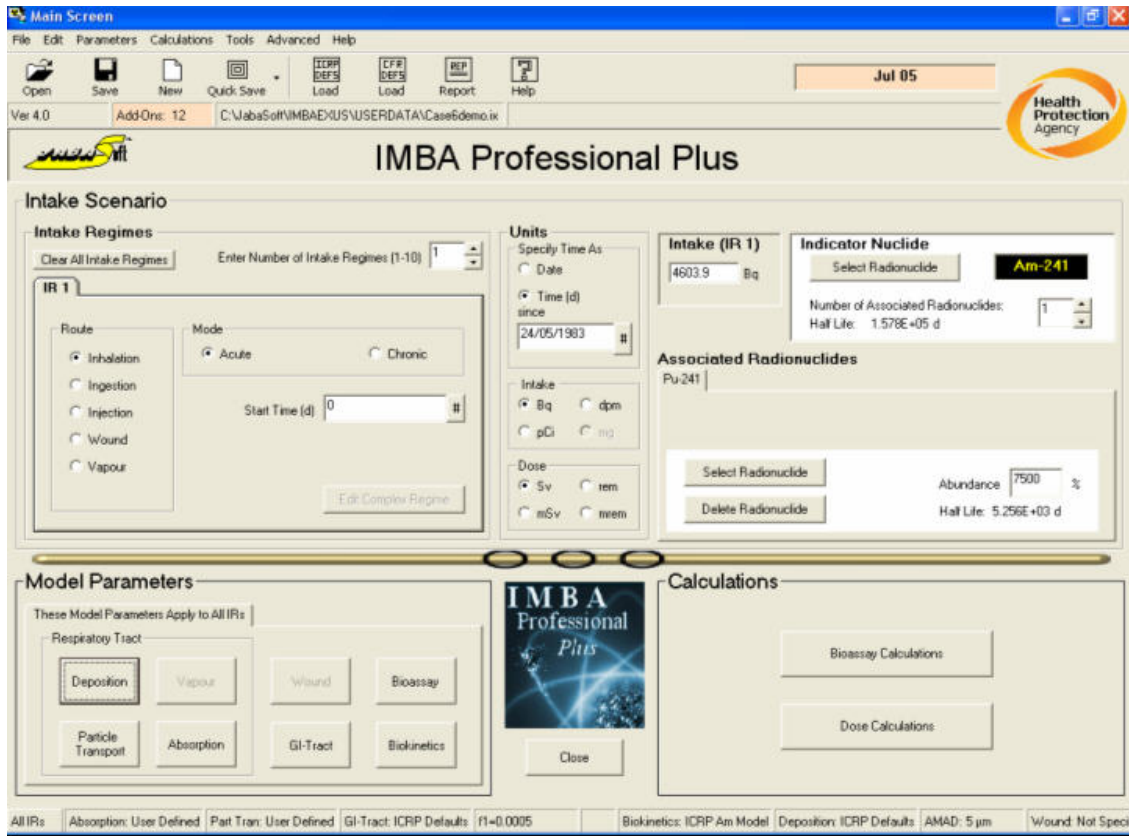


Figure 7: The Main Screen of IMBA

IMBA, which is an acronym for Integrated Modules for Bioassay Analysis, is an assortment of software units. The software aids in the performance of the existing ICRP biokinetic and dosimetric models that approximate the ingestion and dosage of radioactive substances. Currently, the Approved Dosimetry Services that are based in the United Kingdom employ components of the IMBA software for the regular dose evaluation in work environments following rigorous quality checks of the software. Although the IMBA modules are approved for use, the Health Protection Agency, Radiation Protection Division (HPA-RPD)* keeps on making adjustments to the

* Health Protection Agency, Radiation Protection Division, Oxford, UK.

components of the IMBA software. Some of the best features of IMBA modules are their personalized, easy-to-use interfaces especially in the IMBA ExpertTM editions, which have been developed under the sponsorship of US and various organizations based in the UK. Such interfaces make it possible to use the conventional ICRP models. They also make it possible for users to alter a large number of the parameter values. These alterations permit the use of highly developed methods of handling data in the computation of internal dosage. Such computations involve using the maximum likelihood technique in the tallying of data and handling a variety of data forms, for example, feces, urine and the entire body data all at once. The computations may also deal with large numbers of acute and chronic intakes (Birchall et al, 2005).

Bioassay quantities and doses from a known intake can be estimated using the base unit. The base unit can also work from back to the front to approximate the best intake from a group comprising a maximum of two hundred bioassay measurements. From the models, it is possible to estimate long-term and short-term inhalation of vapors as well as the intake of radionuclides through food and injections. On the IMBA interface, there are keys that enable users to pick any of the ICRP default factors. One can also specify each value to be used if all the values in the model are not needed. The software consists of a variety of tools that facilitate the input and output of data and graphical features. The software, which employs about seventy-five of the most frequently encountered radioactive nuclides, also has report writing and online help facilities (Birchall et al, 2005).

The IMBA Professional Plus was used in this investigation the ICRP 67 default parameters was employed to provide fit of data and predict an intake for each case. Data

obtained from urine and feces were also input into the software for simultaneous computation to estimate the best approximation of intake. The model was tested by using transfer rates that had previously been calculated using geometric mean parameter values of eleven instances from the SAAM II software.

3.4 IMBA Statistics

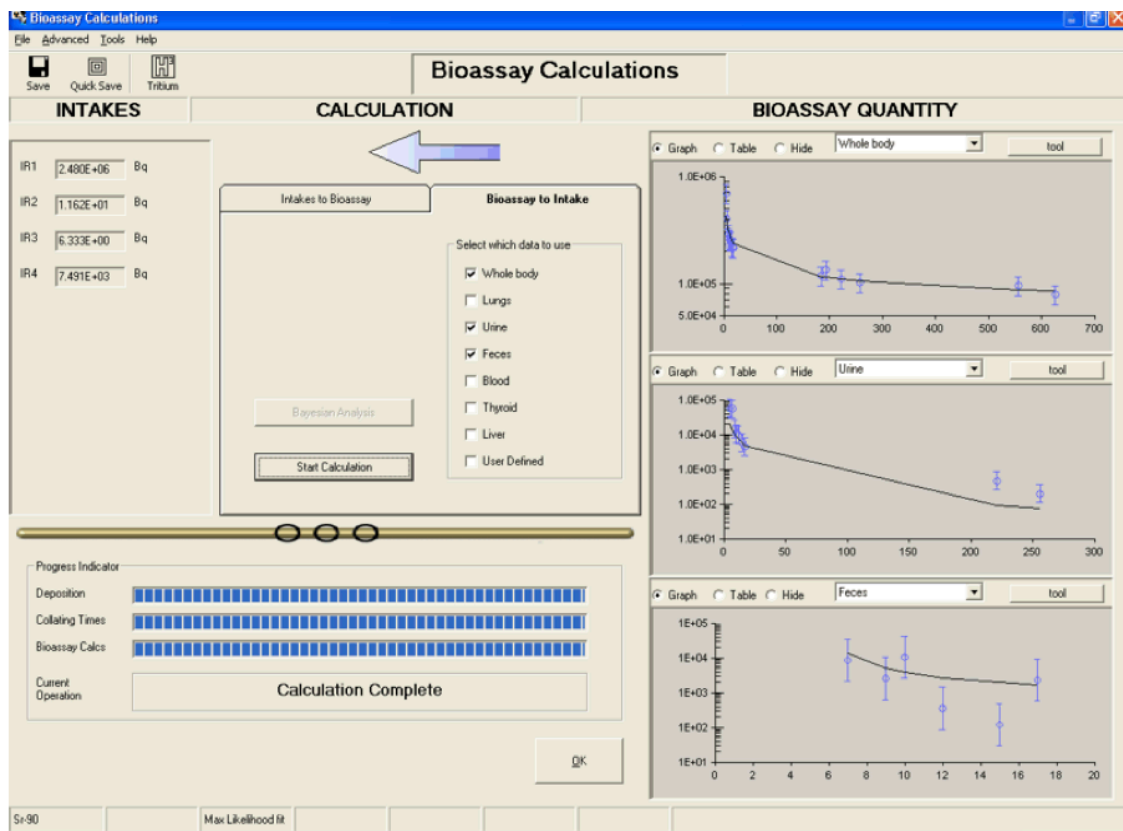


Figure 8: Calculated Intake amount with Maximum Likelihood Method “best fit”

3.4.1 Maximum Likelihood Method

The maximum likelihood method defines the ‘best fit’ quantity of the intake (I) as the intake that has the highest probability of fitting the measurement data. The IMBA fit employs the maximum likelihood technique of fitting using numerous chronic and acute

intakes. It also handles diverse data types such as urine, feces and whole body count data all at once. Small quantities below normal detection limits can be used in the analyses. Any number of independent intake regimens can be enumerated (Birchall et al, 2003). In these investigations, the mean value of intake is not identified, although a known part of data set. Therefore, the mean is approximated from the data and denoted as μ' for a test distribution. The range of error in the distribution is approximated to be equal to the probable error of the main population. Therefore, the probability function is given by Equation 7.

$$P(\mu) = \left(\frac{1}{\sigma\sqrt{2\pi}}\right)^N \text{EXP} \left[-\frac{1}{2} \sum \left(\frac{x_i - \mu'}{\sigma}\right)^2 \right] \quad \text{Equation 7}$$

Where:

σ = the standard deviation of the parent function.

μ' = the estimated mean for the data.

x_i = the value at each measurement (Bevington, 2003).

IMBA professional plus makes use of two major statistics to establish an association between predicted and calculated data. These two statistics are the chi-square statistics, which is denoted by χ^2 and the autocorrelation coefficient that is represented by the symbol ρ .

3.4.2 Chi-Square Statistics

The chi-square test statistic measured the degree of fit between the measured values and the predicted values (Puncher 2007). The incorporation of the chi-square test into the IMBA software enables it to approximate the bioassay intake function. Consequently, the probability of a chi-square test statistics of a given size can be computed (with degrees of freedom equal to the measured values less one), assuming the model fits the data. This probability, called a p-value indicates the relative plausibility or implausibility of the fitted model. The following equation illustrates how the chi parameter is computed.

$$\chi^2 = \frac{1}{\mu'} \sum_{i=1}^N (x_i - \mu')^2 \quad \text{Equation 8}$$

In the above equation, μ' signifies the average of the experimental data while x_i denotes the actual value in the group of data (Knoll 2000).

Small values of chi-square are obtained when the P-value is greater than 0.20, indicating the fitted model is quite plausible. Such small values show that there is a close match between the calculated and predicted variations in the data. In contrast, high chi-square values are obtained when the P-value is smaller than 0.005, indicating the fitted model is quite implausible. Such high values indicate of inadequate fits between the measured and expected variations in the data.

3.4.3 Autocorrelation Coefficient

The autocorrelation coefficient is useful in uncovering lack of independence between observed values close in time. For a string of residuals, the autocorrelation coefficient is computed using the equation 9.

$$\rho = \frac{\sum_{i=1}^{N-1} R_{i+1}}{\sum_{i=1}^N R_i^2} \quad \text{Equation 9}$$

In this equation, R_i denotes the residual in the i th position in a succession of N residuals. The value of N must always be greater than 4 (Puncher 2007). Provided that the tallying process presumes the evaluated uncertainties are in a lognormal fashion with an equal geometric standard deviation presupposed for each quantity, then each residual is computed as (Puncher 2007).

$$R_i = \frac{\ln(M_i) - \ln[I * B(t_i)]}{\ln \sigma_g} \quad \text{Equation 10}$$

Where:

$\ln(M_i)$ = the i th measurement, at time t_i after the intake.

I = the estimate intake.

$B(t_i)$ = A fraction the relevant bioassay quantity, at time t_i after the intake.

σ_g = the geometric standard deviation assumed to represent the uncertainty of data.

A point worth noting is that it is impossible to employ the ρ test in instances where a given data array contains less than four values (Puncher 2007). Table 4 summarizes how the two test statistics generated by IMBA can be used together in order to make overall judgments concerning the “goodness of fit” of the fitted models (Derryberry, 2013).

Autocorrelation Test	Chi-Square Test	
	Large p-value (good model fit to the data)	Small p-value (poor model fit to the data)
Large p-value (no systematic bias in the data)	Data is consistent with null hypothesis. Interpretation of p-value obtained from the chi-square test is not problematic.	Data is consistent with alternative hypothesis. Interpretation of p-value obtained from the chi-square test is not problematic.
Small p-value (systematic bias in the data)	Data is consistent with null hypothesis. P-value obtained from the chi-square test would be larger if there were no data clumping.	The results are ambiguous. P-value obtained from the chi-square test would be larger if there were no data clumping, so there is uncertainty that the p-value is small.

Table 4: An explanation of how the Chi-square test and autocorrelation coefficient are utilized together to assess model “goodness of fit”

CHAPTER 4: RESULTS AND DISCUSSION

4.1 Non-human Primates Data and SAAM II Predictions Results

The retention of strontium (Sr) in bioassay data type (urine and feces) was predicted with the aid of the SAAM II software. The ICRP 67 strontium systemic model was employed in the process. Strontium-90 was administered intravenously to 21 Non-human primates. The time between the administration of Sr-90 and death of the animals was between 1 and 7,168 days. The details of the 21 non-human primates were already summarized in Table 1.

Comparisons, were made between the data obtained from the non-human primates and the predicted values of intake, and other end point data based on the ICRP 67 systemic model. SAAM II employed the default parameters as provided in ICRP 67 to estimate the retention values in urine, feces, and skeleton in the comparison of measured and expected values. In this study, the urine and fecal bioassay data were analyzed simultaneously except in, 11 cases where they were analyzed separately.

The information illustrated the variations in the concentration of Sr activity in bioassay data with changes in time. Figures 9 to 30 illustrate the retention of Sr for predicted data and the measured data with respect to time, all instances that were assessed are provide in the figures.

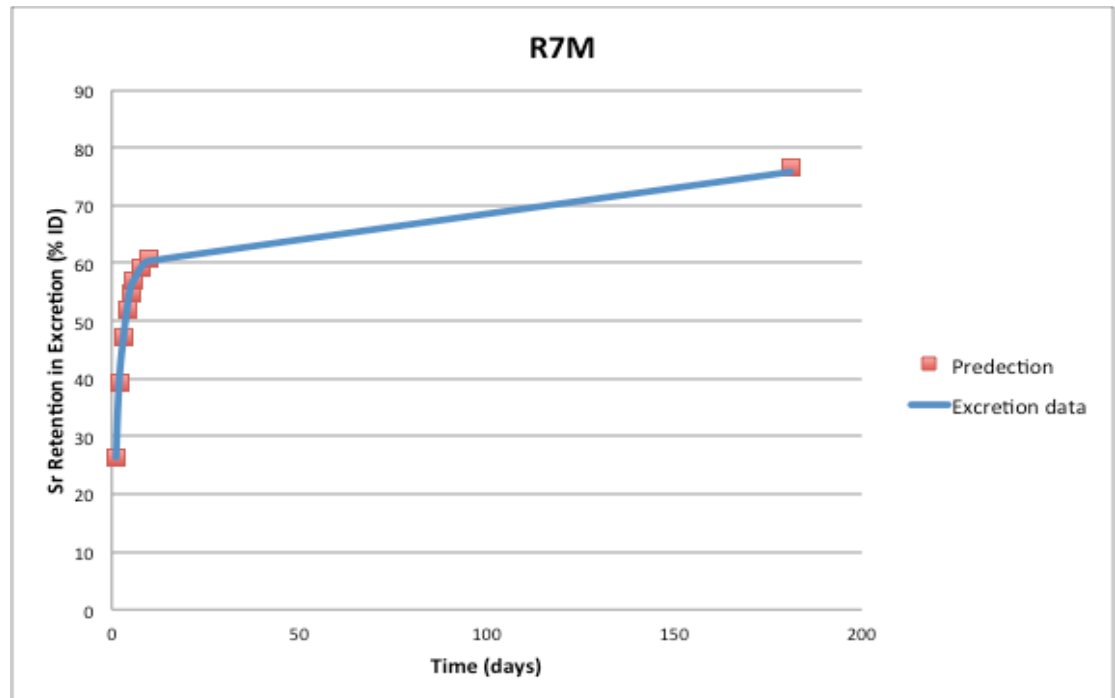


Figure 9: Case R7M, urine and feces are combined

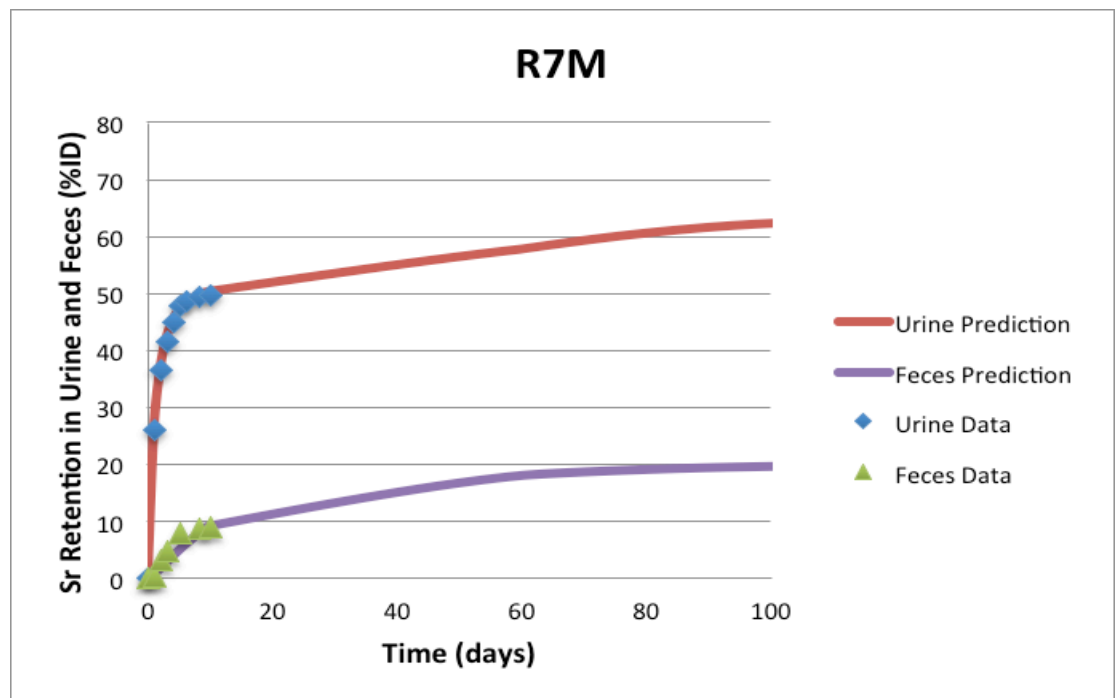


Figure 10: Case R7M, urine and feces are separate

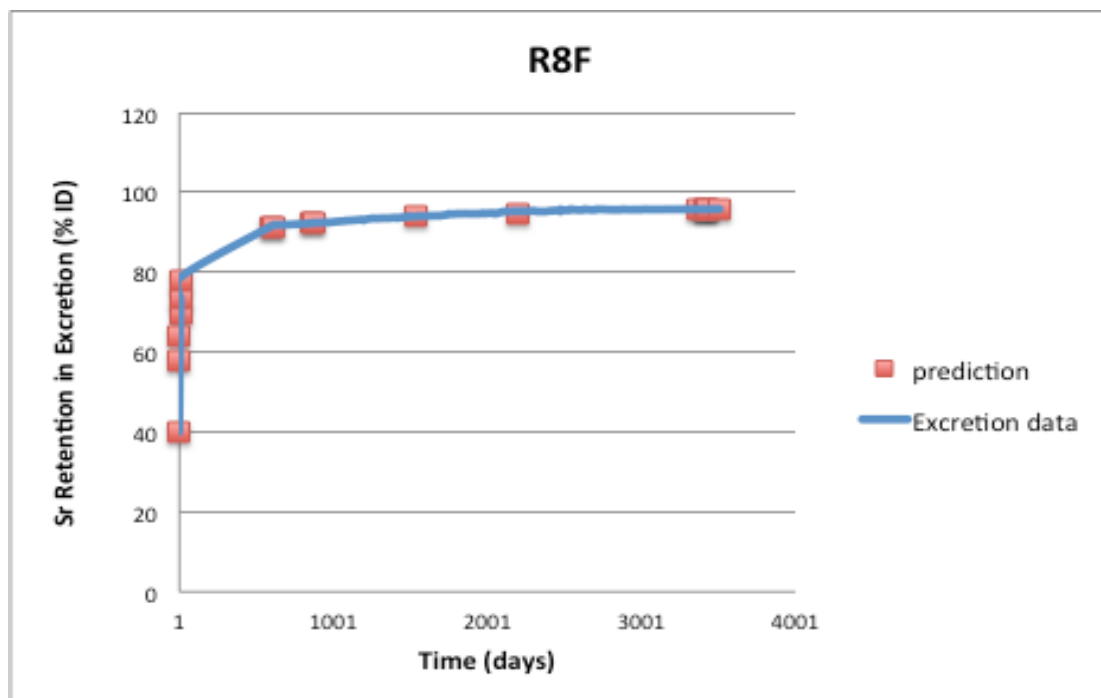


Figure 11: Case R8F, urine and feces are combined

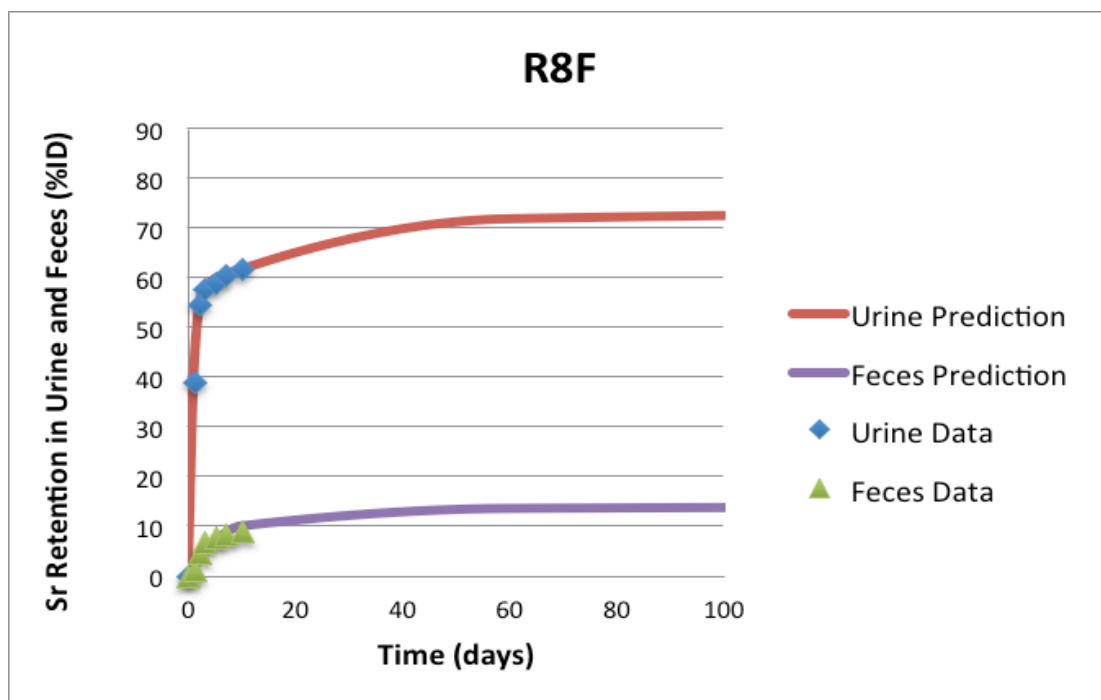


Figure 12: Case R8F, urine and feces are separate

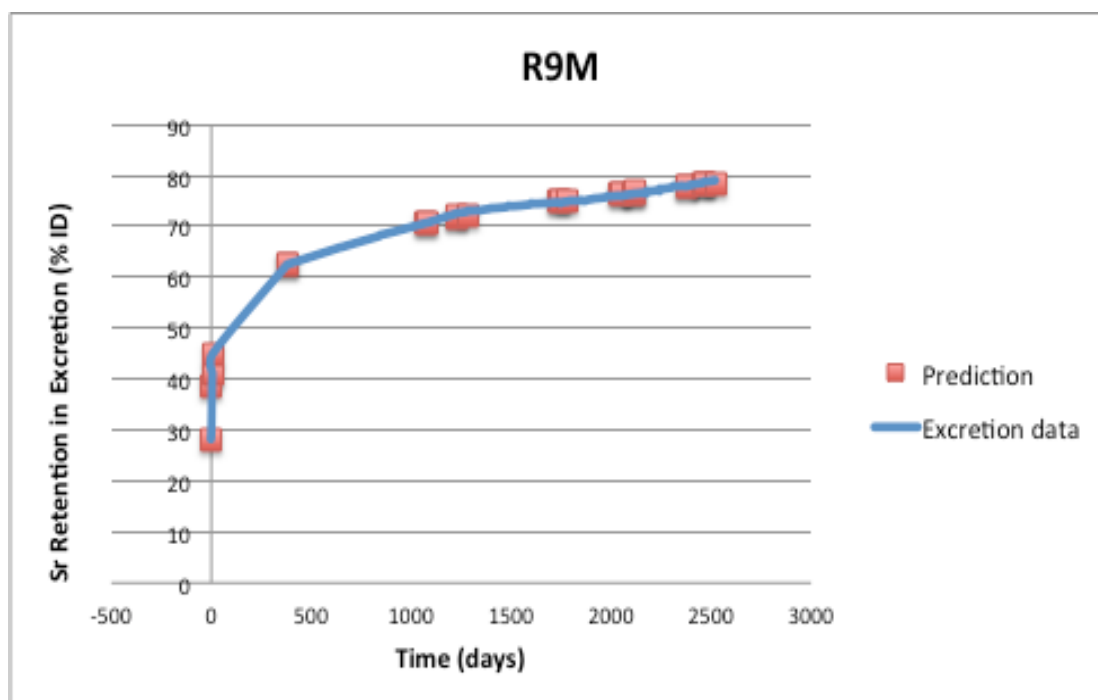


Figure 13: Case R9M, urine and feces are combined

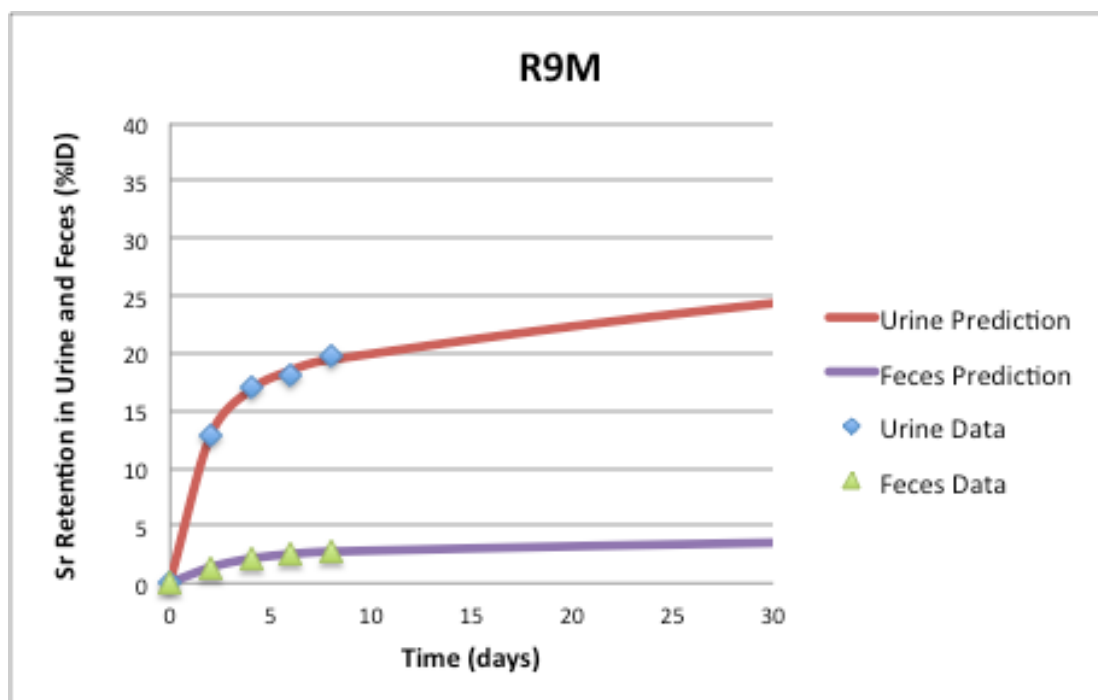


Figure 14: Case R9M, urine and feces are separate

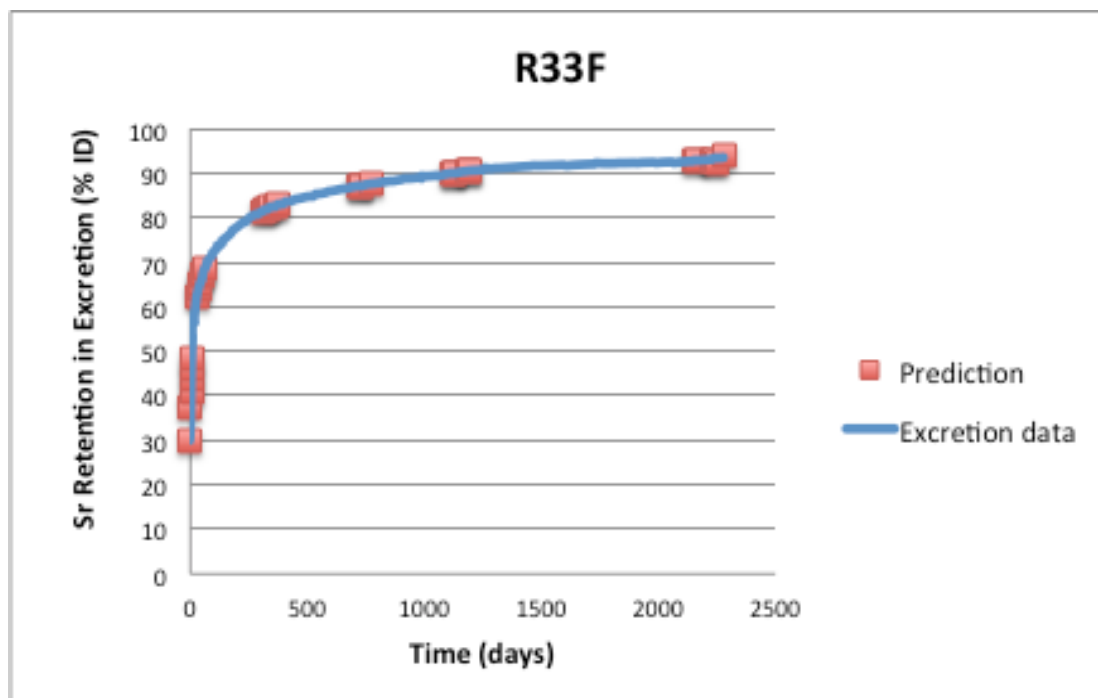


Figure 15: Case R33F, urine and feces are combined

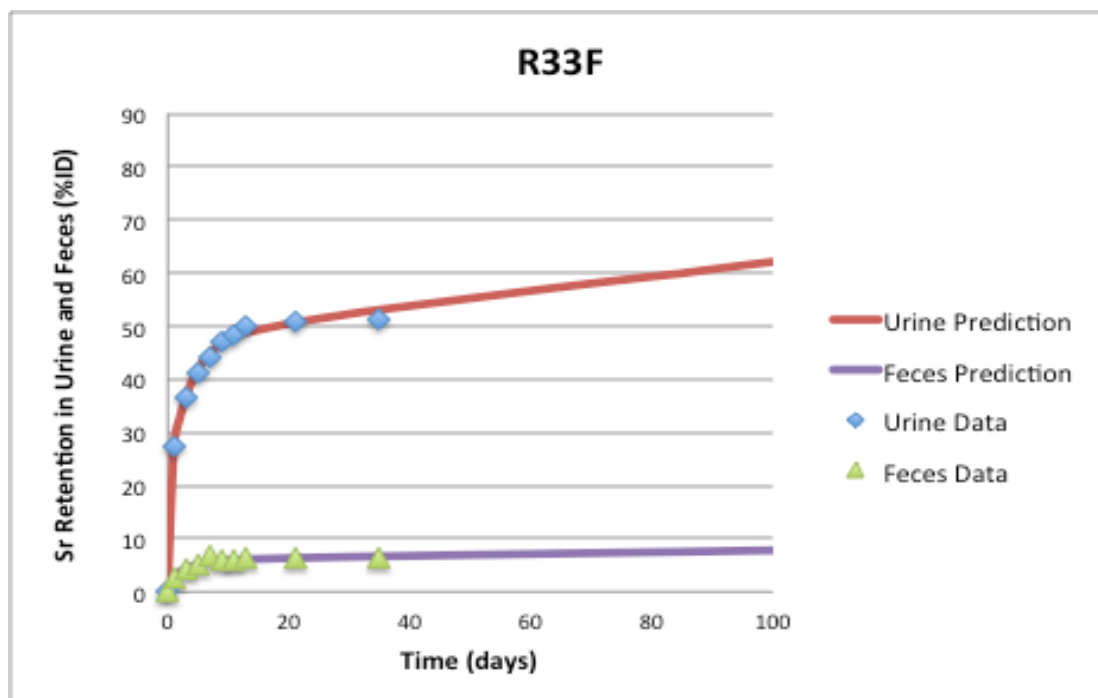


Figure 16 Case R33F, urine and feces are separate

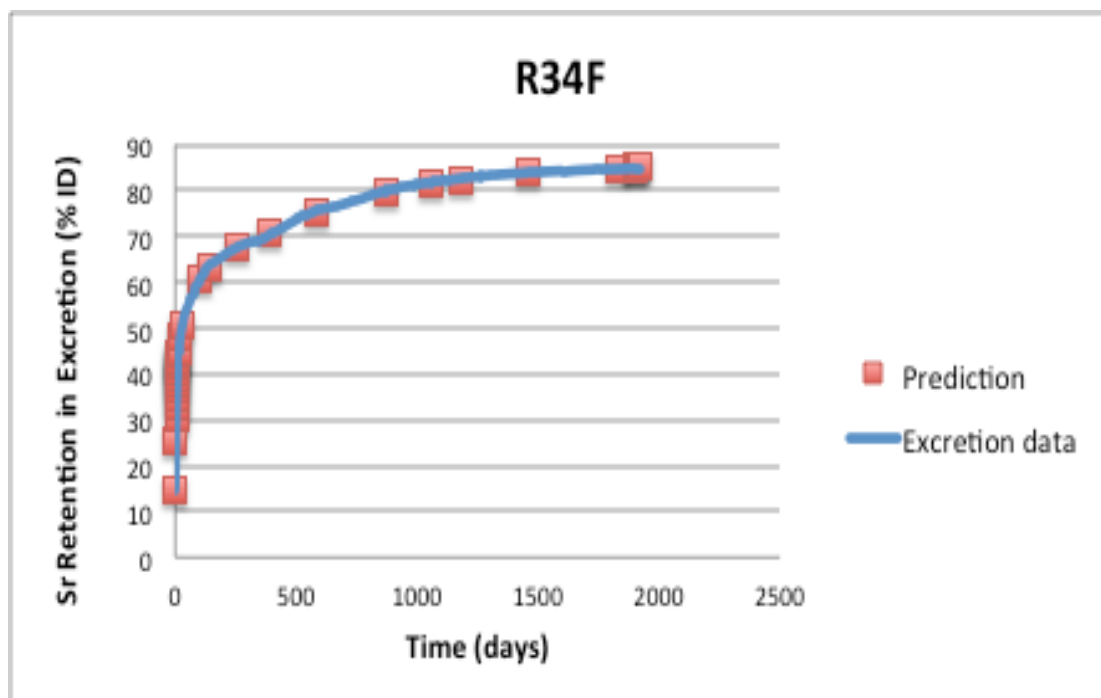


Figure 17: Case R34F, urine and feces are combined

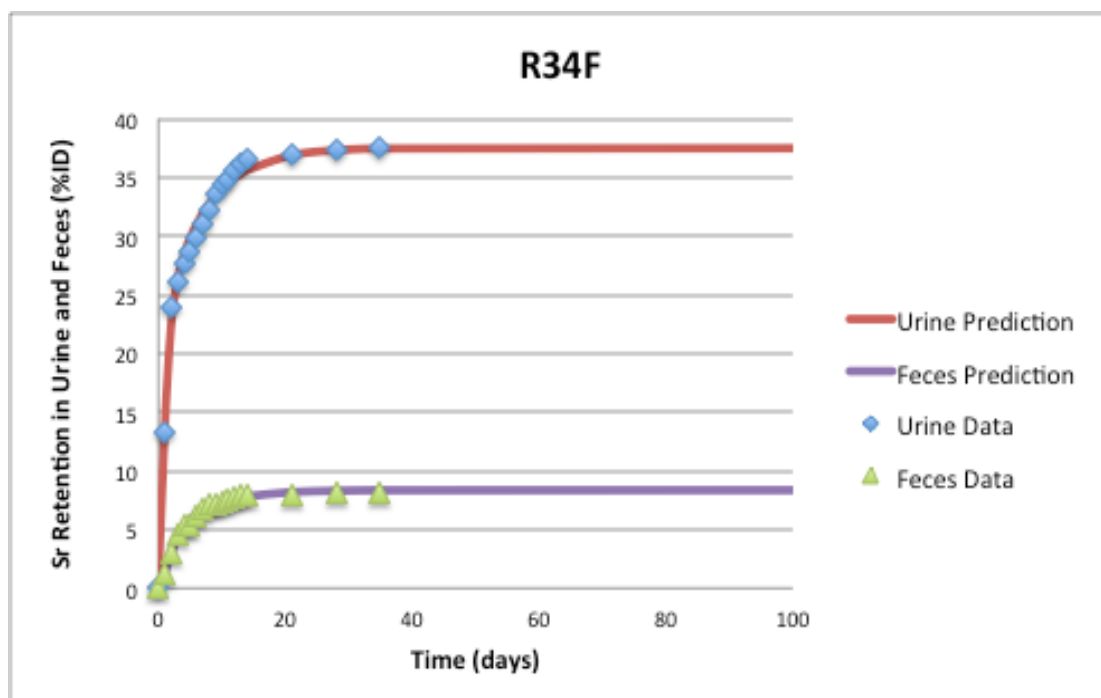


Figure 18: Case R34F, urine and feces are separate

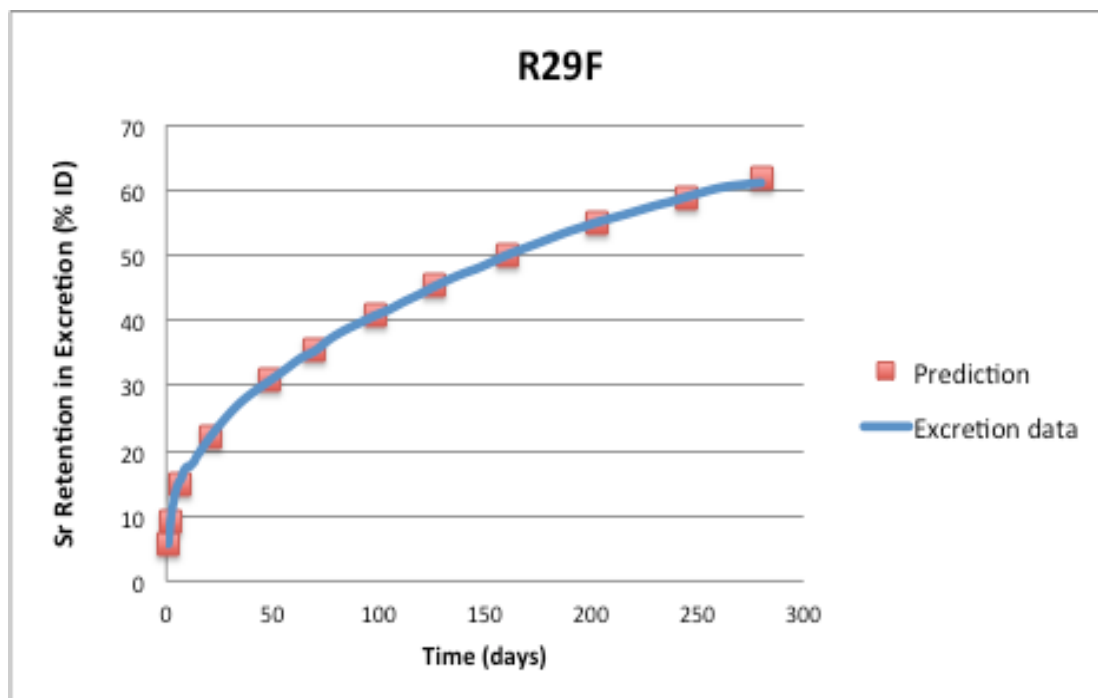


Figure 19: Case R29F, urine and feces are combined

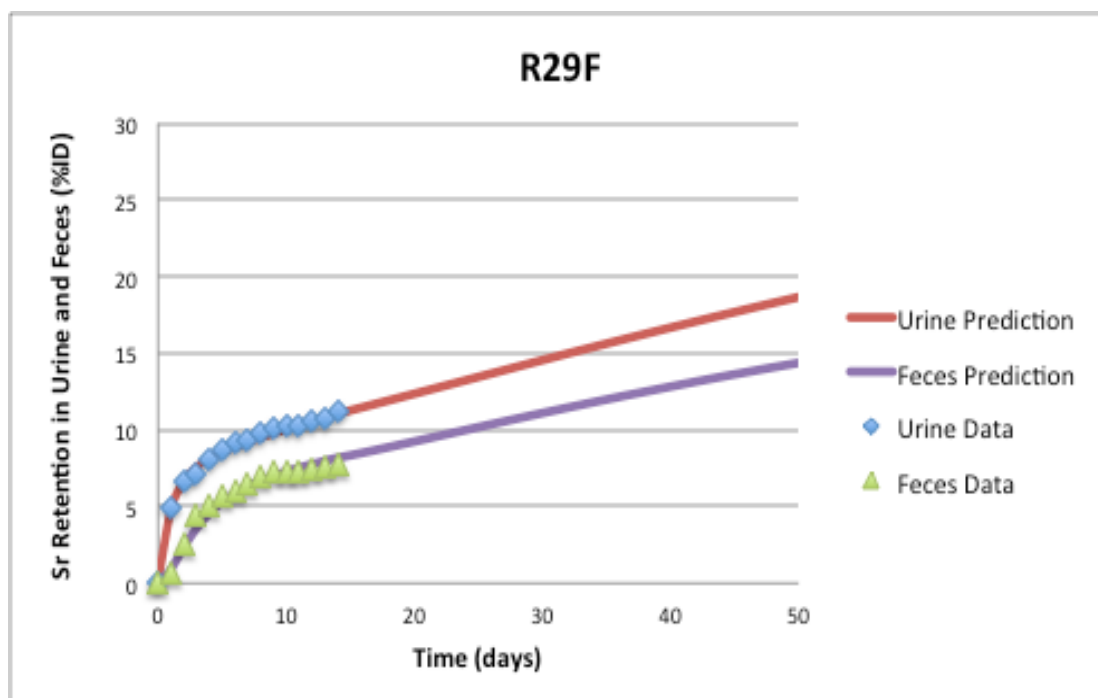


Figure 20: Case R29F, urine and feces are separate

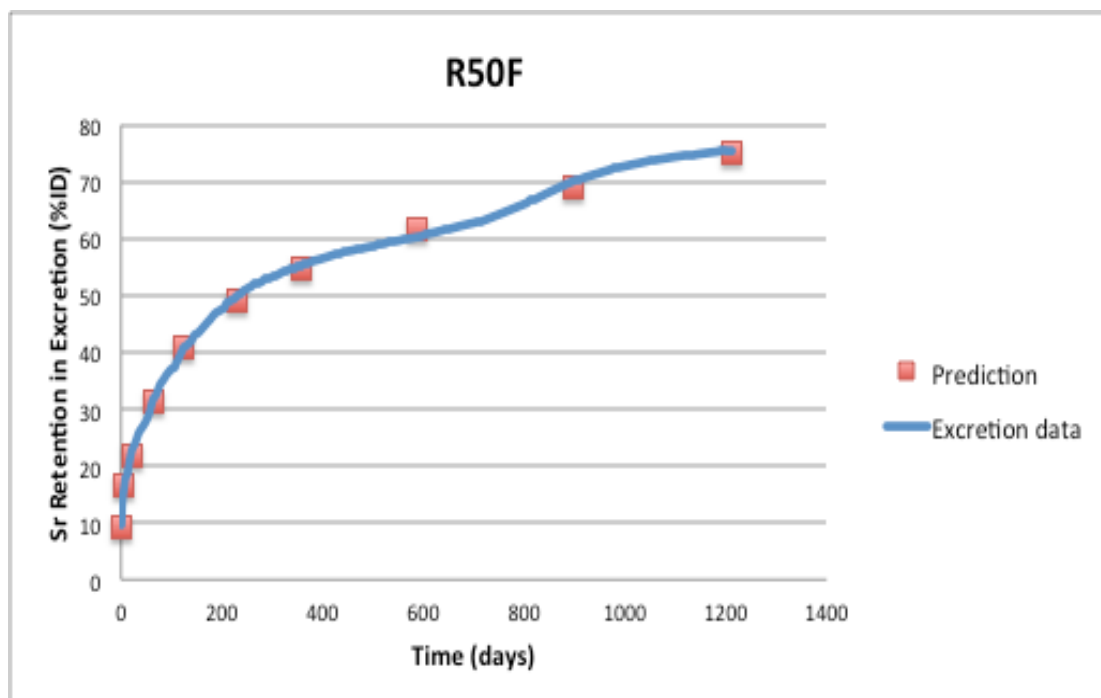


Figure 21: Case R50F, urine and feces are combined

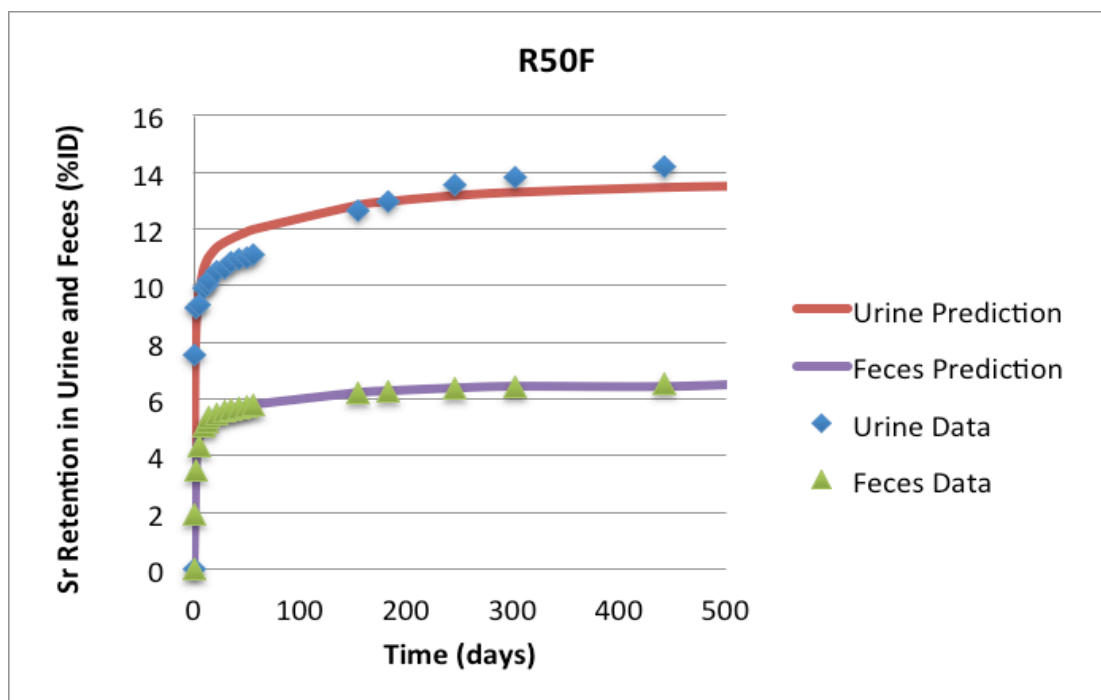


Figure 22: Case R50F, urine and feces are separate

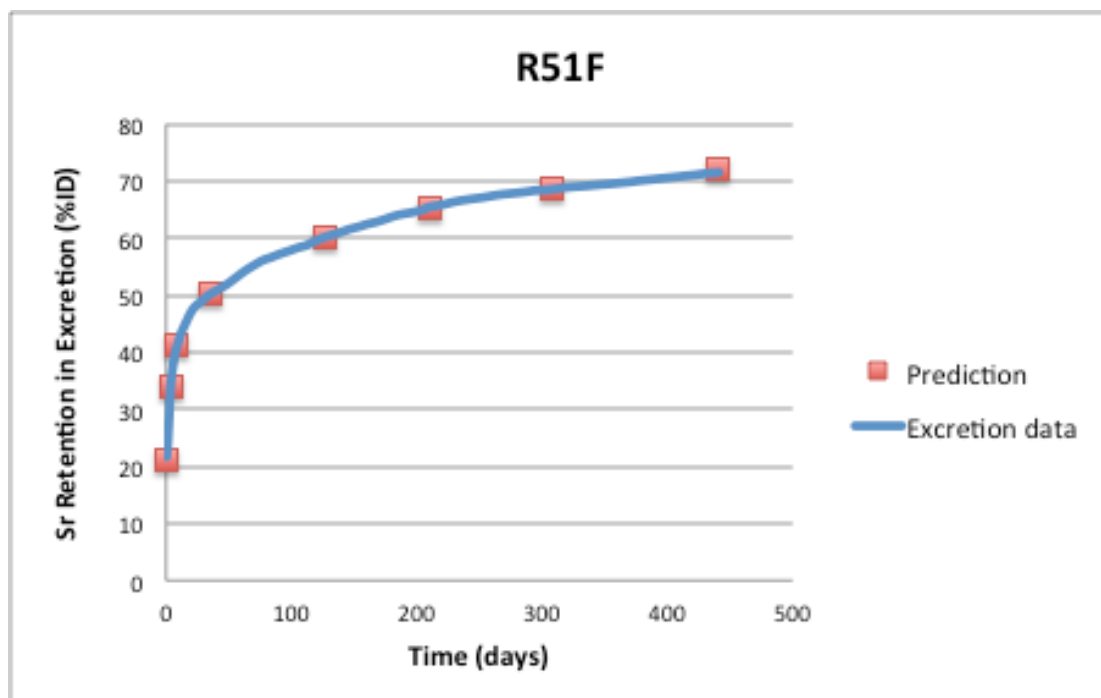


Figure 23: Case R51F, urine and feces are combined

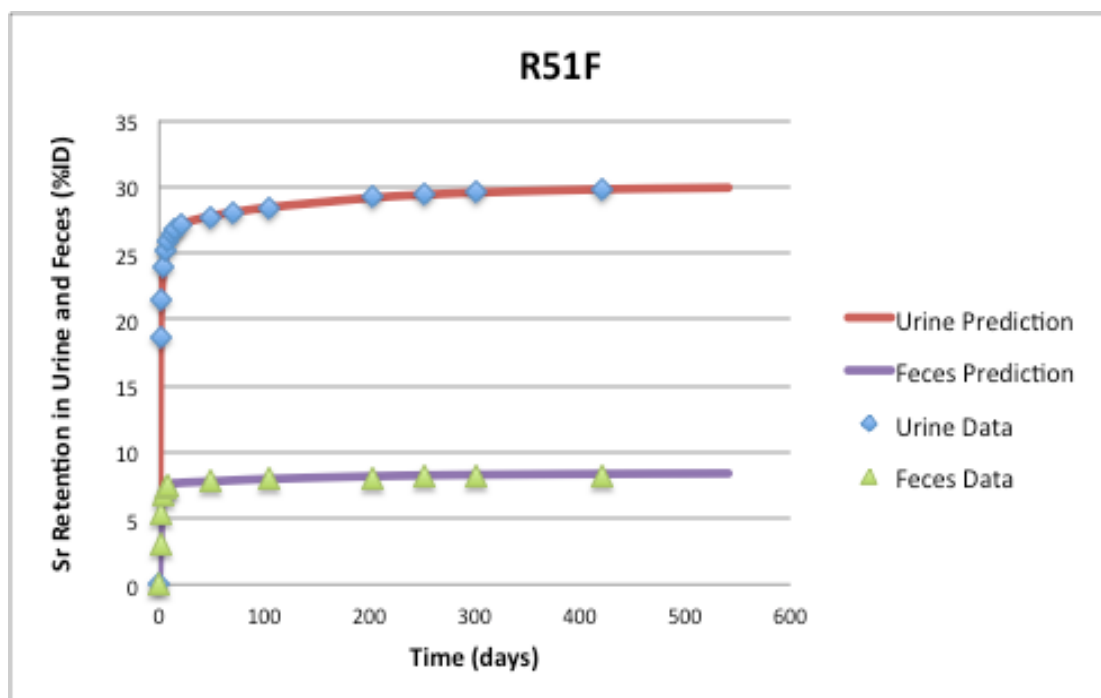


Figure 24: Case R51F, urine and feces are separate

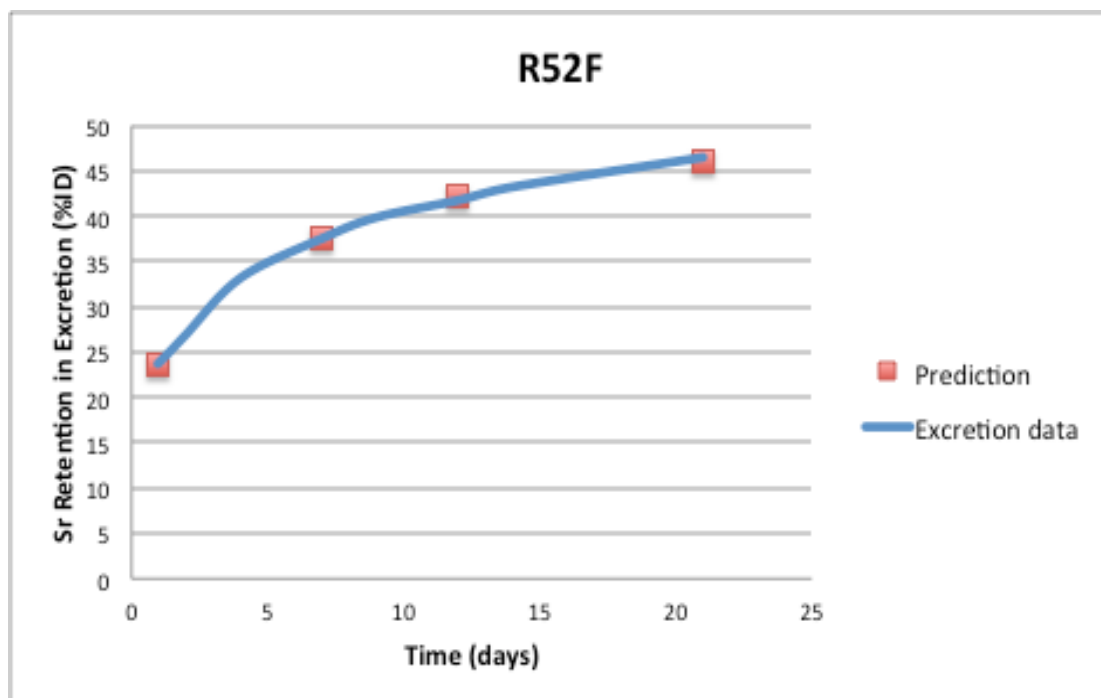


Figure 25: Case R52F, urine and feces are combined

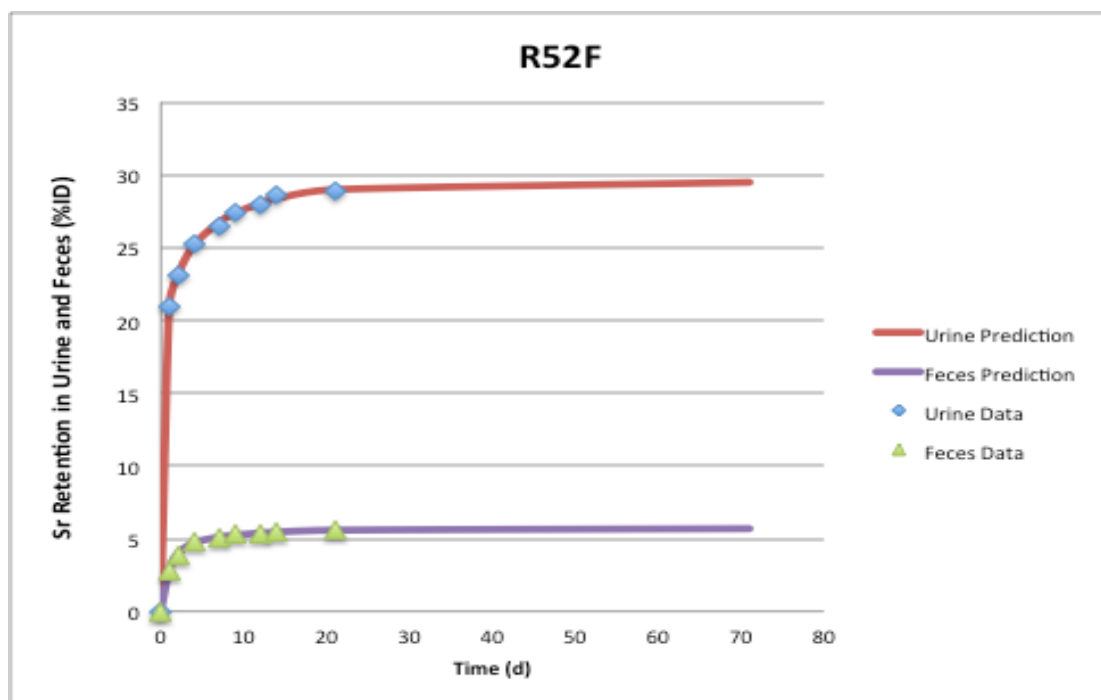


Figure 26: Case R52F, urine and feces are separate

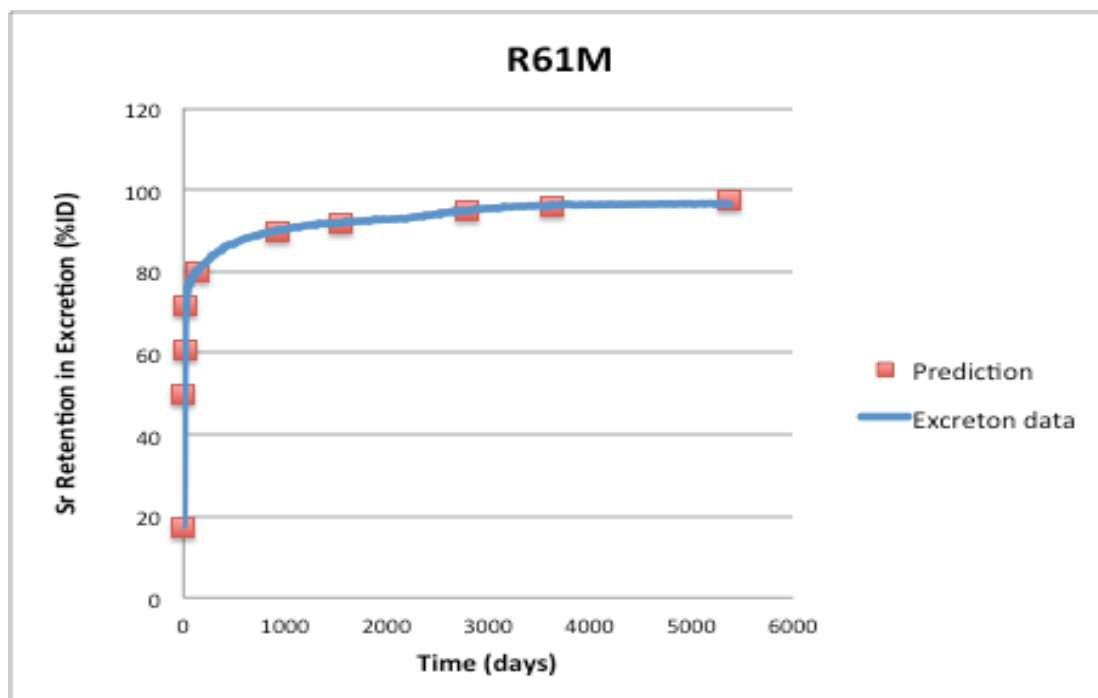


Figure 27: Case R61M, urine and feces are combined

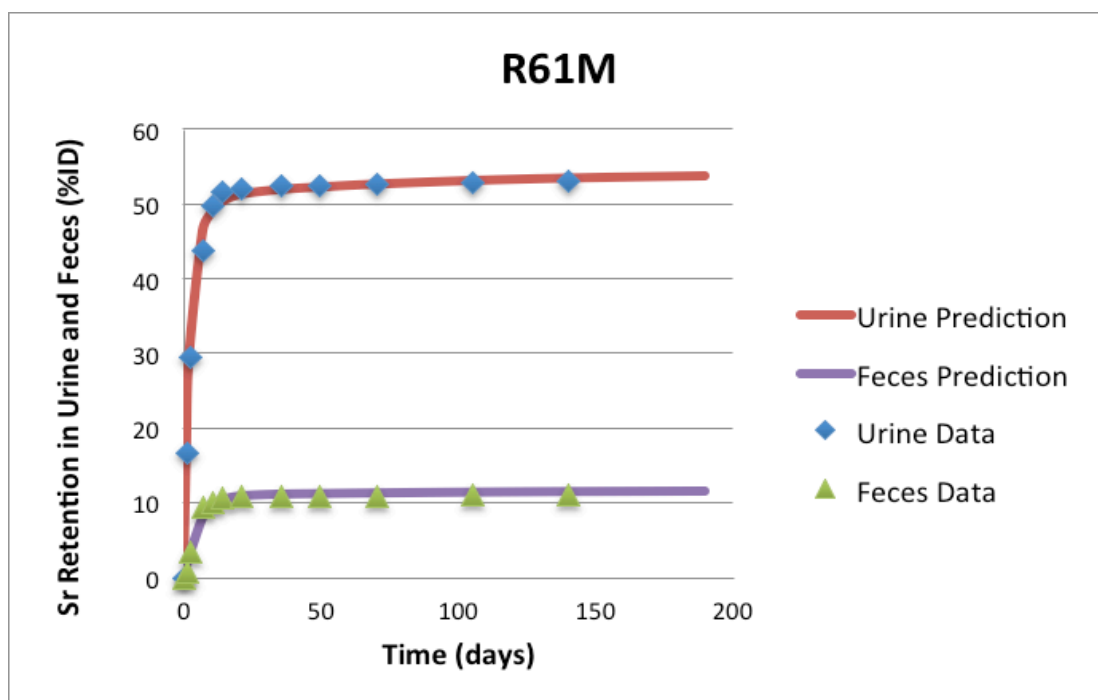


Figure 28: Case R61M, urine and feces are separate

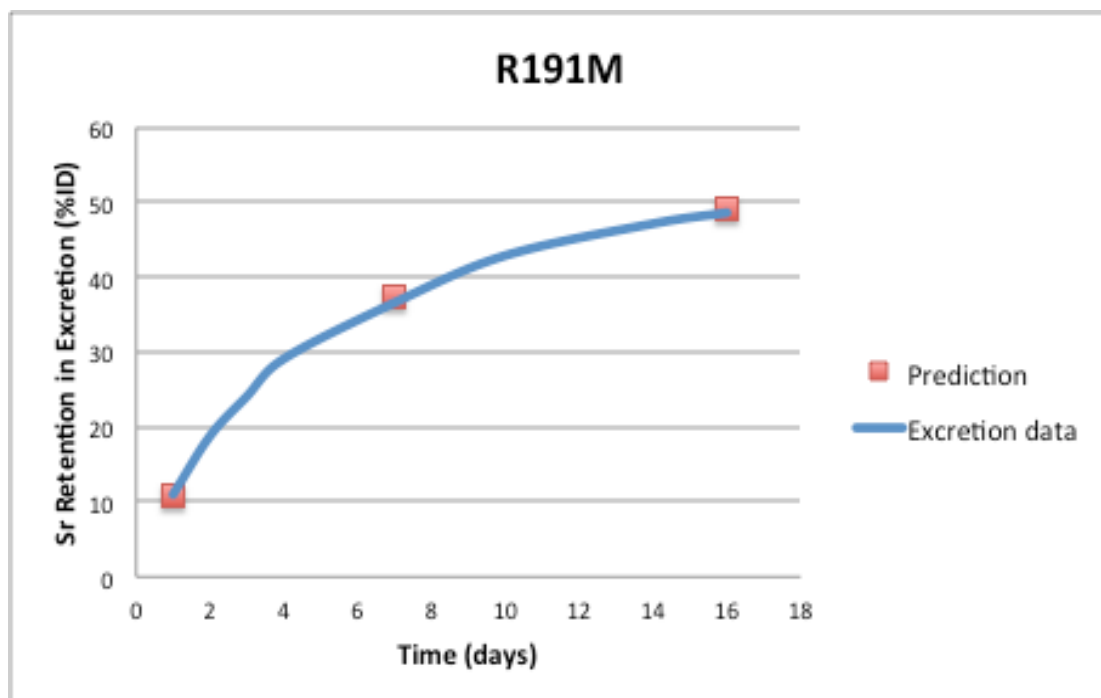


Figure 29: Case R191M, urine and feces are combined

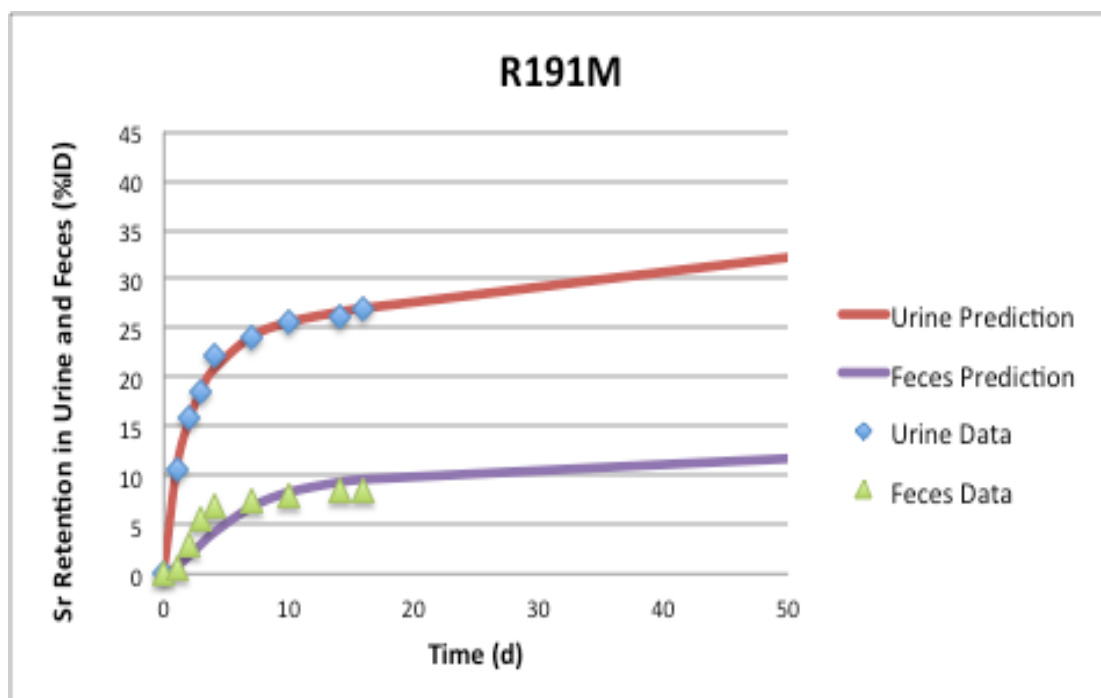


Figure 30: Case R191M, urine and feces are separate

Case R7M (Figure 9) illustrated Sr-90 retention in excretion as a function of time. It was shown that the percentage Sr-90 retained increased as time progressed. The rate of increase was very high within the first 50 days. From there, the rate increased gradually. It was noted that the predicted values and calculated values were almost similar. Figures 10 to 30 also exhibited trends similar to what was observed in Figure 9. However, there were slight variations in the initial Sr-90 retention values. The lowest initial values were observed in Cases R9M, R33F, R34F, R29F, and R50F, whereas the highest initial retention rates of 80% were observed in Cases R8F and R61M. In the rest of the figures, the initial rates ranged from 10% to 40%.

The SAAM II software and the ICRP 67 default transfer rates were used to evaluate the strontium activity held in the skeleton against the measured values. The quantified amounts of Sr-90 were compared with the estimated values when death occurred. The proportion of the predicted values established was mapped out as a function of time. The number of days after injection of Sr-90 varied from one day to 7,168 days. In a large number of instances, it was observed that the skeleton retained all the Sr-90 thereby giving a retention ratio of 1. In addition, during the late stages of the primates' lives (just before death), it was realized that the ratio of predicted to measured values in the skeleton was also 1. Those observations could be attributed to the fact that Sr-90 exhibited behavior that was similar to calcium. It was known that any calcium taken into the body went to the bones to assist in the development of healthy bones as well as teeth. In addition, calcium requirements increased with an increase in age. That implied that more calcium was directed to the bones and stored as the primate aged. That

explained why the measured values of Sr-90 retention in the skeletons of the primates were high at around the time of death.

The retention values of the skeleton were similar to the predicted values because only slight differences in the two categories were observed. This information was summarized in Table 5. Figure 31 was used to further illustrate the information in Table 5.

Skeleton

	Days Post	SAAM	Measured	Fraction	
Case #	Injection	Predicted	(% ID)	P/M	%Differences
R7M	181	23.3	23.3	1	0
R8F	3506	3.13	2.81	1.1	10.77
R9M	2520	20.9	20.9	1	0
R10F	94	42.7	42.7	1	0
R33F	2278	6.54	5.9	1.1	
R34F	1921	16.1	16.3	0.98	10.33
R35F	2040	16.1	16.3	0.99	1.23
R27F	3159	14.55	14.50	1	0
R28F	2087	14.79	14.8	1	0
R29F	280	36.99	37	1	0
R32F	7168	5.22	5.20	1	0
R36F	4	55.8	55.8	1	0
R37F	1	41.2	41.3	0.99	0.24
R50F	1212	22.9	22.9	1	0
R51F	441	27.3	27.2	0.99	0.36
R52F	21	51.7	51.7	1	0
R61F	5372	2.47	2.48	0.99	0.40
R62M	5853	1.09	1.1	0.99	2.71
R1881M	2	27.6	27.6	1	0
R191M	16	43.16	48.7	0.88	12.06

Table 5: Summary of the retention fraction of SAAM II prediction and measured values in skeleton.

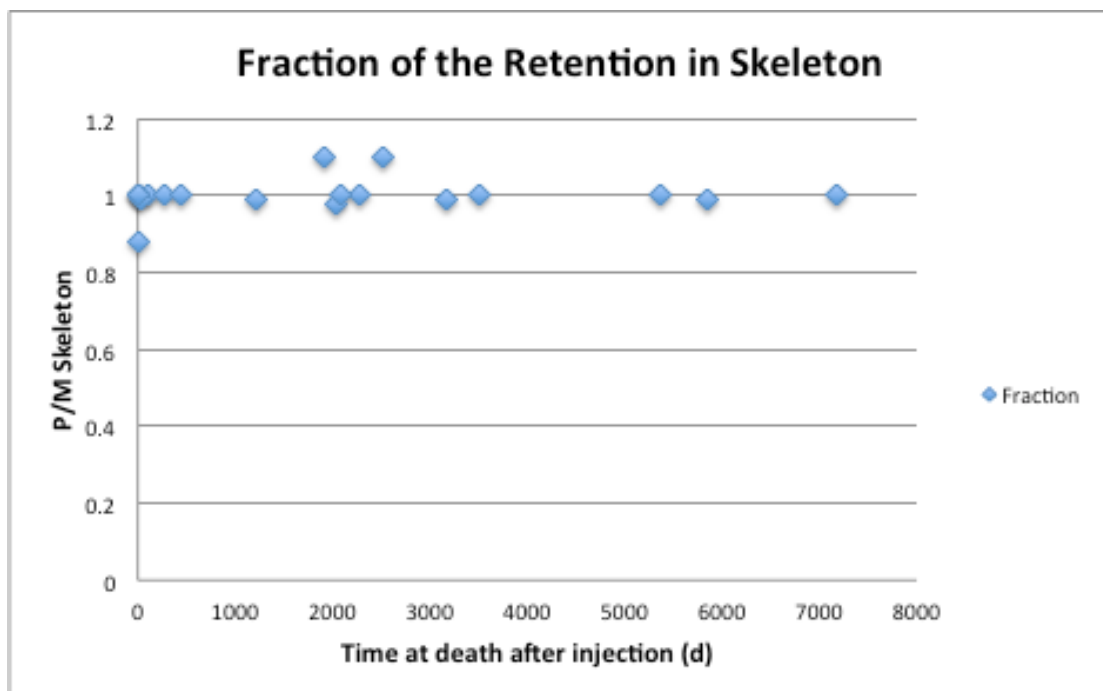


Figure 31: Scatter plots of the retention fraction of SAAM II prediction and measured values in skeleton

4.2 Modification of Default Parameters based on Intravenously Injected Non-human Primates Data

SAAM II software was used to improve the efficiency of the original transfer rates explained in the ICRP 67 systemic model for strontium. The improvement of the parameters was carried out in the range of a tenth and tenfold the initial parameters. The original parameters were used to improve data from the 21 non-human primates that received intravenous injections of Sr-90. Particularly, excretion and skeleton data were employed in the optimization process with the aid of the Bayesian technique. In total, 22 parameters explained in the model were optimized. Therefore, the adjusted parameters were produced by the SAAM II software. The values of the total objective function and AIC were also obtained from the software.

Fit parameters for the bioassay data together with the modified transfer rates were provided by the SAAM II software. The computed statistical figures were minimized thereby giving predicted and measured values, which differed by a maximum of $\pm 20\%$. The data showing the parameters for systemic model for Strontium were summarized in Table 6 to 10. The bioassay data (urine and feces) was analyzed simultaneously (and separately for eleven cases).

The modified parameters were used in the computation of the geometric means as well as the geometric standard deviations (GSD). The results of the geometric means and geometric standard deviations of the systemic model are provided in Table 11 and 12. In addition, the estimate excretion in the different samples (feces, urine) and retention in skeleton, and soft tissue were evaluated against the default model predictions using the

geometric mean parameters. Figures 32, 33, 34 and 35 provide the summaries of those comparisons.

Part I

Model Parameters	Route	default	R7M	R8F	R9M	R10F	R33F	R34F	R35F
Plasma to ST0	K(1,4)	7.5	11.07	7.23	36.15	79.7	73.95	74.54	0.83
Plasma to ST1	k(2,4)	1.53	10.23	1.51	1.62	2.20	1.50	1.50	1.50
Plasma to ST2	k(3,4)	0.003	0.021	0.03	0.02	0.002	0.03	0.104	3.00×10^{-4}
ST0 TO Plasma	k(4,1)	2.5	0.825	11.184	22.94	2.763	20.97	19.042	0.5047
ST1 TO Plasma	k(4,2)	0.116	0.0578	0.1666	0.1663	0.0358	0.0529	0.0224	0.0233
ST2 TO Plasma	k(4,3)	3.80×10^{-4}	1.76×10^{-4}	3.80×10^{-5}	2.00×10^{-4}	3.86×10^{-4}	3.80×10^{-5}	3.80×10^{-5}	2.70×10^{-3}
Cor. Surface to Plasma	k(4,6)	0.578	1.2668	0.8313	0.0578	3.6057	0.0592	0.2133	0.0578
Non-exchang Cor. Vol. to Plasma	k(4,8)	8.21×10^{-4}	8.46×10^{-5}	1.79×10^{-5}	4.83×10^{-4}	3.55×10^{-5}	3.23×10^{-5}	8.21×10^{-6}	8.21×10^{-6}
Non-exchang Trab. Vol. to Plasma	k(4,9)	4.93×10^{-4}	0.0013	0.0013	0.0024	8.58×10^{-5}	0.0017	0.004	0.0042
Trabecular Surface to plasma	k(4,11)	5.78×10^{-1}	0.8661	8.65×10^{-1}	5.77	3.32	2.87×10^{-1}	5.78×10^{-2}	4.29×10^{-1}

Part I Cont'd

Mod Parameters	Rout	default	R7M	R8F	R9M	R10F	R33F	R34F	R35F
Plasma to Cortical Surfaces	k(6,4)	1.67	9.9277	0.167	0.6026	1.18x10 ⁻¹	1.67	3.7158	0.7442
Ex. Cor. bone vol. to Cor.Surf.	k(6,7)	4.30x10 ⁻³	5.84x10 ⁻⁴	4.40x10 ⁻⁴	4.30x10 ⁻⁴	8.73x10 ⁻⁴	2.30x10 ⁻²	4.32x10 ⁻⁴	4.32x10 ⁻⁴
Cor. Surf. to Cor. Ex. Vol.	k(7,6)	0.116	0.444	1.1536	1.16	3.30x10 ⁻¹	0.116	0.0259	0.0464
Ex. Cor. bone vol. to Non-Ex. cor. Vol	k(8,7)	4.30x10 ⁻³	5.21x10 ⁻⁴	9.74x10 ⁻⁴	4.60x10 ⁻⁴	2.88x10 ⁻²	4.30x10 ⁻³	2.03x10 ⁻²	2.47x10 ⁻²
Ex. Trab. bone vol. to Non-Ex Trab. Vol.	k(9,10)	4.30x10 ⁻³	0.0067	0.0013	0.007	2.98x10 ⁻²	0.0054	0.0041	0.0037
Trab. Surf. to Trab. Ex. Vol.	k(10,11)	0.116	5.03x10 ⁻¹	1.12	1.14	4.43x10 ⁻¹	8.86x10 ⁻²	1.16	8.96x10 ⁻²
Plasma to Trabecular Surfaces	k(11,4)	2.08	13.7227	3.15x10 ⁻¹	3.9076	2.01x10 ⁻¹	9.1094	1.0049	4.0583
Ex. Trab. bone Vol. to Trab. Surf.	K(11,10)	4.30x10 ⁻³	6.11x10 ⁻⁴	4.30x10 ⁻⁴	7.56x10 ⁻⁴	8.75x10 ⁻⁴	7.00x10 ⁻⁴	4.30x10 ⁻⁴	4.38x10 ⁻⁴
Plasma to Urinary bladder contents	k(14,4)	1.73	17.3	1.14	0.3971	2.60x10 ⁻¹	1.3442	2.12	0.1825
Urinary bladder to Urine	k(15,14)	5.00	7.89x10 ⁻¹	2.18	1.44	2.77x10 ⁻¹	3.34	1.60	5.0x10 ⁻¹
Plasma to G.I tract contents	k(18,4)	5.25x10 ⁻¹	5.157	1.54	1.623	3.79	4.54	0.3188	1.5717
G.I tract contents to Feces	k(19,18)	1.00	4.38	1.90	1.40	2.45x10 ⁻¹	3.44	1.83	3.33

Table 6: Summary of the modified transfer rates for each case with the default values described in ICRP 67 (COMBINED)

Part II

Model Parameters	Route	default	R27M	R28F	R29M	R32F	R36F	R37F	R50F
Plasma to ST0	K(1,4)	7.5	2.4088	0.8061	41.514	75	0.75	0.75	16.7539
Plasma to ST1	k(2,4)	1.53	1.6067	37.787	1.50	1.50	1.50	1.50	2.052
Plasma to ST2	k(3,4)	0.003	0.0299	0.03	0.0065	0.03	0.0027	0.0018	0.007
ST0 TO Plasma	k(4,1)	2.5	2.1964	15.795	2.8963	20.736	2.9432	2.7967	0.5047
ST1 TO Plasma	k(4,2)	0.116	0.0649	0.2431	0.0581	0.05	4.90x10 ⁻¹	1.1449	0.0306
ST2 TO Plasma	k(4,3)	3.80x10 ⁻⁴	3.91x10 ⁻⁵	3.80x10 ⁻⁵	1.50x10 ⁻³	5.77x10 ⁻⁵	3.80x10 ⁻⁴	3.80x10 ⁻⁵	1.500x10 ⁻³
Cor. Surface to Plasma	k(4,6)	0.578	0.1841	5.6813	0.0578	0.0578	5.78x10 ⁻²	0.0578	4.5166
Non-exchang Cor. Vol. to Plasma	k(4,8)	8.21x10 ⁻⁴	1.75x10 ⁻⁴	5.24x10 ⁻⁵	8.87x10 ⁻⁶	1.39x10 ⁻⁴	8.21x10 ⁻⁵	8.21x10 ⁻⁵	1.85x10 ⁻⁴
Non-exchang.Trab. Vol.to Plasma	k(4,9)	4.93x10 ⁻⁴	0.0049	0.0031	4.93x10 ⁻⁵	6.40x10 ⁻⁴	4.93x10 ⁻⁴	4.93x10 ⁻⁴	1.50x10 ⁻³
Trabecular Surface to plasma	k(4,11)	5.78x10 ⁻¹	5.89x10 ⁻¹	1.30x10 ⁻¹	1.61	5.78	5.78x10 ⁻²	5.78x10 ⁻²	2.47x10 ⁻¹

Part II Cont'd

Model Parameters	Rout	default	R27M	R28F	R29F	R32F	R36F	R37F	R50F
Plasma to Cortical Surfaces	k(6,4)	1.67	0.3566	6.5083	1.52x10 ⁺¹	2.02	3.44	5.37	1.68x10 ⁻¹
Ex. Cor. bone vol. to Cor.Surf.	k(6,7)	4.30x10 ⁻³	1.90x10 ⁻³	9.40x10 ⁻³	1.79x10 ⁻²	4.30x10 ⁻²	4.30x10 ⁻³	4.30x10 ⁻³	2.58x10 ⁻²
Cor. Surf. to Cor. Ex. Vol.	k(7,6)	0.116	1.0823	1.1544	1.84x10 ⁻²	6.51x10 ⁻¹	1.57x10 ⁻¹	1.61x10 ⁻¹	1.16x10 ⁻²
Ex. Cor. bone vol. to Non-Ex. cor. Vol	k(8,7)	4.30x10 ⁻³	4.0x10 ⁻²	1.55x10 ⁻²	4.30x10 ⁻⁴	8.64x10 ⁻⁴	4.30x10 ⁻³	4.30x10 ⁻³	4.60x10 ⁻⁴
Ex. Trab. bone vol. to Non-Ex Trab. Vol.	k(9,10)	4.30x10 ⁻³	4.63x10 ⁻⁴	0.0042	5.40x10 ⁻³	1.37x10 ⁻²	4.30x10 ⁻³	4.30x10 ⁻³	2.07x10 ⁻²
Trab. Surf. to Trab. Ex. Vol.	k(10,11)	0.116	1.04	9.70x10 ⁻²	3.01x10 ⁻¹	1.16	1.72x10 ⁻¹	1.81x10 ⁻¹	1.51x10 ⁻¹
Plasma to Trabecular Surfaces	k(11,4)	2.08	3.59	17.4061	1.15x10 ⁺¹	8.81x10 ⁻¹	4.88	7.83	2.70
Ex. Trab. bone Vol. to Trab. Surf.	K(11,10)	4.30x10 ⁻³	2.07x10 ⁻²	3.61x10 ⁻²	1.23x10 ⁻²	4.30x10 ⁻⁴	4.30x10 ⁻³	4.30x10 ⁻³	2.12x10 ⁻²
Plasma to Urinary bladder contents	k(14,4)	1.73	7.07x10 ⁻¹	1.6506	1.77	2.51x10 ⁻¹	4.56	1.72x10 ⁺¹	2.00x10 ⁻¹
Urinary bladder to Urine	k(15,14)	5.00	3.53x10 ⁺¹	5.00x10 ⁺¹	8.02x10 ⁻¹	5.45x10 ⁻¹	3.65	4.74x10 ⁺¹	2.84
Plasma to G.I tract contents	k(18,4)	5.25x10 ⁻¹	1.0	2.2844	1.11	2.43	7.76x10 ⁻¹	5.25x10 ⁻²	4.20x10 ⁻¹
G.I tract contents to Feces	k(19,18)	1.00	2.99	1.0x10 ⁻¹	8.38	3.15x10 ⁻¹	1.40	3.56	2.84

Table 7: Summary of the modified transfer rates for each case with the default values described in ICRP 67 (COMBINED)

Part III

Model Parameters	Route	default	R51F	R52F	R61M	R62M	R188M	R191M
Plasma to ST0	K(1,4)	7.5	14.9869	6.8966	70.4372	73.2757	0.75	41.8716
Plasma to ST1	k(2,4)	1.53	1.5523	1.5	1.5	1.7018	1.5	4.0599
Plasma to ST2	k(3,4)	0.003	0.0297	3.00×10^{-4}	0.016	0.0056	0.0027	0.0039
ST0 TO Plasma	k(4,1)	2.5	0.9735	0.6288	3.8753	16.0134	3.7782	5.3813
ST1 TO Plasma	k(4,2)	0.116	0.0943	0.1586	0.0254	0.2357	0.5602	0.3712
ST2 TO Plasma	k(4,3)	3.80×10^{-4}	3.96×10^{-5}	4.18×10^{-4}	3.80×10^{-5}	3.80×10^{-5}	3.8×10^{-4}	1.1×10^{-3}
Cor. Surface to Plasma	k(4,6)	0.578	0.2986	0.0873	0.1115	0.0578	0.8106	2.5319
Non-exchang Cor. Vol. to Plasma	k(4,8)	8.21×10^{-4}	6.95×10^{-4}	8.21×10^{-5}	3.68×10^{-4}	8.21×10^{-6}	8.21×10^{-5}	8.21×10^{-6}
Non-exchang Trab. Vol. to Plasma	k(4,9)	4.93×10^{-4}	8.84×10^{-4}	4.93×10^{-4}	4.90×10^{-3}	6.90×10^{-4}	4.93×10^{-4}	1.30×10^{-3}
Trabecular Surface to plasma	k(4,11)	5.78×10^{-1}	8.64×10^{-2}	5.78×10^{-1}	3.33	5.77	8.55×10^{-1}	1.37

Part III Cont'd

Model Parameters	Rout	default	R51F	R52F	R61M	R62M	R188M	R191M
Plasma to Cortical Surfaces	k(6,4)	1.67	3.56	7.87	8.42	3.29x10 ⁻¹	4.32	1.33x10 ⁺¹
Ex. Cor. bone vol. to Cor.Surf.	k(6,7)	4.30x10 ⁻³	3.41x10 ⁻²	4.30x10 ⁻²	5.30x10 ⁻³	4.30x10 ⁻²	4.30x10 ⁻³	4.10x10 ⁻³
Cor. Surf. to Cor. Ex. Vol.	k(7,6)	0.116	6.68x10 ⁻¹	1.16x10 ⁻¹	5.81x10 ⁻²	3.78x10 ⁻²	1.04x10 ⁻¹	4.39x10 ⁻¹
Ex. Cor. bone vol. to Non-Ex. cor. Vol	k(8,7)	4.30x10 ⁻³	1.10x10 ⁻³	4.30x10 ⁻⁴	2.29x10 ⁻²	7.80x10 ⁻³	4.30x10 ⁻³	8.10x10 ⁻³
Ex. Trab. bone vol. to Non-Ex Trab. Vol.	k(9,10)	4.30x10 ⁻³	1.06x10 ⁻¹	4.30x10 ⁻³	9.20x10 ⁻³	3.90x10 ⁻³	4.30x10 ⁻³	4.33x10 ⁻⁴
Trab. Surf. to Trab. Ex. Vol.	k(10,11)	0.116	8.29x10 ⁻¹	1.16x10 ⁻¹	5.25x10 ⁻¹	1.16	9.75x10 ⁻²	1.61x10 ⁻¹
Plasma to Trabecular Surfaces	k(11,4)	2.08	1.98	2.08	1.72x10 ⁺¹	3.98	623	2.08x10 ⁻¹
Ex. Trab. bone Vol. to Trab. Surf.	K(11,10)	4.30x10 ⁻³	2.04x10 ⁻²	4.30x10 ⁻²	4.30x10 ⁻³	4.10x10 ⁻³	4.30x10 ⁻³	5.40x10 ⁻³
Plasma to Urinary bladder contents	k(14,4)	1.73	3.75	4.37	1.39x10 ⁺¹	3.77	7.64	1.73
Urinary bladder to Urine	k(15,14)	5.00	1.57x10 ⁻¹	2.16x10 ⁺¹	1.01	1.11	1.04x10 ⁻¹	5.00
Plasma to G.I tract contents	k(18,4)	5.25x10 ⁻¹	6.87x10 ⁻²	5.25x10 ⁻²	3.79	5.25x10 ⁻²	8.97x10 ⁻¹	5.25x10 ⁻¹
G.I tract contents to Feces	k(19,18)	1.00	8.32	6.32	1.39x10 ⁻¹	1.76x10 ⁻¹	1.90	1.00

Table 8: Summary of the modified transfer rates for each case with the default values described in ICRP 67 (COMBINED)

Part IV

Model Parameters	Route	default	R7M	R8F	R9M	R29F	R33F	R34F
Plasma to Cortical Surfaces	k(6,4)	1.67	75	75	0.75	30.4117	2.2666	73.6346
Plasma to ST1	k(2,4)	1.53	4.7255	6.5343	4.6881	1.7278	1.5	1.5
Plasma to ST2	k(3,4)	0.003	0.03	0.0021	0.003	0.0264	0.03	0.0154
ST0 TO Plasma	k(4,1)	2.5	4.573	9.4834	0.25	25	0.6433	25
ST1 TO Plasma	k(4,2)	0.116	0.0116	0.0242	0.0121	0.0402	0.0116	0.2421
ST2 TO Plasma	k(4,3)	3.80x10 ⁻⁴	3.80x10 ⁻⁵	3.83x10 ⁻⁴	3.81x10 ⁻⁴	4.57x10 ⁻⁵	3.80x10 ⁻⁵	3.8010 ⁻⁵
Cor. Surface to Plasma	k(4,6)	0.578	0.578	0.578	0.578	0.5535	0.578	0.0578
Non-exchang Cor. Vol. to Plasma	k(4,8)	8.21x10 ⁻⁴	8.21x10 ⁻⁵	8.21x10 ⁻⁵	8.21x10 ⁻⁵	7.98x10 ⁻⁵	8.21x10 ⁻⁵	8.21x10 ⁻⁶
Non-exchang.Trab. Vol.to Plasma	k(4,9)	4.93x10 ⁻⁴	4.93x10 ⁻⁴	4.93x10 ⁻⁴	4.93x10 ⁻⁴	2.82x10 ⁻⁴	4.93x10 ⁻⁴	4.93x10 ⁻⁵
Trabecular Surface to plasma	k(4,11)	5.78x10 ⁻¹	5.78x10 ⁻¹	5.78x10 ⁻¹	5.78x10 ⁻¹	4.47x10 ⁻¹	5.78x10 ⁻¹	5.78x10 ⁻²

Part IV Cont'd

Model Parameters	Route	default	R7M	R8F	R9M	R29F	R33F	R34F
Plasma to Cortical Surfaces	k(6,4)	1.67	1.67	1.67	1.67	1.69x10 ⁻¹	1.67	1.62
Ex. Cor. bone vol. to Cor.Surf.	k(6,7)	4.30x10 ⁻³	4.30x10 ⁻³	4.30x10 ⁻³	4.30x10 ⁻³	7.01x10 ⁻⁴	4.30x10 ⁻³	4.30x10 ⁻⁴
Cor. Surf. to Cor. Ex. Vol.	k(7,6)	0.116	1.16x10 ⁻¹	1.16	1.16x10 ⁻¹	3.16x10 ⁻²	1.16x10 ⁻¹	1.16
Ex. Cor. bone vol. to Non-Ex. cor. Vol	k(8,7)	4.30x10 ⁻³	4.30x10 ⁻³	4.30x10 ⁻³	4.30x10 ⁻³	5.30x10 ⁻³	4.30x10 ⁻³	1.46x10 ⁻²
Ex. Trab. bone vol. to Non-Ex Trab. Vol.	k(9,10)	4.30x10 ⁻³	4.30x10 ⁻³	4.30x10 ⁻³	4.30x10 ⁻³	4.80x10 ⁻³	4.30x10 ⁻³	4.30x10 ⁻⁴
Trab. Surf. to Trab. Ex. Vol.	k(10,11)	0.116	1.16x10 ⁻¹	1.16x10 ⁻¹	1.16x10 ⁻¹	8.23x10 ⁻²	1.16x10 ⁻¹	1.16
Plasma to Trabecular Surfaces	k(11,4)	2.08	2.08	2.08	2.08	2.10x10 ⁻¹	2.08	2.08x10 ⁻¹
Ex. Trab. bone Vol. to Trab. Surf.	K(11,10)	4.30x10 ⁻³	4.30x10 ⁻³	4.30x10 ⁻³	4.30x10 ⁻³	7.23x10 ⁻⁴	4.30x10 ⁻³	4.30x10 ⁻⁴
Plasma to Urinary bladder contents	k(14,4)	1.73	7.61	1.57x10 ⁺¹	1.33	1.73x10 ⁻¹	2.21	1.22
Urinary bladder to Urine	k(15,14)	5.00	8.57	1.96	1.03	5.0x10 ⁺¹	5.0x10 ⁺¹	2.77
Plasma to G.I tract contents	k(18,4)	5.25x10 ⁻¹	2.41	2.96	1.96x10 ⁻¹	1.34x10 ⁻¹	2.78x10 ⁻¹	2.72x10 ⁻¹
G.I tract contents to Feces	k(19,18)	1.00	1.00x10 ⁻¹	2.09x10 ⁻¹	5.37x10 ⁻¹	4.82x10 ⁻¹	2.07	6.07x10 ⁻¹

Table 9: Summary of the modified transfer rates for some case with the default values described in ICRP 67 (Individually)

Part V

Model Parameters	Route	default	R35F	R50F	R51F	R52F	R61M	R191M
Plasma to Cortical Surfaces	k(6,4)	1.67	13.6829	74.2288	52.52	0.75	75	75
Plasma to ST1	k(2,4)	1.53	1.5	1.5	1.57	16.03	1.5	4.9834
Plasma to ST2	k(3,4)	0.003	0.0032	0.0288	0.0014	0.006	3.33x10 ⁻⁴	0.0299
ST0 TO Plasma	k(4,1)	2.5	0.4782	4.99752	24.9992	0.25	3.5986	5.469
ST1 TO Plasma	k(4,2)	0.116	0.0116	0.259	0.2289	1.1582	0.0116	0.0116
ST2 TO Plasma	k(4,3)	3.80x10 ⁻⁴	3.80x10 ⁻⁵	3.87x10 ⁻⁵	1.0x10 ⁻⁴	3.48x10 ⁻⁴	8.01x10 ⁻⁵	3.80x10 ⁻⁵
Cor. Surface to Plasma	k(4,6)	0.578	0.0578	0.0578	0.283	0.0578	1.41x10 ⁻¹	0.578
Non-exchang Cor. Vol. to Plasma	k(4,8)	8.21x10 ⁻⁴	8.21x10 ⁻⁶	8.21x10 ⁻⁶	8.41x10 ⁻⁶	8.21x10 ⁻⁴	8.21x10 ⁻⁶	8.21x10 ⁻⁵
Non-exchang Trab. Vol.to Plasma	k(4,9)	4.93x10 ⁻⁴	4.93x10 ⁻⁵	5.02x10 ⁻⁵	6.44x10 ⁻⁵	4.93x10 ⁻⁵	4.93x10 ⁻⁵	4.93x10 ⁻⁴
Trabecular Surface to plasma	k(4,11)	5.78x10 ⁻¹	4.67	6.24x10 ⁻²	9.23x10 ⁻¹	5.78x10 ⁻²	3.59	5.78x10 ⁻¹

Part V Cont'd

Model Parameters	Route	default	R35F	R50F	R51F	R52F	R61M	R191M
Plasma to Cortical Surfaces	k(6,4)	1.67	5.72	3.49	6.17	1.67x10 ⁺¹	1.67x10 ⁺¹	1.67
Ex. Cor. bone vol. to Cor.Surf.	k(6,7)	4.30x10 ⁻³	4.30x10 ⁻⁴	1.92x10 ⁻²	3.80x10 ⁻³	4.30x10 ⁻⁴	4.30x10 ⁻⁴	4.30x10 ⁻³
Cor. Surf. to Cor. Ex. Vol.	k(7,6)	0.116	1.16	1.16	7.52x10 ⁻¹	9.01x10 ⁻²	1.51x10 ⁻¹	1.16x10 ⁻¹
Ex. Cor. bone vol. to Non-Ex. cor. Vol	k(8,7)	4.30x10 ⁻³	2.71x10 ⁻²	5.70x10 ⁻³	6.40x10 ⁻³	1.48x10 ⁻²	4.30x10 ⁻²	4.30x10 ⁻³
Ex. Trab. bone vol. to Non-Ex Trab. Vol.	k(9,10)	4.30x10 ⁻³	1.35x10 ⁻²	1.14x10 ⁻²	1.80x10 ⁻³	1.05x10 ⁻²	3.20x10 ⁻²	4.30x10 ⁻³
Trab. Surf. to Trab. Ex. Vol.	k(10,11)	0.116	2.08x10 ⁺¹	1.88x10 ⁻¹	2.34x10 ⁻¹	2.08x10 ⁻¹	1.16x10 ⁻²	1.16x10 ⁻¹
Plasma to Trabecular Surfaces	k(11,4)	2.08	4.30x10 ⁻⁴	1.66	3.18x10 ⁻¹	2.08x10 ⁺¹	2.08x10 ⁺¹	2.08
Ex. Trab. bone Vol. to Trab. Surf.	K(11,10)	4.30x10 ⁻³	4.34	3.16x10 ⁻²	4.00x10 ⁻³	4.30x10 ⁻⁴	4.30x10 ⁻⁴	4.30x10 ⁻³
Plasma to Urinary bladder contents	k(14,4)	1.73	4.34	6.13x10 ⁻¹	1.88	1.20x10 ⁺¹	1.38x10 ⁺¹	2.17
Urinary bladder to Urine	k(15,14)	5.00	5.00x10 ⁺¹	4.97x10 ⁻¹	5.00x10 ⁺¹	9.86	1.35	5.00x10 ⁺¹
Plasma to G.I tract contents	k(18,4)	5.25x10 ⁻¹	7.11x10 ⁻¹	2.98x10 ⁻¹	5.27x10 ⁻¹	2.31	2.94	8.05x10 ⁻¹
G.I tract contents to Feces	k(19,18)	1.00	5.77x10 ⁻¹	1.44	1.33	1.34	2.97x10 ⁻¹	3.06x10 ⁻¹

Table 10: Summary of the modified transfer rates for some case with the default values described in ICRP 67 (Individually)

Model Parameters	default	Geo. Mean	GSD
Plasma to ST0	7.5	11.01	6.0813
Plasma to ST1	1.53	2.109	2.233
Plasma to ST2	0.003	7.53E-03	4.902
ST0 TO Plasma	2.5	4.583	3.492
ST1 TO Plasma	0.116	0.105	3.111
ST2 TO Plasma	3.80×10^{-4}	1.79×10^{-4}	4.375
Cor. Surface to Plasma	0.578	0.275	5.296
Non-exchang Cor. Vol. to Plasma	8.21×10^{-4}	6.365	4.531
Non-exchang.Trab. Vol.to Plasma	4.93×10^{-4}	9.89×10^{-4}	3.381
Trabecular Surface to plasma	5.78×10^{-1}	0.618	4.666
Plasma to Cortical Surfaces	1.67	2.392	4.236
Ex. Cor. bone vol. to Cor.Surf.	4.30×10^{-3}	4.08×10^{-3}	5.00
Cor. Surf. to Cor. Ex. Vol.	0.116	0.174	4.248
Ex. Cor. bone vol. to Non-Ex. cor. Vol.	4.30×10^{-3}	3.55×10^{-3}	4.873
Ex. Trab. bone vol. to Non-Ex Trab. Vol.	4.30E-03	5.19E-03	3.396
Trab. Surf. to Trab. Ex. Vol.	0.166	0.322	2.781
Plasma to Trabecular Surfaces	2.8	3.646	3.517
Ex. Trab. bone Vol. to Trab. Surf.	4.30×10^{-3}	2.60×10^{-3}	4.627
Plasma to Urinary bladder contents	1.73	1.774	4.144
Urinary bladder to Urine	5.00	4.085	4.567
Plasma to G.I tract contents	5.25×10^{-1}	0.747	4.484
G.I tract contents to Feces	1.00	1.422	3.809

Table 11: Summary of Geometric mean and GSD values along with the default values for systemic model for 21 non-human primates *using combined* urine and feces data

Model Parameters	default	Geo. Mean	GSD
Plasma to ST0	7.5	18.78	6.048
Plasma to ST1	1.53	2.677	2.203
Plasma to ST2	0.003	0.0067	4.368
ST0 TO Plasma	2.5	3.5827	5.870
ST1 TO Plasma	0.116	0.0465	5.025
ST2 TO Plasma	3.80×10^{-4}	8.8×10^{-5}	2.830
Cor. Surface to Plasma	0.578	0.240	2.917
Non-exchang Cor. Vol. to Plasma	8.21×10^{-4}	4.8×10^{-5}	5.292
Non-exchang.Trab. Vol.to Plasma	4.93×10^{-4}	1.6×10^{-4}	3.128
Trabecular Surface to plasma	5.78×10^{-1}	0.4694	3.990
Plasma to Cortical Surfaces	1.67	2.5608	3.316
Ex. Cor. bone vol. to Cor.Surf.	4.30×10^{-3}	2.04×10^{-3}	3.588
Cor. Surf. to Cor. Ex. Vol.	0.116	0.2462	3.537
Ex. Cor. bone vol. to Non-Ex. cor. Vol.	4.30×10^{-3}	7.6×10^{-3}	2.225
Ex. Trab. bone vol. to Non-Ex Trab. Vol.	4.30×10^{-3}	4.99×10^{-3}	2.816
Trab. Surf. to Trab. Ex. Vol.	0.166	0.1928	5.563
Plasma to Trabecular Surfaces	2.8	0.9220	15.02
Ex. Trab. bone Vol. to Trab. Surf.	4.30×10^{-3}	0.01794	172.0
Plasma to Urinary bladder contents	1.73	2.58473	3.698
Urinary bladder to Urine	5.00	11.3111	4.771
Plasma to G.I tract contents	5.25E-01	0.6603	2.952
G.I tract contents to Feces	1.00	0.58374	2.395

Table 12: Summary of Geometric mean and GSD values along with the default values for systemic model for 11 non-human primates *using separate* urine and feces data

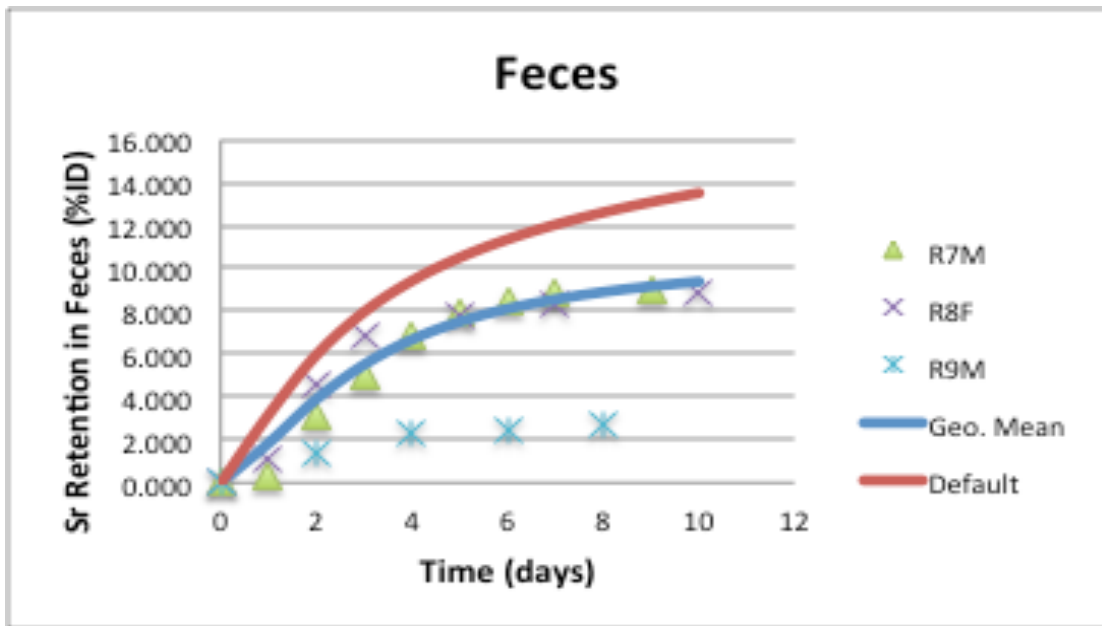


Figure 32: Strontium-90 retentions in feces predicted by the systemic model using default and geometric mean parameters respectively

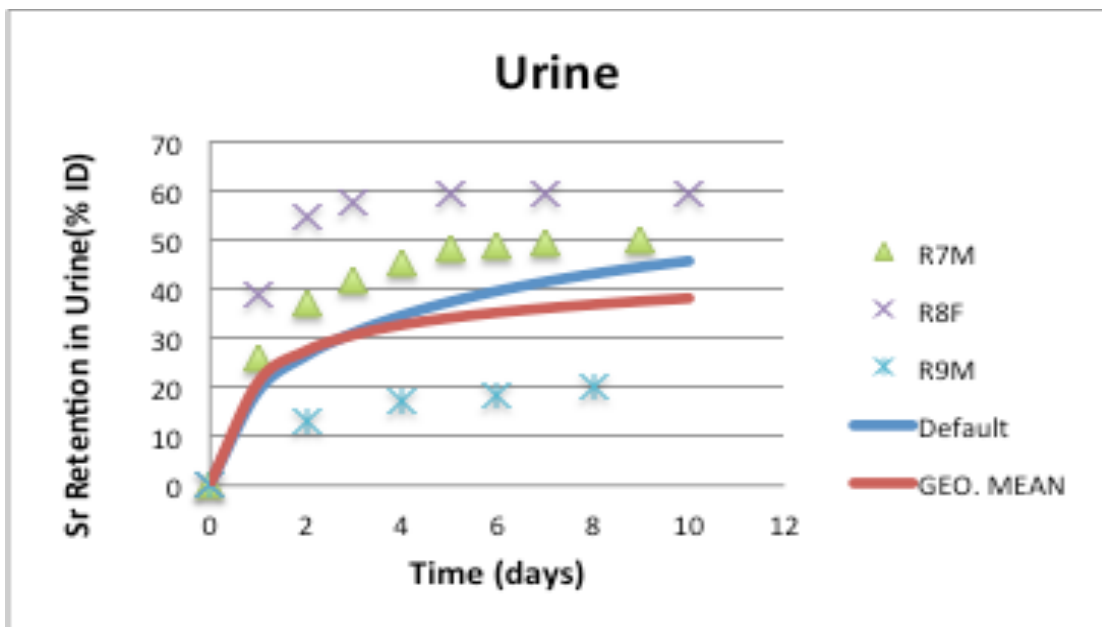


Figure 33: Strontium-90 retentions in urine predicted by the systemic model using default and geometric mean parameters respectively

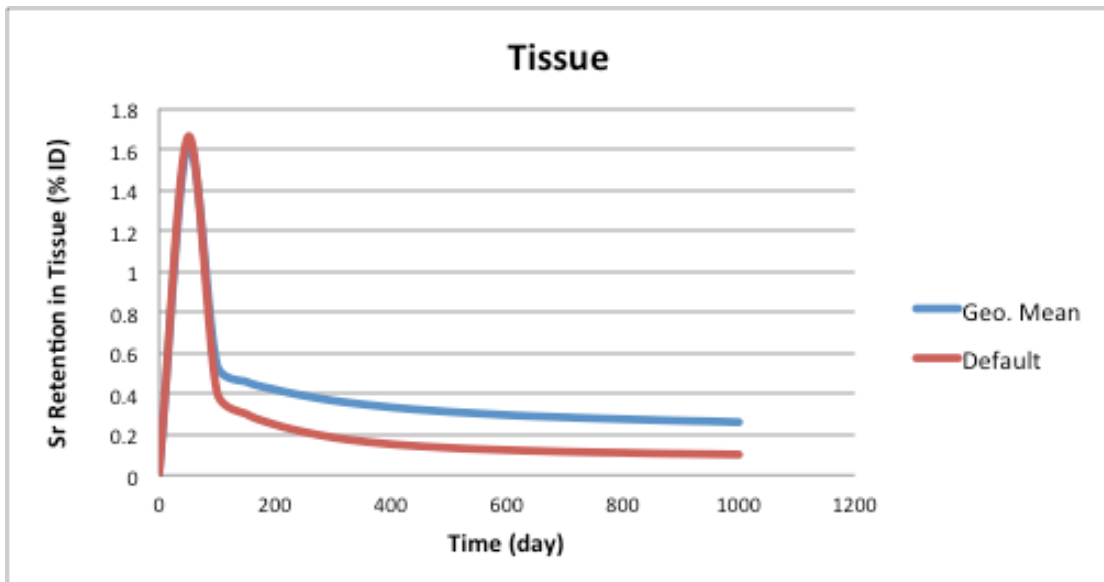


Figure 34: Strontium-90 retentions in soft tissue predicted by the systemic model using default and geometric mean parameters respectively

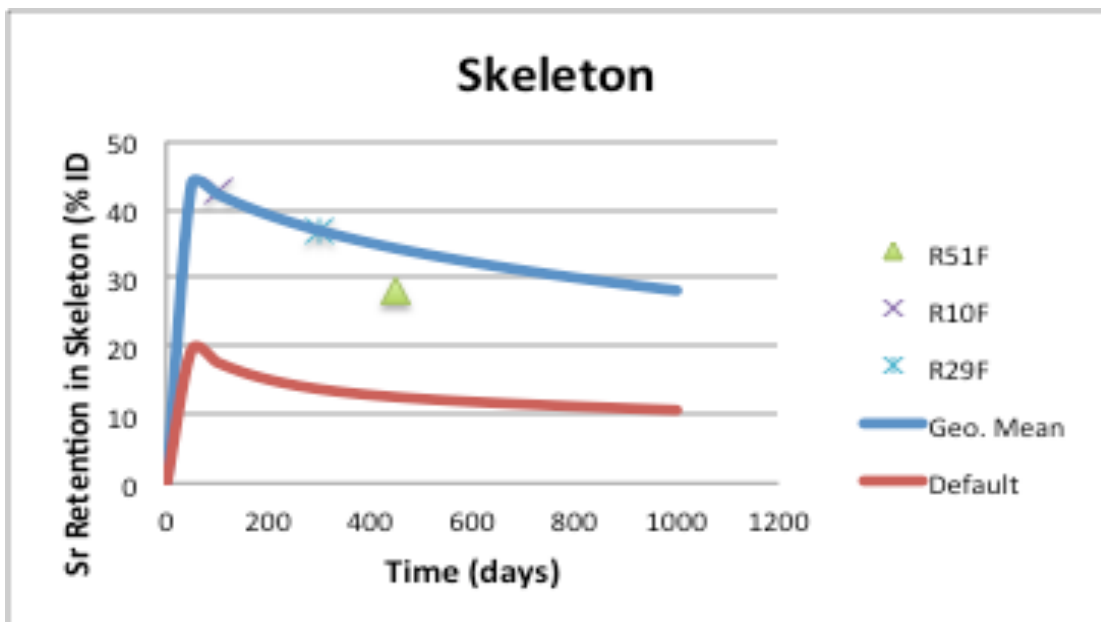


Figure 35: Strontium-90 retentions in skeleton predicted by the systemic model using default and geometric mean parameters respectively.

Figure 32 showed the percentage of Sr-90 retained in feces as predicted by the systemic model using parameters of the geometric mean and the default parameters. It was realized that the default values were slightly higher than the predicted values especially between days 4 and 10. Figure 33 showed that the predicted retention in urine was significantly lower than the default values by about 10%. Figure 34, on the other hand, illustrated strontium retention in soft tissues. The default retention values and the predicted retention values were similar within the first 100 days. However, there were slight variations between the default values and the predicted retention values from day 100. The predicted retention values were higher than the default values by about 0.2%. The overall trend that was observed was the retention values increased from the time of injection and reached a peak of 1.6 % at around day 50. The peak dropped drastically to about 0.5% and decreased gradually. There is no clear evidence illustrate the difference that occurs between default and geometric mean parameters after 100 days.

Figure 35 illustrated Sr-90 retention in the skeleton. It was realized that the predicted retention values were significantly higher than the default retention values by about 25%. In addition, both retention values were high immediately after injection. However, the rate of retention decreased gradually after day 100. There are many factors may dominate predictions at various stages, these factors are age, fasting, low dietary levels of calcium, magnesium, phosphorus, milk diets and vitamin D (ICRP 1993).

Table 10 and 11 indicated a summary of the geometric means and GSD values along with the default values of the systemic model. In total, twenty-two different parameters were used in the computation of the geometric means and GSD values. Seven out of the twenty-two parameters showed the movement of Sr-90 from various surfaces

to plasma. The remaining parameters showed the movement of Sr-90 from plasma to other surfaces as well as into the bladder and the gastrointestinal tract. It is important to note that there is no real difference between default and geometric mean values when considering the GSD values (range from 6.08 to 2.2).

The values of total objective function and AIC are indicated in Table 13 and 14. The values were automatically calculated by SAAM II software. It can be seen that the optimized model is fitting the measured data much better than the default model.

Case #	AIC default model	AIC optimized model	Δ AIC
R7M	3.53042	2.728445	0.801
R8F	3.54758	0.7529	2.794
R9M	4.22343	1.3889	2.834
R10F	4.94420	3.3892	1.555
R33F	3.20152	0.4602	2.741
R34F	4.25279	1.3497	2.903
R35F	4.37072	0.9267	3.444
R27M	4.52358	1.2713	3.252
R28F	5.93133	1.95305	3.978
R29F	5.37549	1.4347	3.940
R32F	4.34712	1.1633	3.183
R36F	5.04723	3.0166	2.030
R37F	5.88062	3.94162	1.939
R50F	5.25007	1.6741	3.575
R51F	4.45882	1.3283	3.130
R52F	4.48748	3.2779	1.209
R61M	2.51854	0.8059	1.712
R62M	3.25084	0.5799	2.670
R188F	4.97428	1.41200	3.562
R199M	4.65843	0.97426	3.684

Table 13: Differences in AIC values between default and optimized model.

Case #	total objective Function	total objective Function
	default model	optimized model
R7M	5.202	2.12
R8F	5.202	-0.60
R9M	6.520	0.415
R10F	7.676	3.7
R33F	4.518	-0.9
R34F	6.614	0.6
R35F	6.852	-0.32
R27M	7.177	0.45
R28F	9.982	1.2
R29F	8.798	0.38
R32F	6.837	0.34
R36F	6.256	2.20
R37F	6.923	4.01
R50F	8.606	1.1
R51F	6.984	0.19
R52F	6.470	3.2
R61M	3.168	-0.44
R62M	4.639	-0.84
R188F	6.111	0.36
R199M	6.812	-1.2

Table 14: The values of total objective function

4.3 Non-human Primates Data and IMBA Professional Plus Predictions

The activity of strontium (Sr) in bioassay data type (urine and feces) was also evaluated with the aid of the IMBA Professional Plus. Eleven of Rhesus Macaques were analyzed using the method of maximum likelihood in IMBA. The ICRP strontium systemic model was employed in the process.

Comparisons, were made between the data obtained from the non-human primates and the predicted values based on the ICRP 67 systemic model. The IMBA Professional Plus software employed the default parameters from ICRP 67 to provide fits to data and predict an intake for each case; furthermore, comparison between measured and expected values were obtained. As mentioned before, the urine and fecal bioassay data were analyzed both simultaneously and separately. In addition, the model was examined by applying transfer rates computed by geometric mean parameter values of 11 cases analyzed by the SAAM II software. The results of this analysis are plotted in Figures 36 to 55.

Case #	Injected	IMBA		
	Activity	predicted Activity (μCi)	Predicted Activity/	% Different
	(μCi)	Using default parameter	Injected Activity	
		Transfer		
R7M	37.50	30.97	0.825	17.5
R8F	39.70	36.75	0.925	-7.5
R9M	37.80	34.35	0.908	-9.2
R29F	41.60	23.51	0.565	-43.5
R33F	56.20	40.54	0.721	-27.9
R35F	56.10	25.47	0.45	-55
R50F	26.10	60	2.29	129
R51F	26.10	44.59	1.70	70
R52F	130.50	68.37	0.523	-47.7
R61M	117.60	90.27	0.767	-23.3
R191M	5	3.60	0.72	-28

Table 15: Measured and predicted intake values of Strontium activity using combined urine and feces data and the maximum likelihood method in IMBA Professional Plus

From Table 15, it was seen that the highest injected activity was 130.5 μCi , whereas the lowest injected activity was 5 μCi . The IMBA predicted quantities using the ICRP default values were lower than the injected activity in most the non-human primate subjects. In addition, the ratio of the predicted activity and the injected activity was less than 1 in eight out of the eleven cases. In two instances, the ratio was more than one (R50F and R51F), whereas the ratio was less than 0.5 in one subject (R53F). It was also observed that the predicted activity values decreased in proportion to the injected activity and vice versa. The highest predicted activity was obtained at the injection activity of

26.10 in subjects R51F and R50F where the predicted activities were approximately two times higher than the injected activities. The overall trend was that IMBA underestimated the amount of injected activity in all cases except in R50F and R51F.

Case #	Injected	IMBA		% Different
	Activity (μCi)	predicted Activity (μCi) Using optimized parameter Transfer	Predicted Activity/ Injected Activity	
R7M	37.50	40.21	1.07	7
R8F	39.70	40.10	1.01	1
R9M	37.80	37.97	1.0	0
R29F	41.60	29.08	0.7	-30
R33F	56.20	37.78	0.67	-33
R35F	56.10	41.54	0.74	-26
R50F	26.10	62.16	2.4	140
R51F	26.10	79.64	3.05	205
R52F	130.50	95	0.73	-27
R61M	117.60	75.67	0.64	-36
R191M	5	5.27	1.05	5

Table 16: Measured and predicted intake values of Strontium activity using combined urine and feces data and the maximum likelihood method in IMBA Professional Plus using optimized Parameter Transfer by SAAM II

The IMBA predicted activity using SAAM parameter transfer values were higher than the injected activity thereby giving high ratios of predicted activity and injected

activities. It was seen that the ratio of the predicted activity and the injected activity was slightly more than 1 in 6 out of the total 12 nonhuman primates. The ratio of the predicted versus injected was twofold in subject R50F and threefold in subject R51F. In the remaining five cases, the ratio of the predicted activity and the injected activity was less than 1 but more than 0.6. Those values showed that IMBA Professional Plus using SAAM parameter transfer overestimated the activity of strontium in non-human cases, in two samples. However, the SAAM parameter prediction was relatively accurate in its predictions in four of the samples (R7M, R8F, R9M, and R191M) since the ratio of the predicted value and the injected value gave 1 and values that exceeded 1 by negligible margins.

A comparison between Table 15 and Table 16 revealed that the IMBA predicted activity using optimized parameter transfer (in Table 16) had higher values than the predicted activity using the default in Table 15. The higher values led to the comparatively higher ratios of predicted activity and injected activity. That observation implied that IMBA prediction using optimized parameter transfer overestimated strontium activity more than the default parameter. In addition, it was realized that Table 15 did not have any instance where the predicted strontium activity was equal to the injected activity. (Further details in section 4.3 based on statistics tests)

Case #	Injected Activity (μCi)	Urine predicted Injected Activity (μCi)	Fraction Predicted / Injected	Feces Predicted Injected Activity (μCi)	Fraction Predicted / Injected
R7M	37.50	25.68	0.68	21.08	0.56
R8F	39.70	31	0.78	29.70	0.75
R9M	37.80	25.22	0.67	12.70	0.34
R29F	41.60	7.87	0.19	17.75	0.43
R33F	56.20	40.97	0.73	10.84	0.20
R35F	56.10	30.72	0.55	15.45	0.28
R50F	26.10	63.78	2.44	57.94	2.22
R51F	26.10	54.62	2.10	37.51	1.44
R52F	130.50	68.29	0.52	47.86	0.37
R61M	117.60	97.70	0.83	85.59	0.73
R191M	5	3.59	0.72	3.0	0.60

Table 17: Measured and predicted intake values of Strontium activity using urine, feces data separately and the maximum likelihood method in IMBA Professional Plus

Table 17 indicated that, in all the samples, higher strontium activity was predicted by IMBA in urine data than in feces data. There was no instance where the separate prediction of strontium activity in urine or feces gave precise estimates. For the urine data, IMBA underestimated the strontium intake in all the samples except in R50F and R51F. In sample R29F and R52F, the predicted activities were five times and two times more than the injected values. For the feces data, similarly, all the strontium intake values

were underestimated by IMBA except for samples R50F and R51F. There was no case where the IMBA predicted value was similar to the injected strontium activity. Therefore, it could be deduced that IMBA did not give correct estimates of strontium activity in separate urine and feces data. (Further details in section 4.3 based on statistics tests).

Case #	Injected Activity (μCi)	Urine predicted Injected Activity (μCi)	Fraction Predicted / Injected	Feces Predicted Injected Activity (μCi)	Fraction Predicted / Injected
R7M	37.50	40.24	1.07	31.62	0.84
R8F	39.70	52.35	1.31	41.62	1.04
R9M	37.80	38.45	1.01	18.27	0.48
R29F	41.60	14.36	0.34	27.02	0.65
R33F	56.20	66.75	1.18	20.75	0.37
R35F	56.10	30.72	0.55	15.45	0.27
R50F	26.10	81.08	3.10	86.21	3.30
R51F	26.10	67.56	2.58	55.13	2.11
R52F	130.50	108.10	0.83	80.18	0.61
R61M	117.60	96.05	0.82	83.75	0.71
R191M	5	5.64	1.13	5.13	1.03

Table 18: Measured and predicted intake values of Strontium activity using urine, feces data separately and the maximum likelihood method in IMBA Professional Plus using optimized Parameter Transfer

Optimized parameter transfer overestimated the injected activity of strontium in all urine data except in cases R29F, R35F, R52F, and R61M. In R29F, the predicted value was five times less than the actual injected value. However, for the feces data, optimized parameter transfer underestimated the strontium activity in all cases except in R8F, R50F, R51F, and R191M. There were significant underestimates in cases R33F and R35F where the predicted activities were five times less than the injected activities. Similar trends were observed in the predicted activities of feces and urine data. For example, when the predicted activity of urine increased in a given case, the feces activity also increased in the same case.

A comparison of Table 17 and Table 18 revealed a similar trend in both tables that the predicted strontium activity was higher in urine than in feces. However, some cases showed opposite trends in the predicted and injected activities using SAAM II optimized parameter transfer and the default parameters. In Table 17, for example, it was seen that the predicted values of urine and feces data for case R191M were lower than the injected values. In Table 18, the same sample had higher predicted activities of urine and feces data than in Table 17. That observation meant that using two different methods of prediction could give totally opposite results for the same sample. (Further details in section 4.3 based on statistics tests).

4.3.1 Chi-square and Autocorrelation Test Results

The Chi-square and Autocorrelation test illustrated the “goodness of fit” between predicted and measured data for default and optimized parameters. This information is summarized in Table 19 for combined urine and feces, and Table 20, 21 for separate urine and feces data.

Case #	Default Model		Optimized Model	
	Chi-square	Autocorrelation (P-value)	Chi-square	Autocorrelation (P- value)
R7M	3.68	1.12×10^{-2}	5.24	5.4×10^{-2}
R8F	4.75	1.9×10^{-2}	2.25	1.2×10^{-1}
R9M	1.34	9.6×10^{-1}	1.99	9.2×10^{-1}
R29F	9.3	6.6×10^{-2}	7.12	3.0×10^{-1}
R33F	1.77	1.6×10^{-2}	3.88×10^{-1}	0.00
R35F	1.43×10^{-1}	2.08×10^{-2}	1.31×10^{-1}	5.6×10^{-3}
R50F	4.11	0.00	3.23	0.00
R51F	1.55	0.00	3.84	0.00
R52F	2.25	9.58×10^{-1}	2.69×10^{-2}	8.5×10^{-2}
R61M	1.38×10^{-1}	0.00	2.2×10^{-1}	0.00
R191M	9.5×10^{-1}	9.35×10^{-1}	1.49×10^{-1}	2.9×10^{-1}

Table 19: Chi-square and Autocorrelation test results for optimized parameters using combined urine and feces data

From Table 19, it was seen that the chi-square tests were within the acceptable range ($P>0.05$), and the autocorrelation tests were also within the acceptable range ($P>0.05$) except the shaded values. Therefore the optimized and default models both fit the data well. However, the optimized model fit the measured data better than the default model in 3 cases.

Case #	Default for Urine		Optimized for Urine	
	Chi-square	Autocorrelation	Chi-square	Autocorrelation
	P- value	P-value	P-value	P- value
R7M	8.22×10^{-1}	2.00×10^{-1}	6.36×10^{-1}	6.70×10^{-2}
R8F	6.92×10^{-1}	2.36×10^{-2}	9.45×10^{-1}	1.08×10^{-1}
R9M	7.25×10^{-1}	8.97×10^{-1}	5.82×10^{-1}	8.12×10^{-1}
R29F	1.00	4.55×10^{-1}	1.00	3.65×10^{-1}
R33F	1.00	2.42×10^{-1}	9.99×10^{-1}	3.97×10^{-2}
R35F	1.00	2.28×10^{-1}	1.00	5.07×10^{-2}
R50F	1.00	0.00	1.00	0.00
R51F	1.00	0.00	1.00	0.00
R52F	9.46×10^{-1}	8.80×10^{-1}	1.00	2.64×10^{-1}
R61M	1.00	4.80×10^{-4}	1.00	0.00
R191M	9.96×10^{-1}	8.53×10^{-1}	1.00	9.08×10^{-2}

Table 20: Chi-square and Autocorrelation test results for Urine data

Table 20 illustrated that the chi-square tests were within the acceptable range ($P>0.05$), and the autocorrelation tests were also within the acceptable range ($P>0.05$) except the shaded values. Therefore the optimized and default models both fit the data well. However, the optimized model fit the measured data better than the default model in 4 cases.

Case #	Default for Feces		Optimized for Feces	
	Chi-square	Autocorrelation	Chi-square	Autocorrelation
	P- value	P-value	P-value	P- value
R7M	1.00	3.27×10^{-1}	1.00	4.03×10^{-1}
R8F	1.00	5.57×10^{-1}	1.00	6.12×10^{-1}
R9M	1.00	5.30×10^{-1}	1.00	4.46×10^{-1}
R29F	8.69×10^{-1}	1.07×10^{-1}	9.58×10^{-1}	3.11×10^{-1}
R33F	1.00	3.52×10^{-3}	8.89×10^{-1}	3.57×10^{-2}
R35F	1.00	4.94×10^{-1}	1.00	5.28×10^{-1}
R50F	1.00	0.00	1.00	0.00
R51F	1.00	0.00	1.00	0.00
R52F	1.00	2.59×10^{-1}	1.00	2.03×10^{-1}
R61M	1.00	6.66×10^{-4}	1.00	2.46×10^{-4}
R191M	1.00	3.97×10^{-1}	1.00	2.98×10^{-1}

Table 21: Chi-square and Autocorrelation test results for feces data.

Table 21 indicated that, the chi-square test (p-value) are large for both models of urine and feces data, while the autocorrelation test (p-value) are large for most cases except the shaded values. However, the optimized model feces did not improve the fit to the measured data, and the chi-square (p-values) and autocorrelation (p-value) are almost matching for both models.

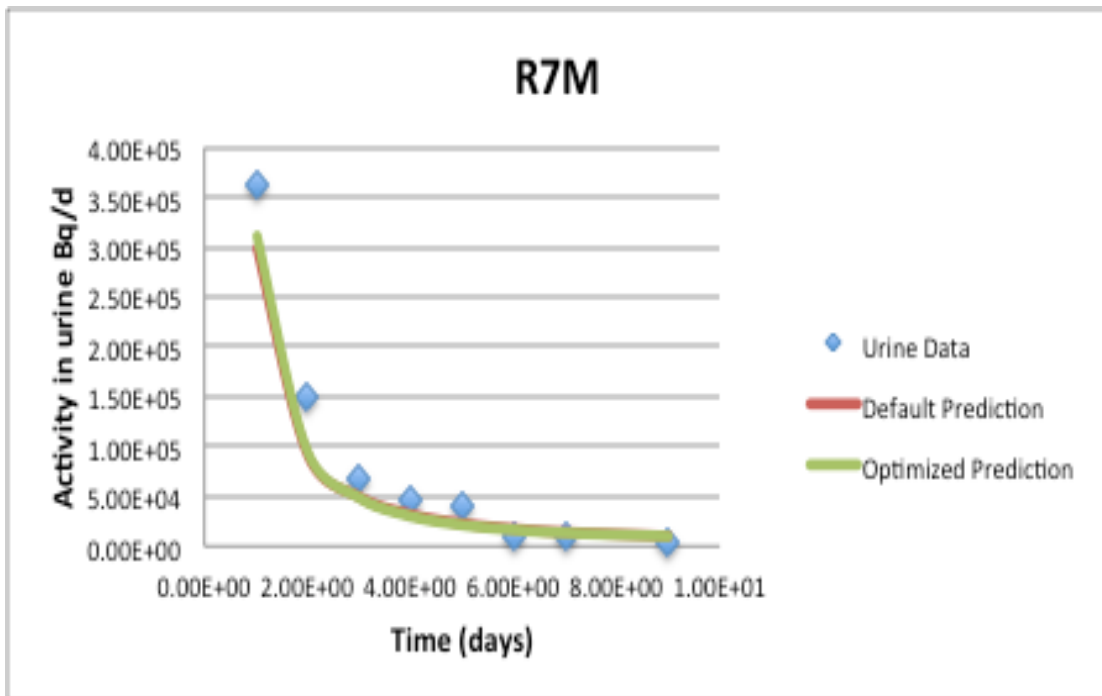


Figure 36: Model fitted activity of urine data using default and optimized parameter transfer

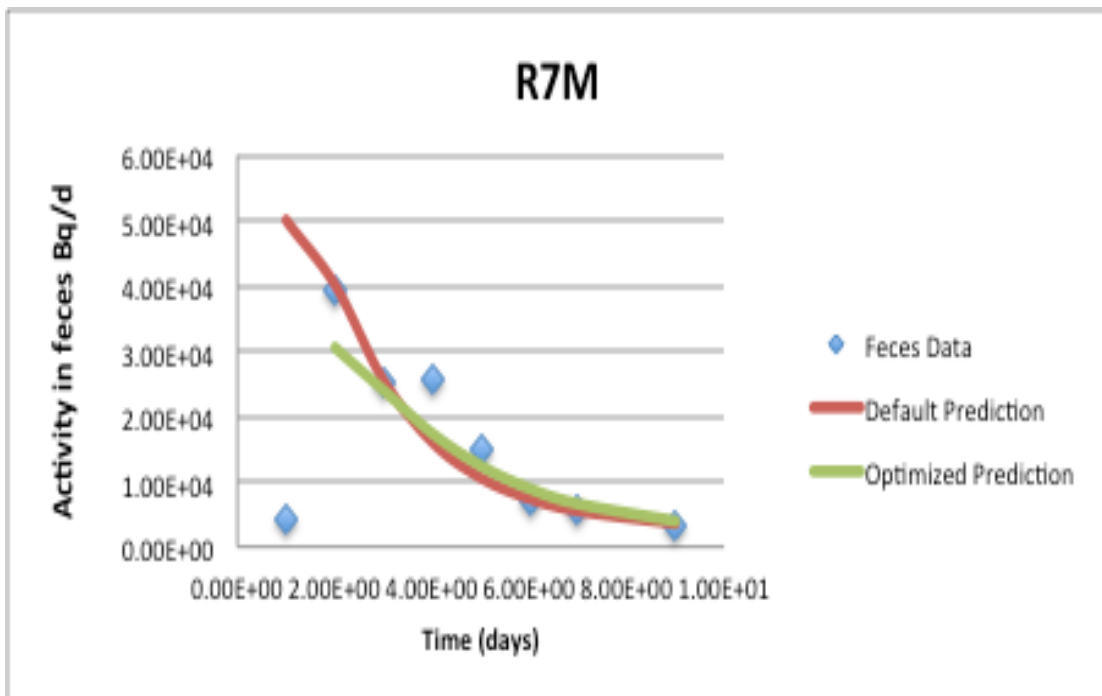


Figure 37: Model fitted activity of feces data using default and optimized parameter transfer

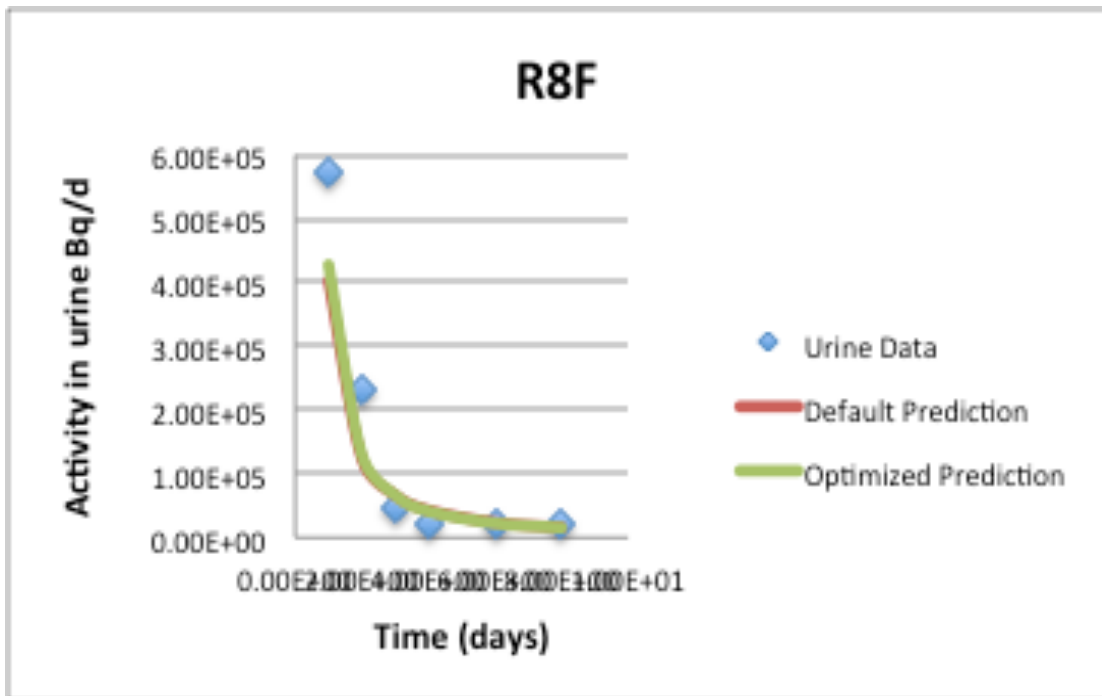


Figure 38: Model fitted activity of urine data using default and optimized parameter transfer

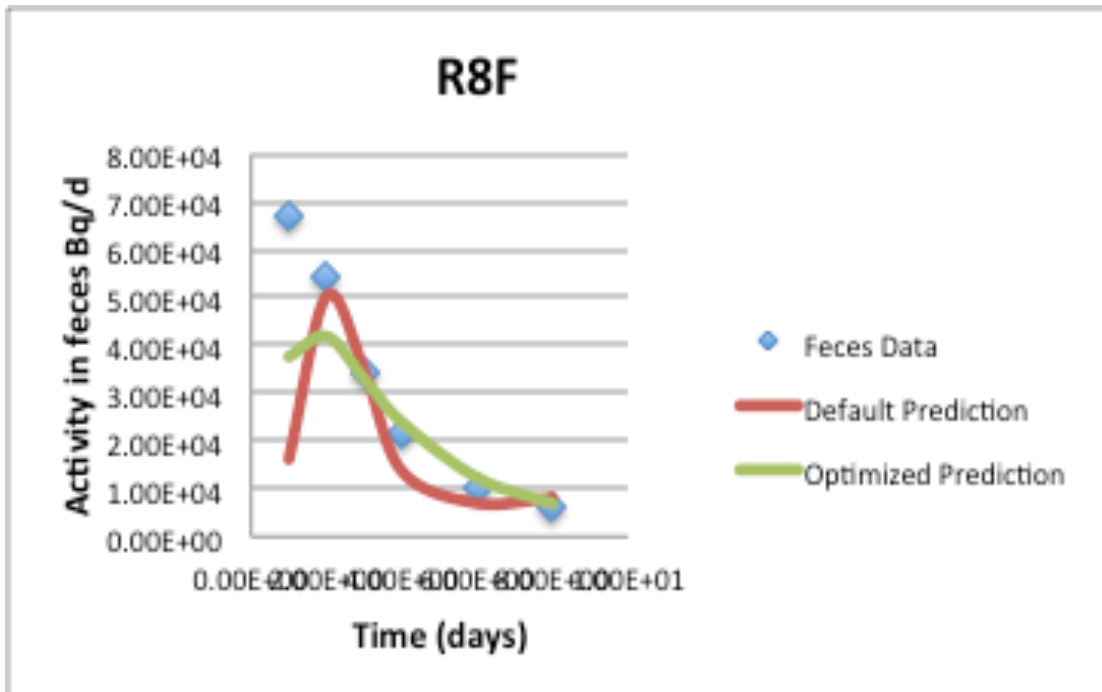


Figure 39: Model fitted activity of feces data using default and optimized parameter transfer

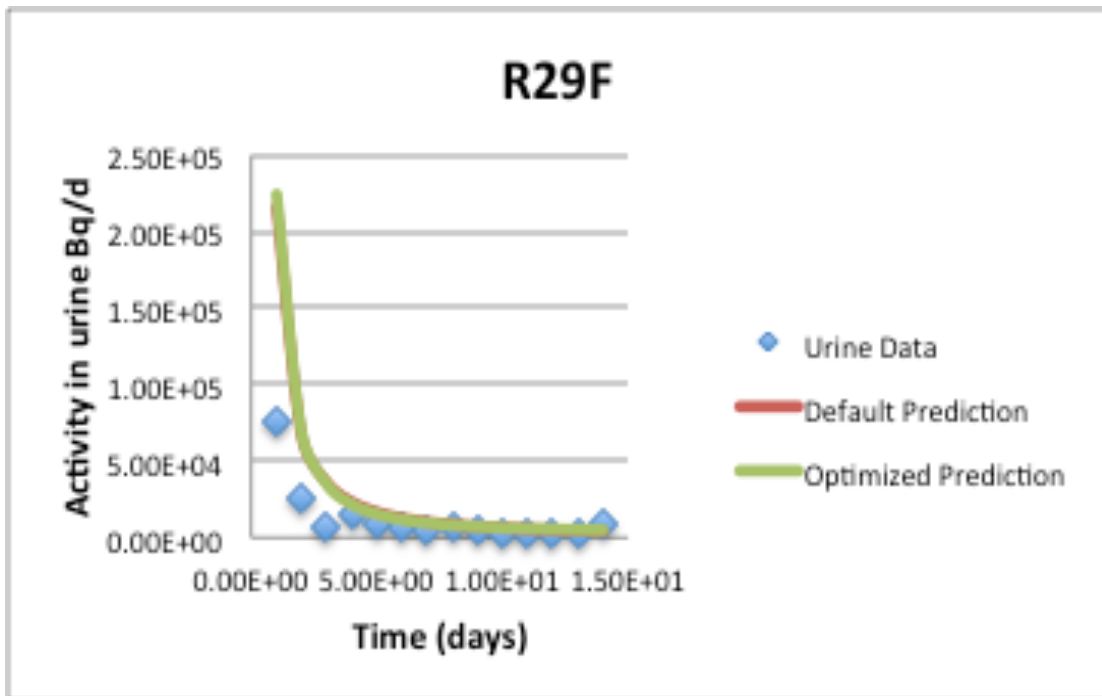


Figure 40: Model fitted activity of urine data using default and optimized parameter transfer

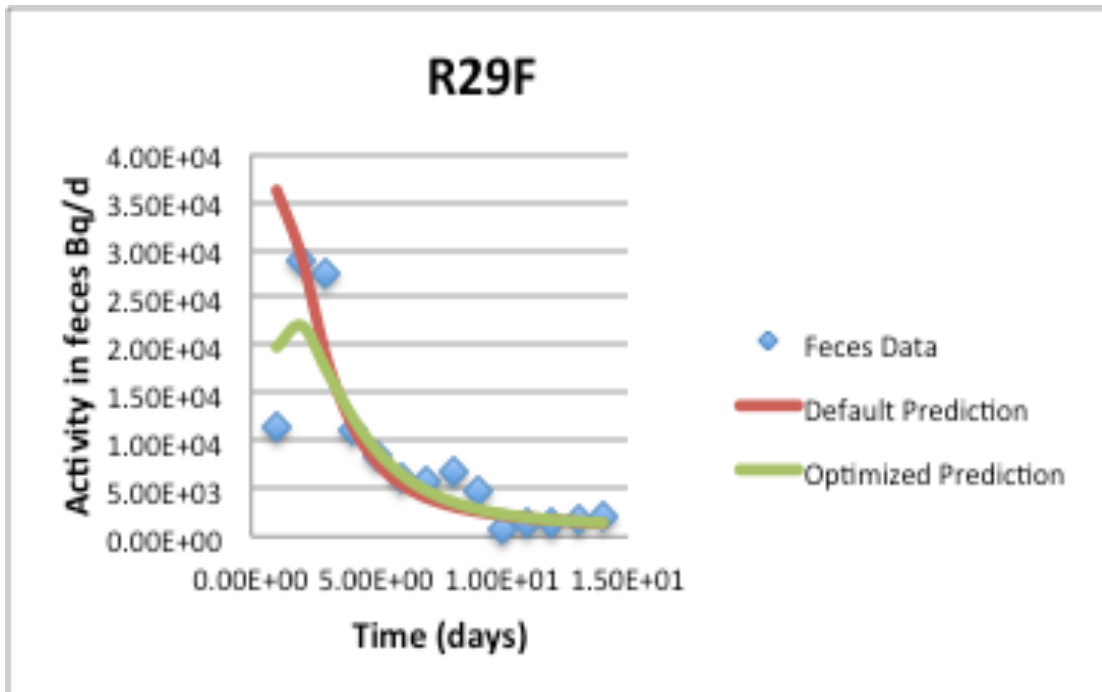


Figure 41: Model fitted activity of feces data using default and optimized parameter transfer

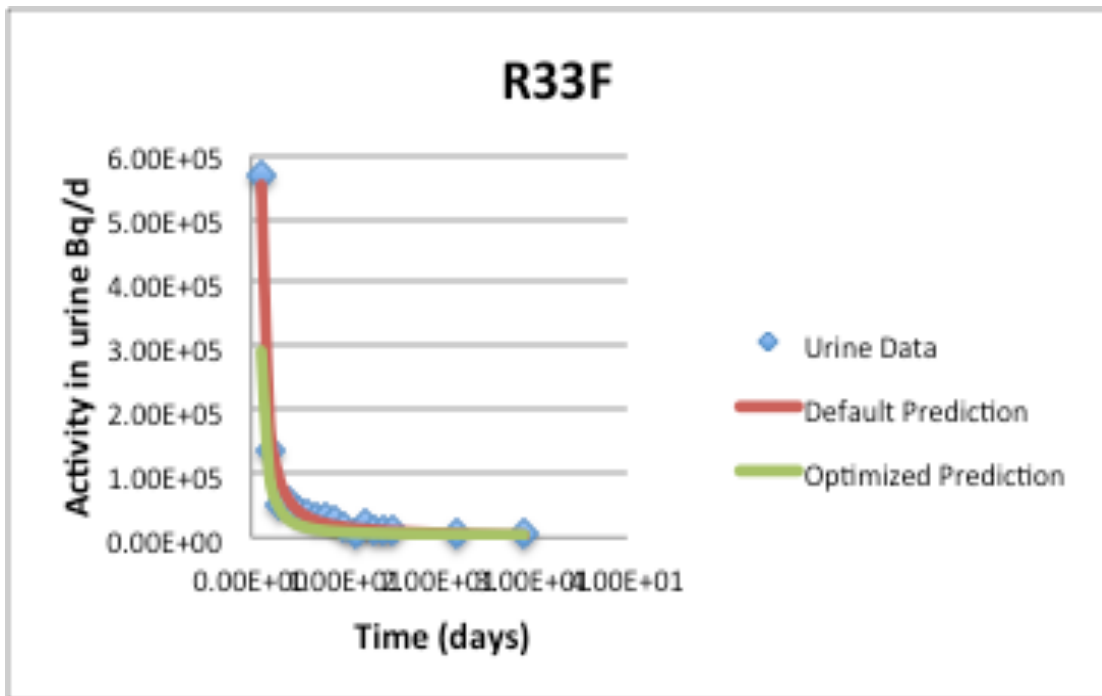


Figure 42: Model fitted activity of urine data using default and optimized parameter transfer

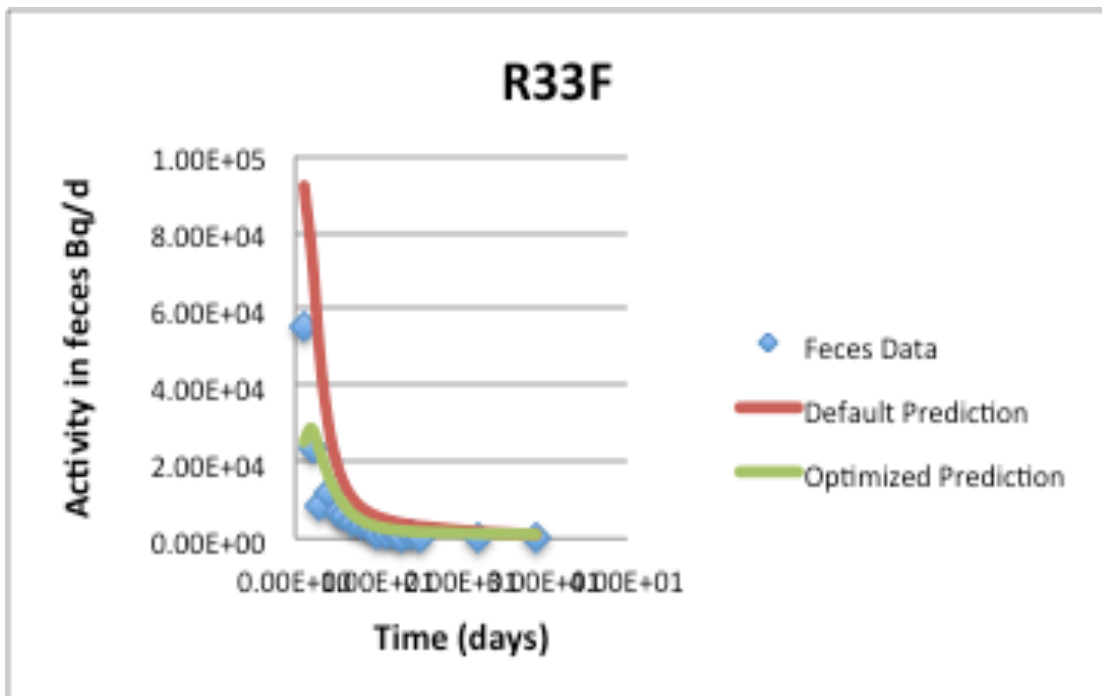


Figure 43: Model fitted activity of feces data using default and optimized parameter transfer

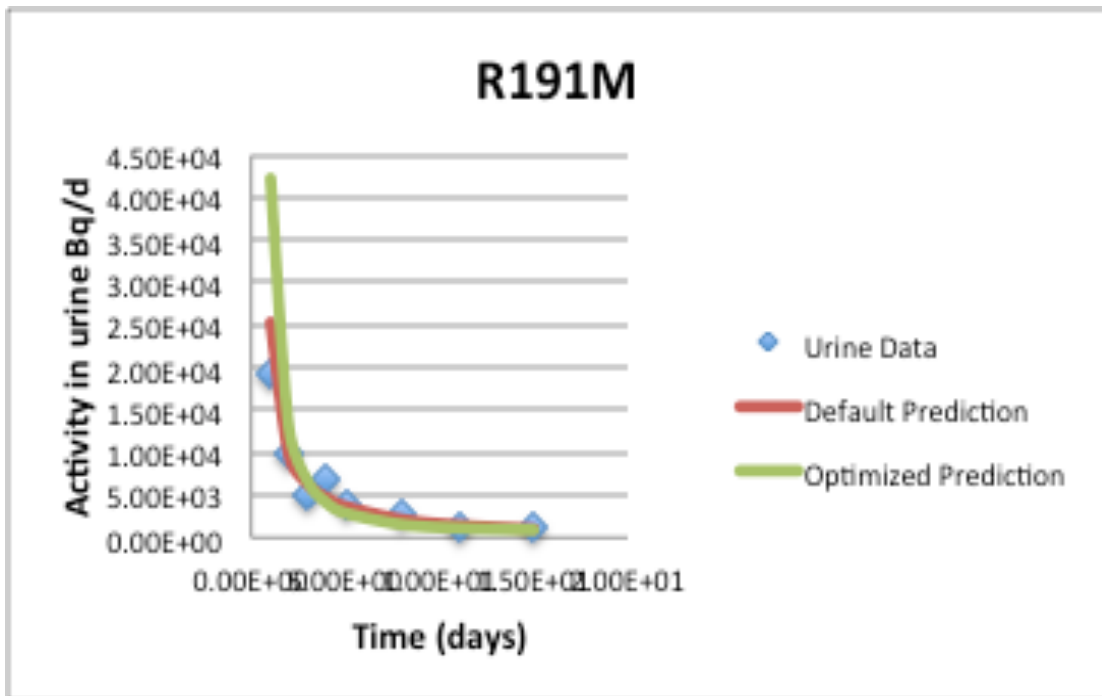


Figure 44: Model fitted activity of urine data using default and optimized parameter transfer

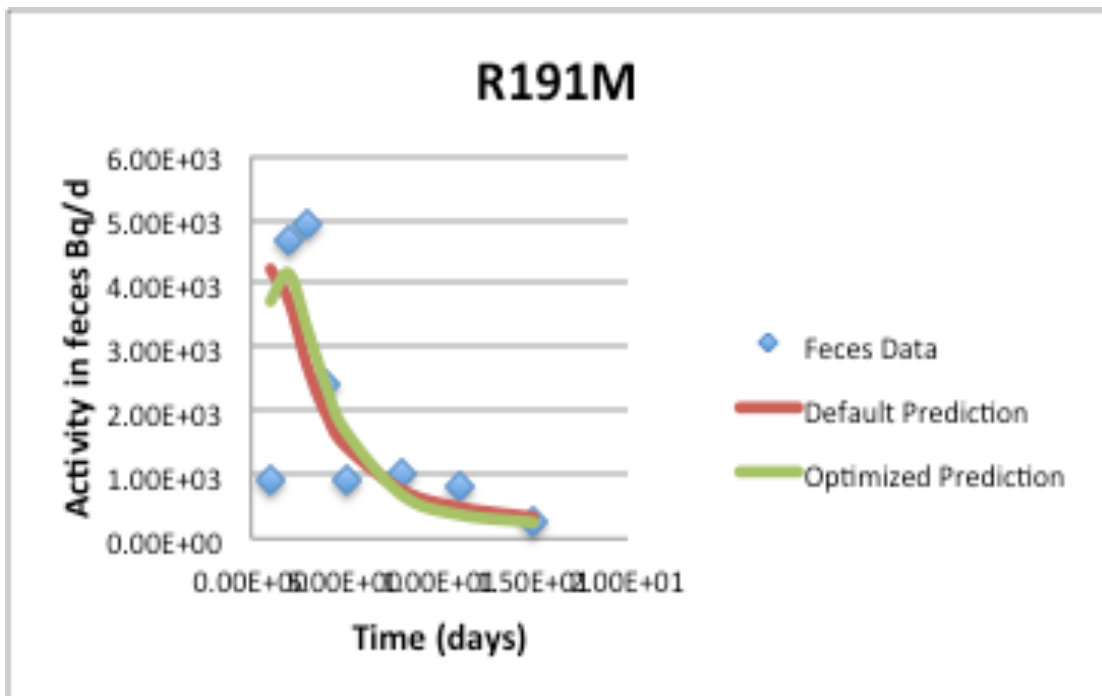


Figure 45: Model fitted activity of feces data using default and optimized parameter transfer

Figures 36 to 45 show the data fitted for urine and feces samples using the default parameter and optimized parameter transfer. It was seen that the data generated from urine samples exhibited different fits from data obtained from feces samples from the ICRP 67 default and SAAM optimized transfers coefficients. The overall trend that was seen in the urine samples (in both parameters) was that the predictions of excretion decrease as time progressed. The initial excretion was very high on the first day after injection. However, that rate reduced exponentially with an increase in time. In the urine samples, optimized and default models gave a good fit for all the cases since the chi-square probabilities are large than 0.05. The predicted transfers and the urine data were in agreement as there were no serious discrepancies between the two values.

However, it was noted that feces samples did not improve the fit for the default model, thus the feces data were not in harmony with the predicted values as proposed by the default and the optimized transfer parameters. In addition, different trends were observed for the SAAM and default transfer parameters. For example, in the default transfer, it was observed that the initial transfer was very high on the first day of injection and decreased as time progressed just as was the case with urine samples. However, a different overall trend was observed for the optimized values. The initial injection value was low. That value increased slightly reaching a peak sometime after injection and finally began decreasing exponentially as time progressed. A similar overall trend in all feces data was seen from most figures. However, it was observed that the predicted values and the feces data had some discrepancies. Those differences could be attributed to the nature of the two samples (urine and feces). Feces, as a sample, contain more

matrix compared to urine. The differences in the matrices were what were likely to have influenced the actual strontium concentration values that were recorded.

CHAPTER 5: SUMMARY AND CONCLUSIONS

Based on the results, the following hypothesis are supported:

First Alternative Hypothesis: The ICRP 67 optimized model will accurately predict the retention in excretion and skeleton using SAAM II software.

Second Alternative Hypothesis: The ICRP 67 default model and optimized model using IMBA software will predict the excretion and deposition of ^{90}Sr from intravenously injected in Rhesus monkeys.

Third Null Hypothesis: The predicted ^{90}Sr intake of urine and feces data using default model and optimized model in IMBA software are significantly different from injected intake.

According to AIC test results for optimized parameters, the predicted retention values yielded acceptable matches to the bioassay data in the combined and independent urine and feces data. While the default parameter underestimated the measured retention values. Strontium retention in excretion as a function of time revealed that the percentage Sr-90 retained increased with time. The rate of increase was very high within the first 50 days after which it declined progressively until the time of death of the non-human primates.

The predictions of the skeletal retention of Sr-90 as given by the SAAM II software gave a near-perfect fit to the data. In many cases, the skeleton retained all the strontium thereby giving a retention ratio of 1. Additionally, the ratio of predicted to measured values in the skeleton was 1 during the final stages of the primates' lives. These

observations could be attributed to strontium metabolism, which resembled the metabolism of calcium. The number of days post injection did not influence the predicted skeleton retention values. The fraction of the predicted over the measured values ranged from 0.88 to 1.1. The fraction was more than one for two cases, case R8F (3,506 days post injection) and case R33F (2,278 days post injection). SAAM II underestimated the skeletal retention in only one of the cases (R191M that had a ratio of 0.88).

The underestimation of the skeletal retention in the above case suggested that the ICRP 67 systemic model could be improved by modifying the biokinetic parameters within the established model structures. Therefore, SAAM II software was used to improve the efficiency of the original transfer rates explained in the ICRP 67 systemic model for strontium. The improvement was performed in the range of a tenth and tenfold the initial parameters. Excretion and skeleton data were used in the optimization process with the Bayesian technique. Twenty-two of the ICRP 67 default parameters explained in the model were optimized. The changes in the default parameters suggested by each individual set of animals data varied to summarized changes for all animals evaluated, the geometric means, geometric standard deviation AIC, and total objective function of each optimized value was calculated. The geometric means for each of the modified parameters for the 11 cases were presumed to represent the optimized model parameters for the population of monkeys. The retentions in feces, urine, skeleton, and soft tissue were evaluated against the default model predictions using the geometric mean parameters.

The activity of strontium in bioassay data type (urine and feces) for the 11 non-human primates was evaluated using the method of maximum likelihood with IMBA.

The ICRP 67 strontium systemic model was employed in the process. For default model, the predicted activity in combined urine and feces data was underestimated by IMBA in nine out of eleven instances. The predicted activity were lower than the injected activity in most cases of non-human primate ranged from 0.523 to 2.29. The same data were overestimated in two instances by twice the original injected values (R50F and R51F). The values of chi-square and correlations tests were computed. The chi-square p-value was greater than 0.05 for all cases and the autocorrelation was greater than 0.05 for six cases out of eleven instances.

The predicted intake values using combined urine and feces data and the maximum likelihood method in IMBA software using optimized parameters also yielded similar results. Almost half (6 out of 11) of the subjects had ratios of predicted activity and the injected activity that were slightly more than 1. The other half (5 out of 11) had ratios that were lower than one. Extreme cases of overestimation were observed in cases R50F (twofold) and R51F (threefold). The optimized model parameters were found to improve the predicted in three of eleven cases. The chi-square test calculated using both models were found to be greater than 0.05, thus it is hard to compare between them based on this test. However the chi-square and autocorrelation tests illustrated that the optimized model fit the observed data better than the default model in only three cases.

In SAAM II, it was impossible to compute the total intake from the bioassay data and skeleton. However, the same feat was possible when using the IMBA software

The ICRP 67 default systemic model prediction for strontium underestimated the measured retention values in excretion. The predicted activity in feces provided estimates that were lower than the bioassay measurement values. Modified parameter transfer provided adequate fits in the model for urine activity data compared to the default transfer rate in four cases out of eleven based on chi-square and autocorrelation test. However, it was noted that feces data could not be fitted properly by the modified model based on chi-square test. The improper fit was probably because the mode of strontium administration was intravenous, which did not allow more of the injected strontium to be detected through the contents of the gastrointestinal tract.

CHAPTER 6: FUTURE WORK

The biokinetic models optimized using the data on non-human primates indicate great variation between the animals themselves. These differences in the parameters may be attributed to the differences in physiology and behavior between the monkeys themselves. Organizing the monkeys into sub-groups based on the characteristics that dominantly affect the physiology may provide a better insight of the biokinetic models. Some of these characteristics may be age of animals, sex, etc.

Animals used in this research, i.e., Rhesus monkeys (*Macaca mulatta*) are phylogenetically very similar to humans, but there exists certain physiological and anatomical differences, e.g., differences in physiology of digestion and the length of the alimentary canal, between these animals and humans. The differences in the biokinetic model parameters may be attributed to the differences in anatomy and physiology of monkeys and humans. In the future, the physiological similarities and the differences between the Rhesus monkeys and humans could be used to determine the applicability limitations of the human biokinetic model to monkeys or vice-versa.

This research uses excretory and skeletal data from the monkeys injected intravenously with ^{90}Sr . Data available on whole body counts and blood retention combined with the excretory and skeletal data can be used to better understand the biokinetics and develop a new model. Furthermore, data from animals injected intramuscularly with ^{90}Sr can also be used to understand NCRP 156 wound model in the future.

REFERENCES

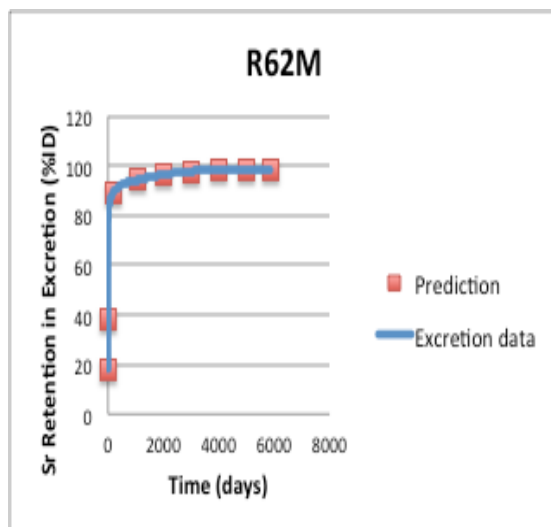
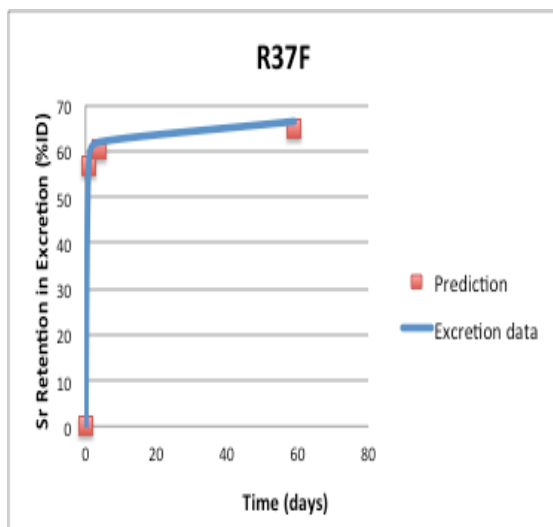
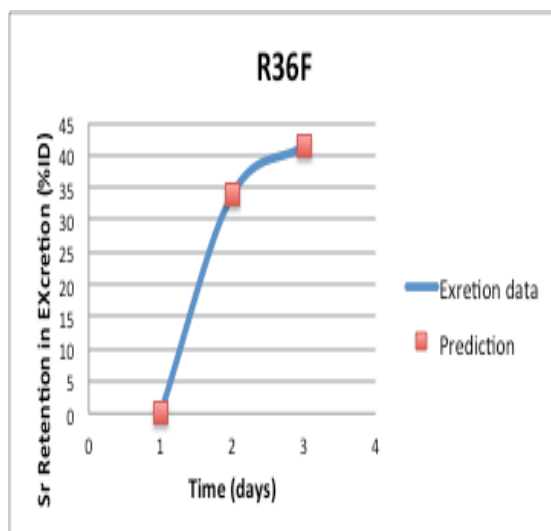
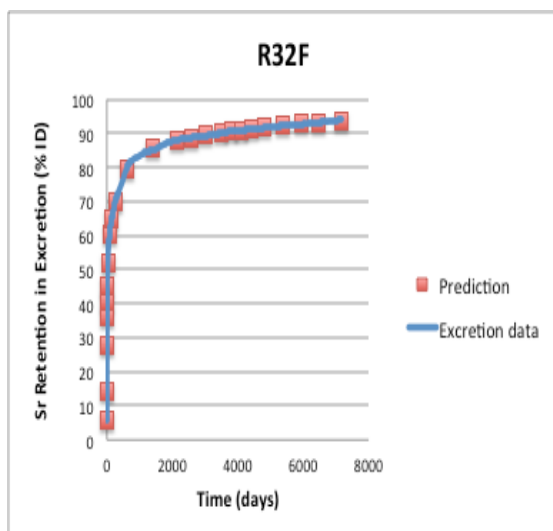
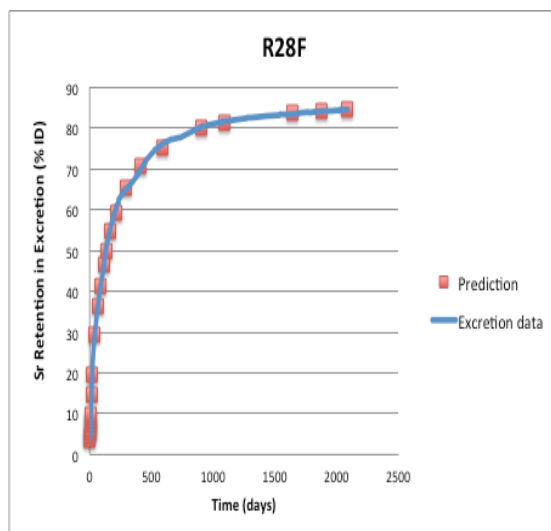
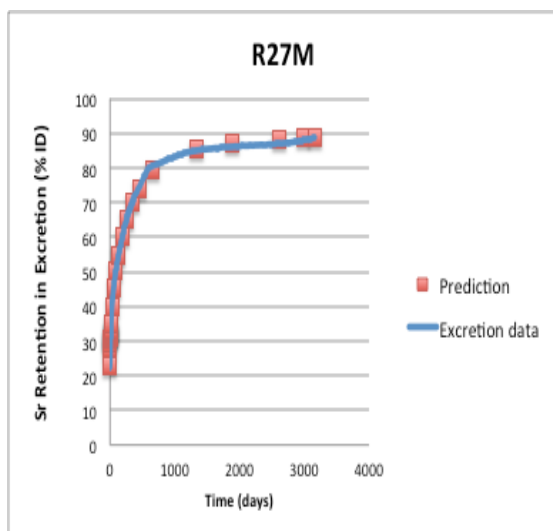
- Barrett, P. H. et al. (1998). SAAM II: simulation, analysis, and modeling software for tracer and pharmacokinetics studies. *Metabolism*.47: 484–492
- Birchall, A., Marsh, J.W., Davis, K., Bailey, M.R., Jarvis, N.S., Peach, A.D., Puncher, M., Dorrian M.D., James, A.C., Using IMBA Professional Plus to estimate intakes and doses SRP, 2005.
- Birchall, A., Puncher, M., James, A. C., Marsh, J. W., Jarvis, N. S., Peace, M. S., Davis, K. and King, D. J. IMBA expert(r): internal dosimetry made simple. *Radiation Protection Dosimetry*.105, pp. 421–425, 2003.
- Burnham, K. A., Anderson, D. R. (2002). Model selection and multimodel inference: a practical information- theoretic approach. 2nd ed. New York: Springer.
- Bligh, P. H.; Taylor, D. M. (1963). Comparative studies of the metabolism of strontium and barium in the rat. *Biochem. J.* 87:612-618.
- Bevington, P., Robinson, D. Data Reduction and Error Analysis for the Physical Sciences. Third Edition, McGraw Hill Higher Education; 2003.
- Derryberry DR. Personal Communication; 2014.
- Durbin PW, Jeung N, Williams MH, Parrott MW, Kullgren B, Tuttle LW. Collected original data on distribution of ⁹⁰Sr in bones of monkeys. Division of Life Sciences. Lawrence Berkeley Laboratory. LBL-28649. 1993a.

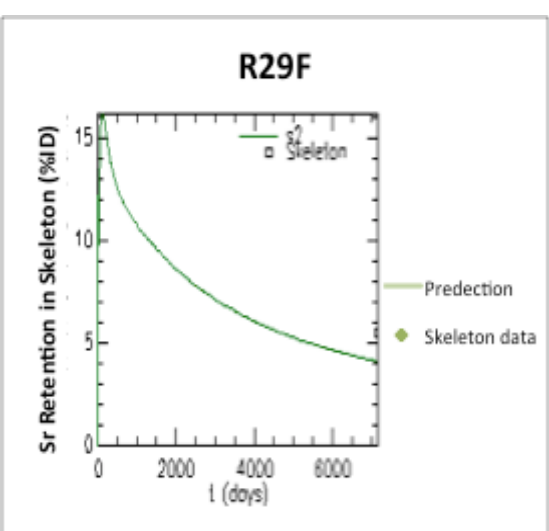
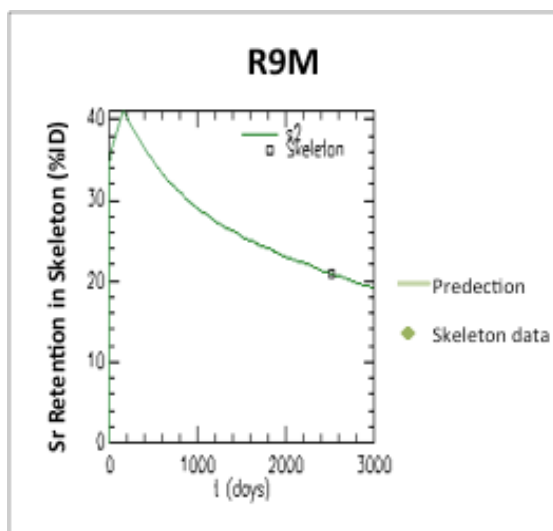
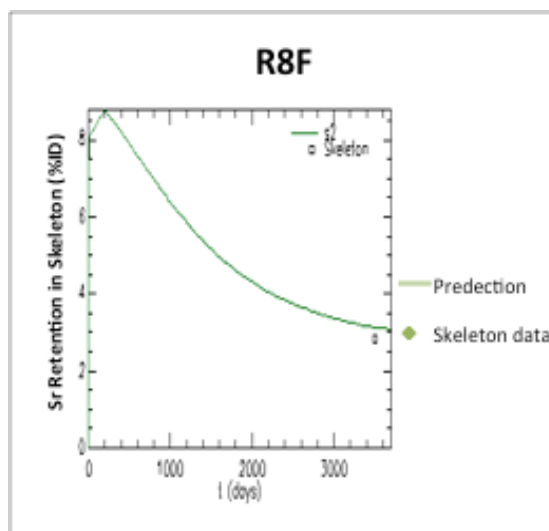
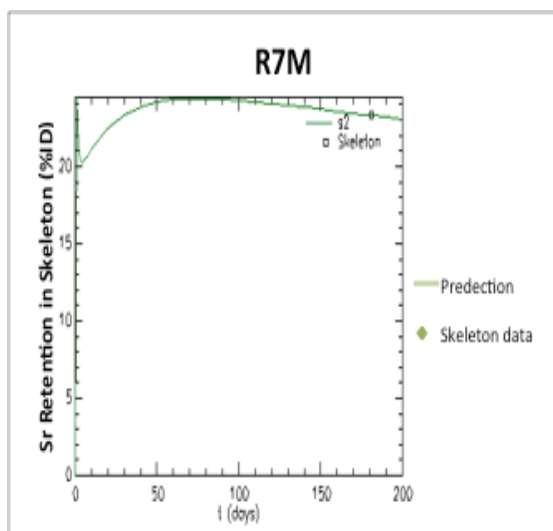
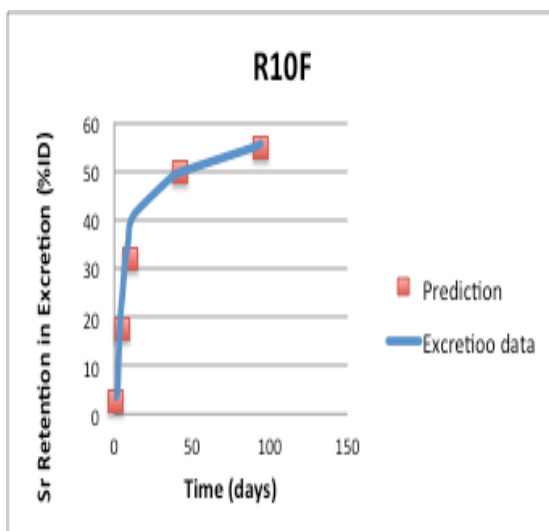
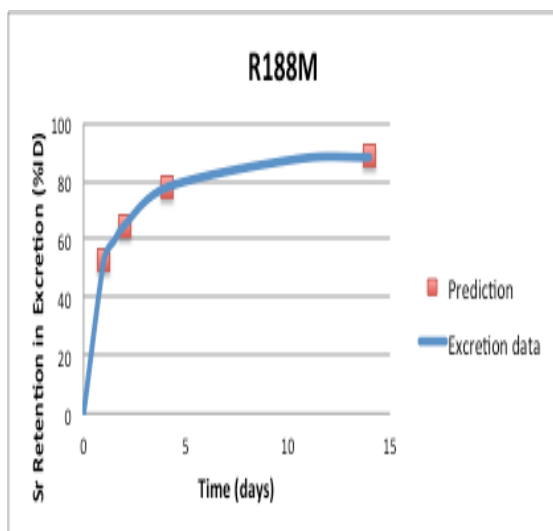
- Durbin PW, Jeung N, Williams MH, Parrott MW, Kullgren B, Tuttle LW. Collected original data on distribution of ^{90}Sr in bones of monkeys. Division of Life Sciences. Lawrence Berkeley Laboratory. LBL-28649. 1993b.
- Domanski, T.; Liniecki, J.; Witkowska, D. (1969). Kinetics of calcium, strontium, barium, and radium in rats. In: Delayed Effects of Bone-Seeking Radionuclides; ed. C.W. Mays, Univ. Utah Press, Salt Lake City pp. 79-
- Domanski, T.; Witkowska, D.; Garlicka, I. (1980). Influence of age on the discrimination of barium in comparison with strontium during their incorporation into compact bone. *Acta Physiol. Pol.* 31:289-296.
- International Commission on Radiological Protection. Age-dependent dose to members of the public from intake of radionuclides: Part 2, ingestion dose coefficients. New York: Pergamon Press; ICRP Publication 67. *Ann. ICRP* 23 (3-4); 1993.
- International Commission on Radiological Protection. Individual monitoring for internal exposure of worker: replacement of ICRP 54. ICRP Publication 78. *Ann. ICRP* 27(3-4);1997.
- James AC. User manual for IMBA Professional Plus (Version 4.0). AJC & Associates, Inc; 2005.
- Kshirsagar, S. G.; Lloyd, E.; Vaughan, J. (1966). Discrimination between strontium and calcium in bone and the transfer from blood to bone in the rabbit. *Br. J. Radiol.* 39:131- 140.

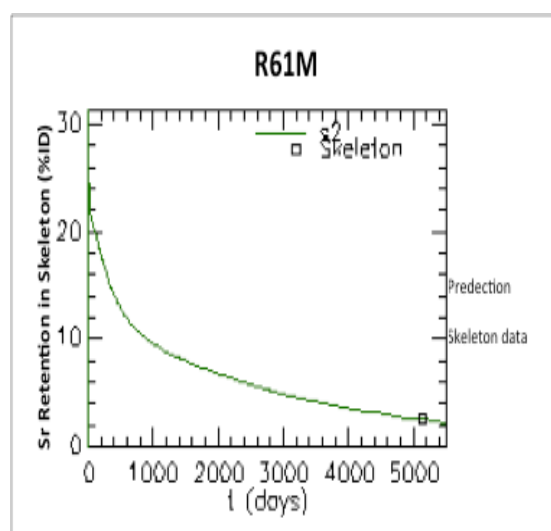
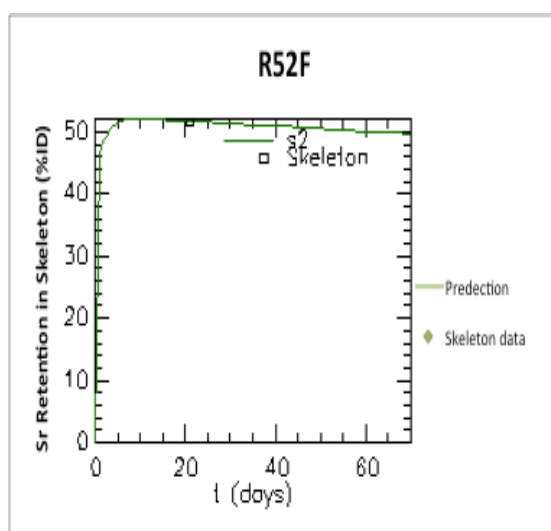
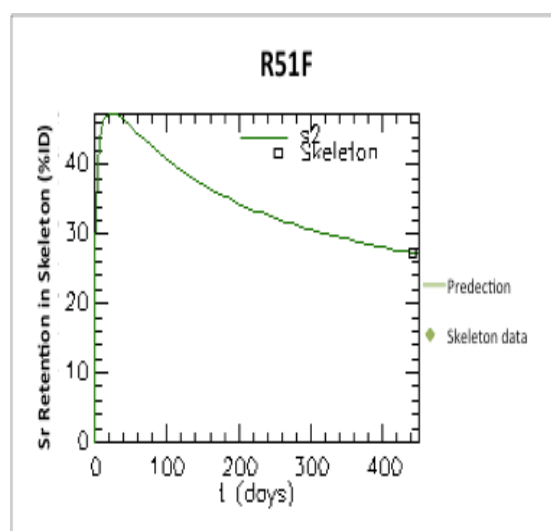
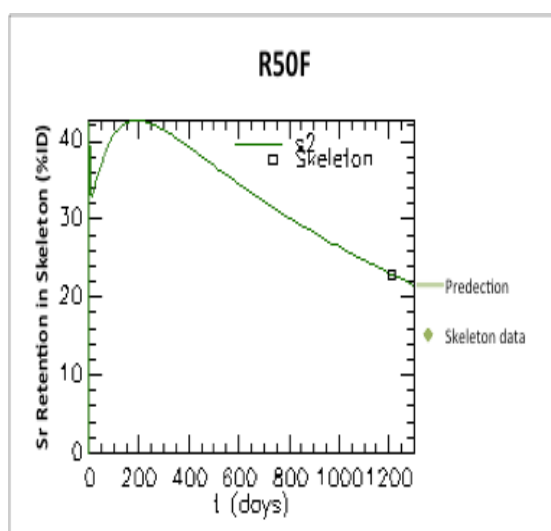
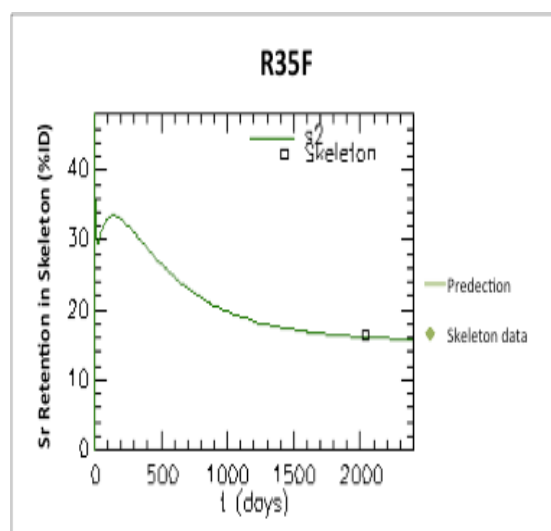
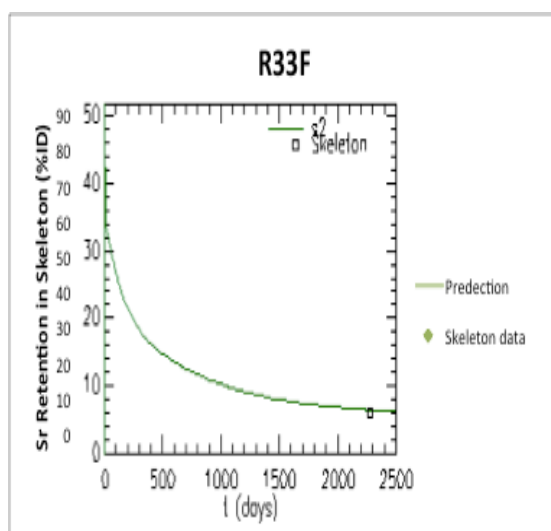
- Leggett, R.W., Eckerman, K.F., Meck, R.A., 2008. Reliability of Current Biokinetic and Dosimetric Models for Radionuclides: A Pilot Study. Oak Ridge National Laboratory: Oak Ridge, TN. ORNL/TM-2008/131.
- Leggett RW, Eckerman KF, Williams, LR. Strontium-90 in bone: a case study in age-dependent dosimetric modeling. Health Phys 43:307-322; 1982.
- Métivier, H. et al. "HUMAN ALIMENTARY TRACT MODEL FOR RADIOLOGICAL PROTECTION". A draft document by a Task Group of Committee 2 of The International Commission on Radiological Protection. 22/263/04. August, 2004
- Schlenker, R. A.; Keane, A. T.; Holtzman, R. B. (1982). The retention of Ra-226 in human soft tissue and bone; implications for the ICRP 20 alkaline earth model. Health Phys. 42:671-693.
- U.S. Department of Health and Human Services, Public Health Service, Agency for Toxic Substances and Disease Registry (ATSDR). "Toxicological profile for Strontium". Atlanta, GA: U.S. 2004.
- U.S. Environmental Protection Agency, Common Radionuclides Found at Superfund Sites. "EPA Facts About Strontium-90". Washington, DC. March, 2002.
- Washington State Department of Health, Division of Environmental Health Office of Radiation Protection. "Strontium-90", Fact Sheet 320-076. July, 2002.

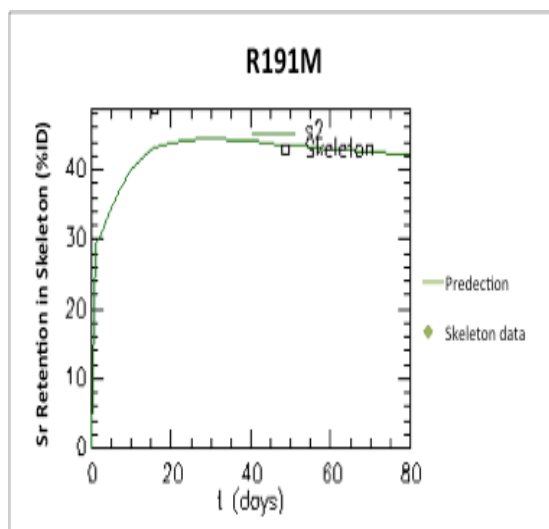
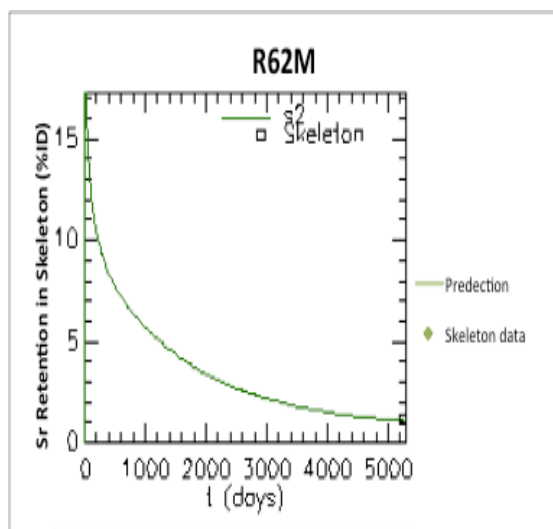
APPENDIX A

This section contains the rest of graphs that not presented in the thesis text. The comparison of measured and expected values were obtained for combined urine and feces data and Skeleton based on ICRP 67 systemic model for Strontium using SAAM II software.









APPENDIX B

Chi-square test and Autocorrelation test values

Case #	Chi-square	p-value	Autocorrelation	P-value
R7M	5.24	9.9×10^{-1}	2.96×10^{-1}	5.4×10^{-2}
R8F	2.25	9.97×10^{-1}	2.07×10^{-1}	1.2×10^{-1}
R9M	1.99	9.61×10^{-1}	-5.22×10^{-1}	9.2×10^{-1}
R29F	7.12	1.00	5.7×10^{-2}	3.0×10^{-1}
R33F	3.88×10^{-1}	3.0×10^{-1}	7.76×10^{-2}	<u>0.00</u>
R35F	1.31×10^{-1}	1.00	3.8×10^{-1}	<u>5.6×10^{-3}</u>
R50F	3.23	1.00	8.83×10^{-1}	<u>0.00</u>
R51F	3.84	1.00	8.99×10^{-1}	<u>0.00</u>
R52F	2.69×10^{-2}	1.00	2.43×10^{-1}	8.5×10^{-2}
R61M	2.2×10^{-1}	1.00	7.26×10^{-1}	<u>0.00</u>
R191M	1.49×10^{-1}	1.00	6.12×10^{-2}	2.9×10^{-1}

Table: Optimized Parameters

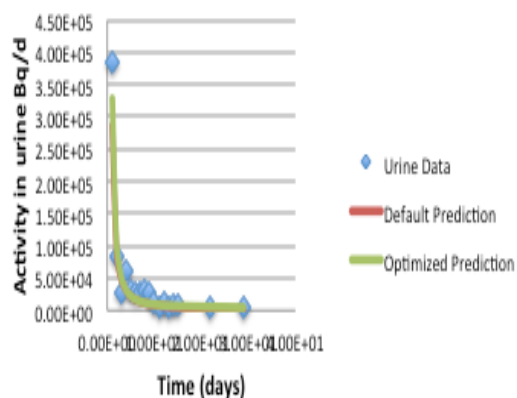
Case #	Chi-square	p-value	Autocorrelation	P-value
R7M	3.68	9.99×10^{-1}	4.48×10^{-1}	1.12×10^{-2}
R8F	4.75	9.43×10^{-1}	4.33×10^{-1}	1.9×10^{-2}
R9M	1.34	9.87×10^{-1}	-6.43×10^{-1}	9.6×10^{-1}
R29F	9.3	9.9×10^{-1}	2.3×10^{-1}	6.6×10^{-2}
R33F	1.77	1.00	3.16×10^{-1}	<u>1.6×10^{-2}</u>
R35F	1.43×10^{-1}	1.00	3.00×10^{-1}	<u>2.08×10^{-2}</u>
R50F	4.11	1.00	9.30×10^{-1}	<u>0.00</u>
R51F	1.55	1.00	7.88×10^{-1}	<u>0.00</u>
R52F	2.25	1.00	-4.50×10^{-1}	9.58×10^{-1}
R61M	1.38×10^{-1}	1.00	5.40×10^{-1}	<u>0.00</u>
R191M	9.5×10^{-1}	1.00	-4.01×10^{-1}	9.35×10^{-1}

Table: Default Parameters

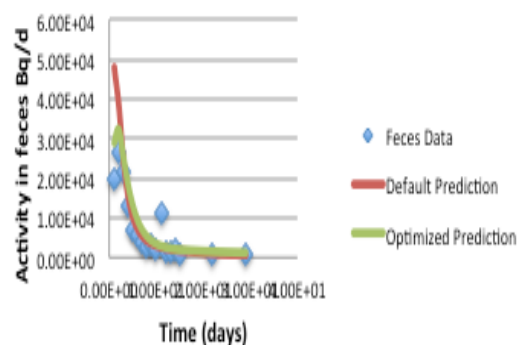
APPENDIX C

This section contains the rest of graphs that not presented in the thesis text. The IMBA Professional Plus employed the default parameters as illustrated in the ICRP 67 and optimized parameters to provide fit to data and predict an intake for each case.

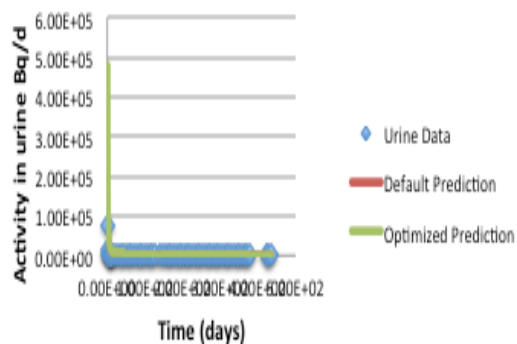
R35F using default and optimized



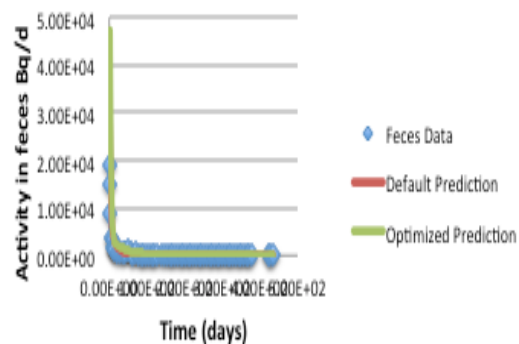
R35F using default and optimized



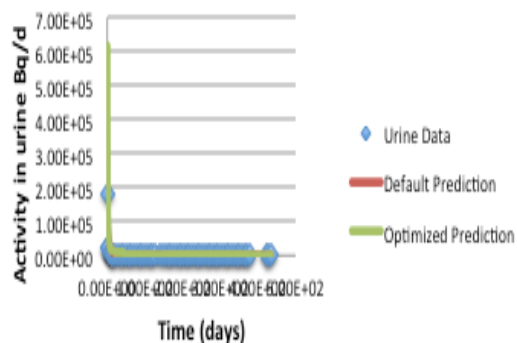
R50F using default and optimized



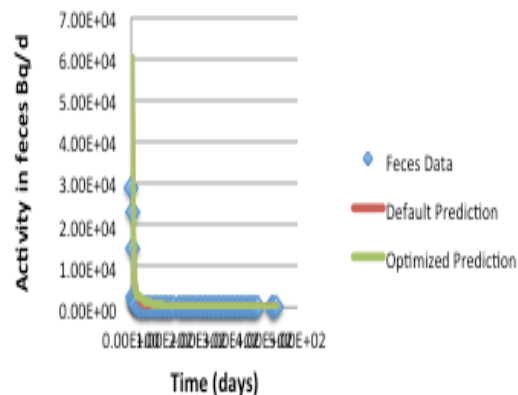
R50F using default and optimized



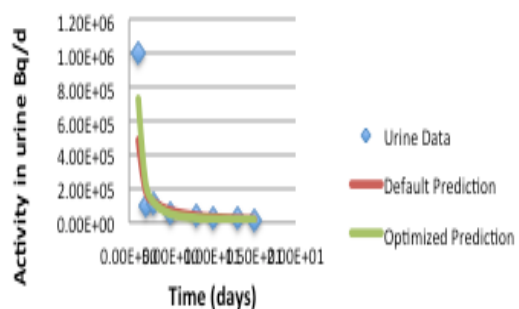
R51F using default and optimized



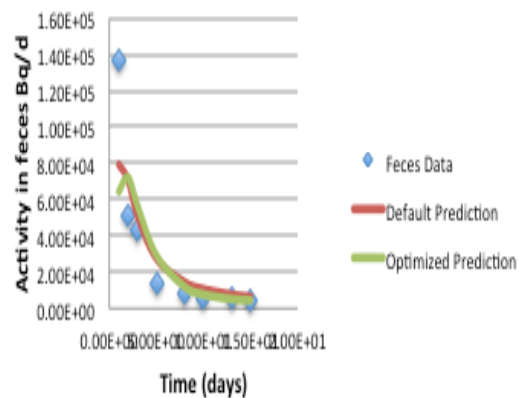
R51F using default and optimized



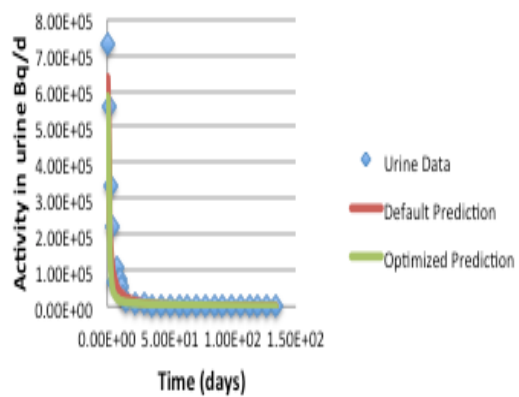
R52F using default and optimized



R52F using default and optimized



R61M using default and optimized



R61M using default and optimized

